



UNIVERSITY of INDONESIA

**RESERVOIR MODELING OF GEOTHERMAL SYSTEM AT
FIELD “X” WITH TOUGH2 SIMULATOR**

THESIS

SARI WIDYANTI

0806326374

FACULTY OF MATHEMATICS AND NATURAL SCIENCE

PHYSICS DEPARTMENT

DEPOK

JUNE 2012



UNIVERSITY of INDONESIA

**RESERVOIR MODELING OF GEOTHERMAL SYSTEM AT
FIELD “X” WITH TOUGH2 SIMULATOR**

THESIS

Proposed as one of the requirements to obtain Bachelor of Science

SARI WIDYANTI

0806326374

FACULTY OF MATHEMATICS AND NATURAL SCIENCE

PHYSICS DEPARTMENT

GEOPHYSICS EXPLORATION

DEPOK

JUNE 2012

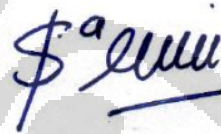
ORIGINALITY STATEMENT PAGE

This thesis is a result of my own work and all sources quoted or referred to, I have stated correctly.

Name : Sari Widyanti

NPM : 0806326374

Signature :



Date : June 13th, 2012

CERTIFICATION PAGE

This thesis is submitted by:

Name : SARI WIDYANTI

NPM : 0806326374

Program Study : Physics

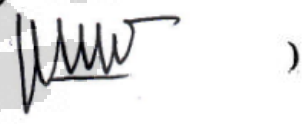
Title of thesis : RESERVOIR MODELING OF GEOTHERMAL SYSTEM
AT FIELD "X" WITH TOUGH2 SIMULATOR

Have been successfully maintained in the presence of Board of Examiners and accepted as part of requirement to obtain a Bachelor of Science in Program Study Physics, Faculty of Mathematics and Natural Science, University of Indonesia.

BOARD OF EXAMINERS

Advisor : Dr. Eng. Yunus Daud, M.Sc. ()

Examiner I : Dr. Eng. Supriyanto Suparno ()

Examiner II : Dr. Djatmiko P. Atmojo ()

Defined at : Depok

Date : June 13th, 2012

PREFACE

Bismillahirrahmanirrahiim.

Thanks to Allah SWT because of His grace and gift, I am able to finish my thesis on reservoir modeling. This thesis is made as a requirement to obtain Bachelor degree in Science from the Physics Department, Faculty of Mathematics and Natural Science, University of Indonesia.

I realize without the help and guidance from various parties, from lecture until preparation of my thesis, it would have been very difficult having it done by myself. Therefore, I would like to send warm and huge thank you to:

- (1) Dr. Eng. Yunus Daud, M.Sc, as my advisor who has provided his time, energy, and mind to guide me in the making of this thesis. Thank you Sir for your wisdom and sharing me your knowledge, support, and useful feedbacks in the making of this thesis and also in life matters.
- (2) Mr. Mulyadi who has taught me about geothermal reservoir. Thank you for taking time and thought in helping me prepared for my thesis. Mas Yuris, Rifka, Wahyudin, Lukman, also the entire staff of STAR ENERGY, thank you for your hospitality & sharing your knowledge.
- (3) Especially to my Mother and sister Mba Ii who has always given me full support and prayed for me nonstop throughout my life. Thank you to have always guides me and protects me.
- (4) The family of Uncle Budi and Aunt Wati, thank you for getting me back on my two feet again. You are like a second family to me.
- (5) Iskandarsyah Mahmuddin who has given full support and prayers from the beginning of the school term until now, thank you for believing in me when I always doubt myself. ☺
- (6) Nurina Kusuma Dewi who has guided me on the beginning to learn reservoir modeling and has spare me time in her busy activities. Also to Kak Lendri, kak Surya, kak Dzil, dan Kak Wambra for the support and feedbacks. May you all succeed and has the best in life.
- (7) Qonita Amriyah, Cut Rulia, dan Ratna Dewi, companion in arms of the same

thesis guidance. Thank you for the togetherness, tears and laughter along the way girls.

- (7) Fanani, Aji, Samuel, James, Kak Shelly, Nita, dan Icha, friends and fellow internship and final thesis fighters at STAR ENERGY. Good luck to us all in the bright future ahead.
- (8) All my close friends, Anggia, Livi, Selita, Tiwi, Iza, Fitha, Zulimatul, Indah, and friends from the Physics Department who I could not mention one by one, thank you for the prayers, support, and togetherness. It would not have been one great chapter of my life without the presence of you all.

Finally, I pray Allah SWT is pleased to reply each of your kindness who have always helped and supported me. May this thesis bring benefits to the world of science and geothermal development, especially to Indonesia.

Author,
June 2012

**PUBLICATION APPROVAL STATEMENT OF THESIS FOR
ACADEMIC INTEREST**

As an academic community of the University of Indonesia, I undersigned below:

Name : Sari Widyanti
NPM : 0806326374
Program Study : Geophysics
Department : Physics
Faculty : Mathematics and Natural Science
Type of Writing : Thesis

for the development in knowledge, agree to grant non - exclusive royalty – free rights (Non - exclusive Royalty Free Right) to the University of on my scientific work, entitled:

**RESERVOIR MODELING OF GEOTHERMAL SYSTEM AT FIELD “X”
WITH TOUGH2 SIMULATOR**

along with the existing devices (if needed). With Non – Exclusive Royalty Free Rights, University of Indonesia is entitled to save, reformat, managing the data base (database), maintain, and publish my final thesis as long as it include my name as author/creator and owner of the Copyright.

I make this statement with the truth.

Made in : Jakarta
Date : June 13th, 2012

Stated by,



(SARI WIDYANTI)

ABSTRAK

Nama : Sari Widyanti
Program Studi : Geofisika
Judul : PEMODELAN RESERVOAR SISTEM GEOTERMAL
LAPANGAN “X” DENGAN SIMULATOR TOUGH2

Lapangan “X” merupakan salah satu lapangan sistem geotermal dengan *high temperature* dan *high enthalpy* yang merupakan bagian dari Bandung *Volcanic Complex*. Ia merupakan peralihan antara jenis sistem *vapor dominated* dengan *liquid dominated*. Hal ini terlihat dari sumur bagian utara yang memproduksi fluida dari sistem jenis *vapor dominated*, sedangkan sumur bagian Selatan memproduksi fluida dari sistem jenis *liquid dominated*. Di lapangan ini terdapat empat pusat *fluid upwelling*, dua di antaranya berasosiasi dengan G.Walawi *andesite stratovolcano* dan dua lainnya dengan G.Lani & G.Intan *andesitic volcanoes*. Untuk mengetahui karakteristik reservoir, letak dan besar energi *heat source*, serta hidrogeologi maka perlu dibuat pemodelan reservoir dengan simulator TOUGH2. Kesesuaian kurva yang didapatkan dari hasil pemodelan dengan 11 data sumur mengindikasikan tercapainya *natural state*. Diperoleh *steam cap* dari reservoir dipisahkan oleh Buri Horst dengan permeabilitas rendah, menghasilkan bagian utara dan selatan. *Heat source* terletak tepat di bawah zona reservoir dengan temperatur 320°C dan reservoir memiliki temperatur rata – rata 257°C dengan luas sekitar 40 km^2 .

Kata Kunci : sistem geotermal, *fluid upwelling*, *heat source*, simulasi reservoir, TOUGH2, *natural state*, reservoir.

ABSTRACT

Name : Sari Widyanti
Study Program : Geophysics
Title : RESERVOIR MODELING OF FIELD “X” GEOTHERMAL SYSTEM WITH TOUGH2 SIMULATOR

Field “X” is one of many geothermal fields located in Bandung Volcanic Complex with high temperature and high enthalpy. It is a transition between vapor dominated with liquid dominated system. This is seen from the well at north producing fluids indicating vapor dominated system, meanwhile fluid is produced from a liquid dominated system at the south. The field has four fluid upwellings, two of them are associated with Mt. Walawi andesitic stratovolcano and two others with Mt. Lani & Mt. Intan andesitic volcanoes. To determine the reservoir's characteristic, location and total energy of heat source, and hydrogeology, modeling of the reservoir needed to be conducted with TOUGH2 simulator. The compatibility of curves gained from the modeling with well data indicates that the natural state has been reached. The result shows the steam cap of the reservoir is separated by the Buri Horst with low permeability, dividing it into the northern and southern sector. The heat source is located beneath the reservoir with temperature of 320°C and the average temperature of reservoir is 257°C with extensive area of 40 km².

Keywords : geothermal system, fluid upwelling, heat source, reservoir simulation, TOUGH2, natural state, reservoir.

TABLE OF CONTENT

Cover Page	i
Title Page	ii
Originality Statement Page	iii
Certification Page.....	iv
Preface.....	v
Publication Approval Statement of Thesis for Academic Interest.....	vii
Abstrak (Indonesian).....	viii
Abstract (English)	ix
Table of Content	x
List of Figures	xiii
List of Tables	xv
Appendices.....	xvi

CHAPTER I. INTRODUCTION

1.1 Background.....	1
1.2 Problem Limitation	3
1.3 Purpose of Research.....	3
1.4 Methodology	4
1.5 Systematics of Writing.....	5

CHAPTER II. LITERATURE REVIEW

2.1 Type of Fluid Phase.....	6
2.1.1 Vapor Dominated System	7
2.1.2 Water Dominated System	7

2.2 Changes Caused by Production	8
2.3 Fractures.....	9
2.4 Tracer Analysis	9
2.5 Fluid Flow	10
2.6 Mass Balance	12
2.7 Energy Balance	15
2.8 Water.....	16
2.9 Reservoir Simulation	17

CHAPTER III. REVIEW OF REGIONAL AREA

3.1 Regional Geology.....	18
3.1.1 Physiography.....	20
3.1.2 Fault Distribution	21
3.1.3 Surface Manifestation	22
3.1.4 Stratigraphy.....	22
3.1.5 Alteration	23
3.1.6 Porosity of Reservoir Rock.....	24
3.1.7 Permeability of Reservoir Rock	24
3.2 Geophysics.....	24
3.2.1 Result of Gravity Method	24
3.2.2 Result of Magnetotelluric (MT) Method	26
3.3 Geochemistry	30
3.4 Conceptual Model.....	32
3.4.1 The Cap Rock Layer	32
3.4.2 The Two – phase Layer.....	33
3.4.3 The Brine Layer	34
3.4.4 The Heat Source.....	34

CHAPTER IV. WELL DATA AND RESERVOIR SIMULATION

4.1 Well Data.....	36
4.2 TOUGH2.....	37
4.3 Simulation Process to Obtain Natural State of Reservoir	38
4.3.1 Boundary & Initial Condition	38
4.3.2 Equation of State.....	39
4.3.3 Making the Grid.....	41
4.3.4 Physical Parameters of Rocks	42
4.3.5 Edit Grid.....	43
4.4 Result of the Simulation.....	44
4.4.1 Layout Block.....	44
4.4.2 Vertical Slice.....	45
4.4.2 Temperature vs Depth Curve.....	45

CHAPTER V. RESULT AND DISCUSSION

5.1 Integrated Interpretation	48
5.2 Vertical Distribution of Layers	50
5.2.1 Cap rock	50
5.2.2 Two – phase Layer	50
5.2.3 Brine Layer	51
5.2.4 Heat Source	51

CHAPTER VI. CONCLUSION AND SUGGESTION

6.1 Conclusion.....	53
6.2 Suggestion.....	54

REFERENCE	55
------------------------	----

LIST OF FIGURES

Figure 1.1 Workflow of Research.....4

Figure 2.1 Vapor dominated system7

Figure 2.2 Water dominated system8

Figure 2.3 Physical changes after production8

Figure 2.4 Use of tracers in monitoring a geothermal reservoir10

Figure 2.5 One – dimensional porous medium held between surfaces at constant pressure.10

Figure 2.6 General mass balance equation for any (sub-) volume of a reservoir, regardless its shape and size13

Figure 2.7 Grid n connected with m in two - dimension13

Figure 2.8 Geometry data in the integral finite difference method14

Figure 2.9 Energy balance equation where fluid also exchange with surroundings15

Figure 2.10 Schematic temperature – pressure diagram of the phase states of pure water16

Figure 2.11 Steam tab17

Figure 3.1 Location of Geothermal Field “X”18

Figure 3.2 Geological map of Geothermal Field “X”19

Figure 3.3 Volcanic Eruption Center Geothermal Field “X”21

Figure 3.4 Stratigraphic cross – section of Geothermal Field “X”23

Figure 3.5 Anomaly Bouger contour of Geothermal Field “X”25

Figure 3.6 Illustration

(a) Temperature distribution, clay alteration, and thermal Features on Geothermal System	26
(b) Conceptual element used on the Integrated Interpretations of MT-TDEM Resistivity, Geology, and Geochemistry	26
Figure 3.7 Distribution of MT stations on topographic map of Geothermal Field “X”	27
Figure 3.8 Resistivity cross - section:	
(a) North – South.....	28
(b) East – West profile 7. With isotherm 225, 250, dan 275OC (White coloured contour)	28
Figure 3.9 Cap rock marked by red line	29
Figure 3.10 Distribution of Resistivity	
(a) Top Elevation.....	29
(b) Base Elevation of Low Resistivity Layer Geothermal Field “X”	29
Figure 3.11 Plotting of CO ₂ - CH ₄ - H ₂ S from a several wells at Geothermal Field “X”	31
Figure 3.12 Conceptual Model of Geothermal Field “X”	32
Figure 4.1 Distribution of lithology and location of water loss zones at geothermal Field “X”	36
Figure 4.2 Main window TOUGH2	37
Figure 4.3 Boundary coordinates of the simulated system	39
Figure 4.4 Initial Condition.....	39
Figure 4.5 Selecting EOS.....	40
Figure 4.6 Making the grid with meshmaker method	41
Figure 4.7 A grid view that has been made	41
Figure 4.8 Input physical parameter of each material	43
Figure 4.9 Edit of grid on each layer	43
Figure 4.10 Distribution of temperature at Layer 8	44
Figure 4.11 Distribution of temperature vertical slice view at Line 13	45

Figure 4.12 Curve matching temperature at natural state	46
Figure 5.1 Geothermal Field “X” Modeling Description	48
Figure 5.2 Reservoir surrounded by permeability barriers	49
Figure 5.3 Distribution of Rock Permeability at Layer 8 using mulGRAPH.....	50
Figure 5.4 Vertical Slice North – South	
(a) Temperature.....	51
(b) Permeability.....	52
Figure 5.5 <i>Vertical Slice</i> Temperature & Permeability East - West	52

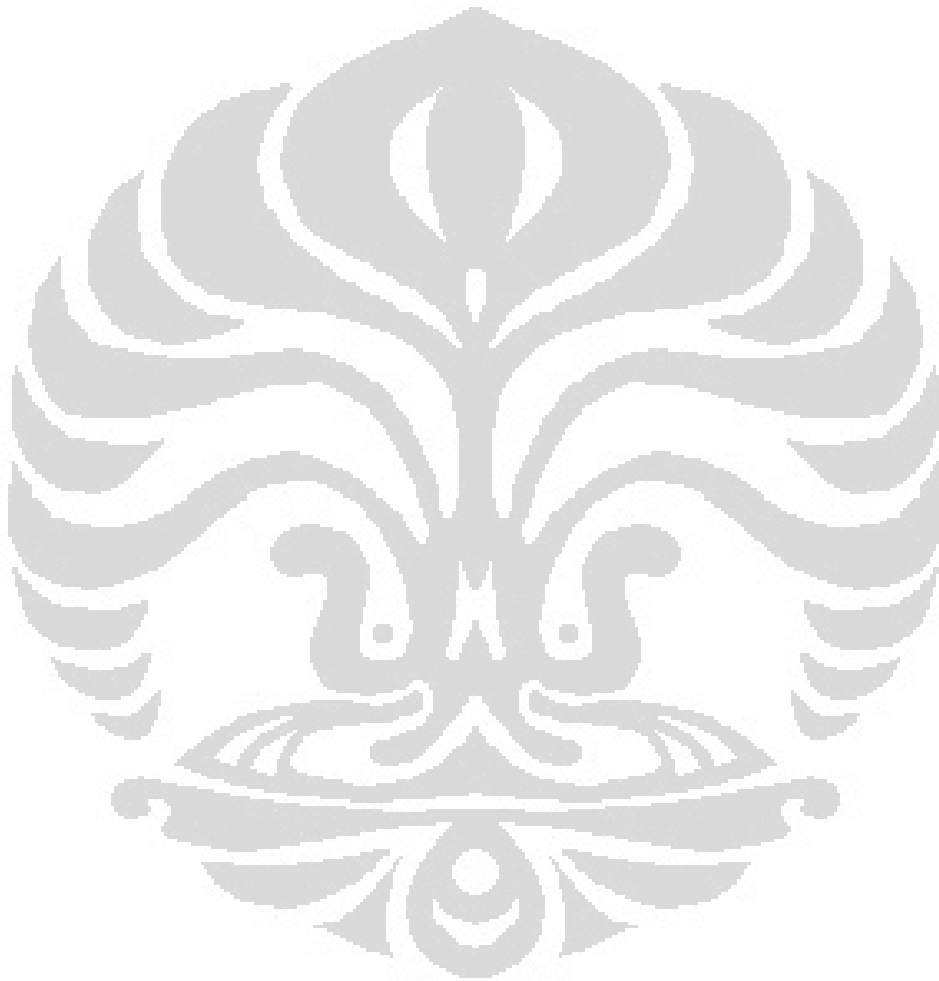
LIST OF TABLE

Table 4.1 Modul EOS fluida	40
Table 4.2 Rocke type with each of the parameter for the simulation	42

APPENDICES

Appendix 1 Horizontal slicing of model simulation at Layer 1.....	57
Appendix 2 Horizontal slicing of model simulation at Layer 2.....	58
Appendix 3 Horizontal slicing of model simulation at Layer 3.....	59
Appendix 4 Horizontal slicing of model simulation at Layer 4.....	60
Appendix 5 Horizontal slicing of model simulation at Layer 5.....	61
Appendix 6 Horizontal slicing of model simulation at Layer 6.....	62
Appendix 7 Horizontal slicing of model simulation at Layer 7.....	63
Appendix 8 Horizontal slicing of model simulation at Layer 8.....	64
Appendix 9 Horizontal slicing of model simulation at Layer 9.....	65
Appendix 10 Horizontal slicing of model simulation at Layer 10.....	66
Appendix 11 Horizontal slicing of model simulation at Layer 11.....	67
Appendix 12 Horizontal slicing of model simulation at Layer 12.....	68
Appendix 13 Horizontal slicing of model simulation at Layer 13.....	69
Appendix 14 Horizontal slicing of model simulation at Layer 14.....	70
Appendix 15 Horizontal slicing of model simulation at Layer 15.....	71
Appendix 16 Horizontal slicing of model simulation at Layer 16.....	72
Appendix 17 Horizontal slicing of model simulation at Layer 17.....	73
Appendix 18 Horizontal slicing of model simulation at Layer 18.....	74
Appendix 19 Horizontal slicing of model simulation at Layer 19.....	75
Appendix 20 Horizontal slicing of model simulation at Layer 20.....	76

Appendix 21 Horizontal slicing of model simulation at Layer 21.....	77
Appendix 22 Horizontal slicing of model simulation at Layer 22.....	78
Appendix 23 Horizontal slicing of model simulation at Layer 23.....	79
Appendix 24 Horizontal slicing of model simulation at Layer 24.....	80
Appendix 25 Horizontal slicing of model simulation at Layer 25.....	81



CHAPTER I

INTRODUCTION

1.1 Background

The demand for energy is never - ending, it is one of the primary need for humans to live their everyday activity. With the increasing amount of demand and consumption for energy, the amount of oil, gas, and coal that has been the main source for daily life is decreasing. With that basic reason, geothermal energy must be developed to reduce dependence on fossil fuel use. Not forgetting to mention that Indonesia has the world's largest potential of geothermal energy.

Indonesia is a country that contains many active volcano because of its geographical position located on plate boundaries. It has the largest potential in geothermal energy in the world, with the total capacity of 20,000 MWe or 40% of the world's geothermal potential with 217 prospective field, 70 of them are included in the high – temperature geothermal system. Unfortunately, only 4% has been developed or only 1,196 MWe is produced from the total potential. It would be such a waste if Indonesia's geothermal energy is not utilized and developed.

Geothermal energy is heat energy from the Earth made by the magmatisation of tectonic plate (Singarimbun dkk., 2011). It is a source of renewable energy and the final disposal produces low rates of carbon dioxide (CO₂) rather than the ones created by fossil fuel energy. Because what it produces is in form of water vapor, not gas. So if we develop this geothermal energy, we are also doing ourselves a favor which is reducing the amount of pollution in the air, water, and soil, or so we can say it is environmentally friendly.

Geothermal energy is so called renewable because the source that it is using and produce are in form of water vapor and hot water to generate the turbines, are injected back into the subsurface to flow back to its reservoir to be reheated back and can be used again. And so on, with a closed cycle system, the geothermal system will never stop producing energy as long as it still has 5

fundamental things needed to be called a geothermal reservoir, they are heat source as the main heat energy for the system, rocks with good permeability to transfer fluid, clay cap to stabilize the pressure in the reservoir, fluid/water as heat carrier, and a reliable recharging system (Daud, 2011).

However, maintaining the condition of a geothermal reservoir to be able to keep producing is not an easy task. We aren't able to see with naked – eye on how the condition on the subsurface is, therefore we don't know if the fluid that we injected back are going into the reservoir, only partially, or none at all. That is why the role of a reservoir modeling simulation and monitoring is important to maintain the conditions of the geothermal reservoir, letting us to understand on how the reservoir responded caused by exploitation. Here, the analysis from geology, geochemistry and geophysics are needed to support in the making of reservoir modeling. With the main objective to determine which well can act as the production and/or the reinjection well to maintain the reservoir in renewable state. Also to predict on how much energy can be produced and guide us on making decisions in managing the reservoir during exploitation.

Geothermal reservoir simulation works on the basic principle of fluid flow and heat transfer, physical properties of the formation in the geothermal reservoir, also thermodynamic and thermo physical properties of the fluid reservoir with the majority in form of water (Pruess, 2002). The simulation will be done by using a computer simulator (software) named TOUGH2. It will make a mathematical model and a numerical simulation of the geothermal reservoir. This simulator is made to test the previous conceptual model and predict the response of a geothermal system for various production scenario's (Newson et al., 2012).

The method used in the modeling is a distributed parameter approach where the system will be divided into several blocks/grid. Each block contains various materials with different permeability, porosity, density, wet heat conductivity, and specific heat distributed vertical and lateral across the reservoir. From here, we can determine the connection between one block to the other.

Parameters used in the reservoir simulator are the dispersion of permeability and porosity, density, change of temperature towards depth, wet heat

conductivity, specific heat, the position and flow rate of the up flow and recharge area, and vapor saturation of fluid inside the reservoir. At the beginning, the parameters of the simulation are not well known or understood. That is why the important step after the modeling is been done, is to calibrate the model or do history matching. This step is to compare data after the simulation with data gained from the field, like distribution of pressure and temperature, change of flow rate fluid and enthalpy in each well, the return of tracer, and other Discrepancy between model from prediction with observation will be recorded and revised so the discrepancy can be reduced (Finsterle et al., 2000).

1.2 Problem Limitation

The making of reservoir simulation model needs parameters of the materials distributed in the reservoir. This information is obtained from the geological, geochemistry, and geophysical data which are integrated with correlating wells. After deciding on the parameters, reservoir simulation is been done by using TOUGH2 software for reservoir simulation modeling. Temperature to depth curve will be plotted from the reservoir modeling and then compared with existing temperature data from well. Compatibility between the two curves indicates that the natural state of the system has been obtained from the reservoir simulation.

1.3 Purpose of Research

Generally, the purposes of this research are:

- ② Knowing the location and characteristics of the geothermal system at field “X”
- ② Knowing the location of the geothermal system located at field “X”
- ② Knowing the hydrogeology of the geothermal system located at field “X”
- ② Knowing the permeability distribution of the geothermal system located at field “X”
- ② Create a reservoir model in natural state condition

1.4 Methodology

Broadly speaking, reservoir simulation activities include:

1. Data collecting and assessment of geological, geochemical, geophysical, well data, and the existing manifestation on the surface.
2. Making of the conceptual model based on existing data.
3. Reservoir modeling (simulation) in natural state condition
4. Curve matching temperature towards depth of well and calculated (simulation).

Methods used in this research can be seen from the following diagram.

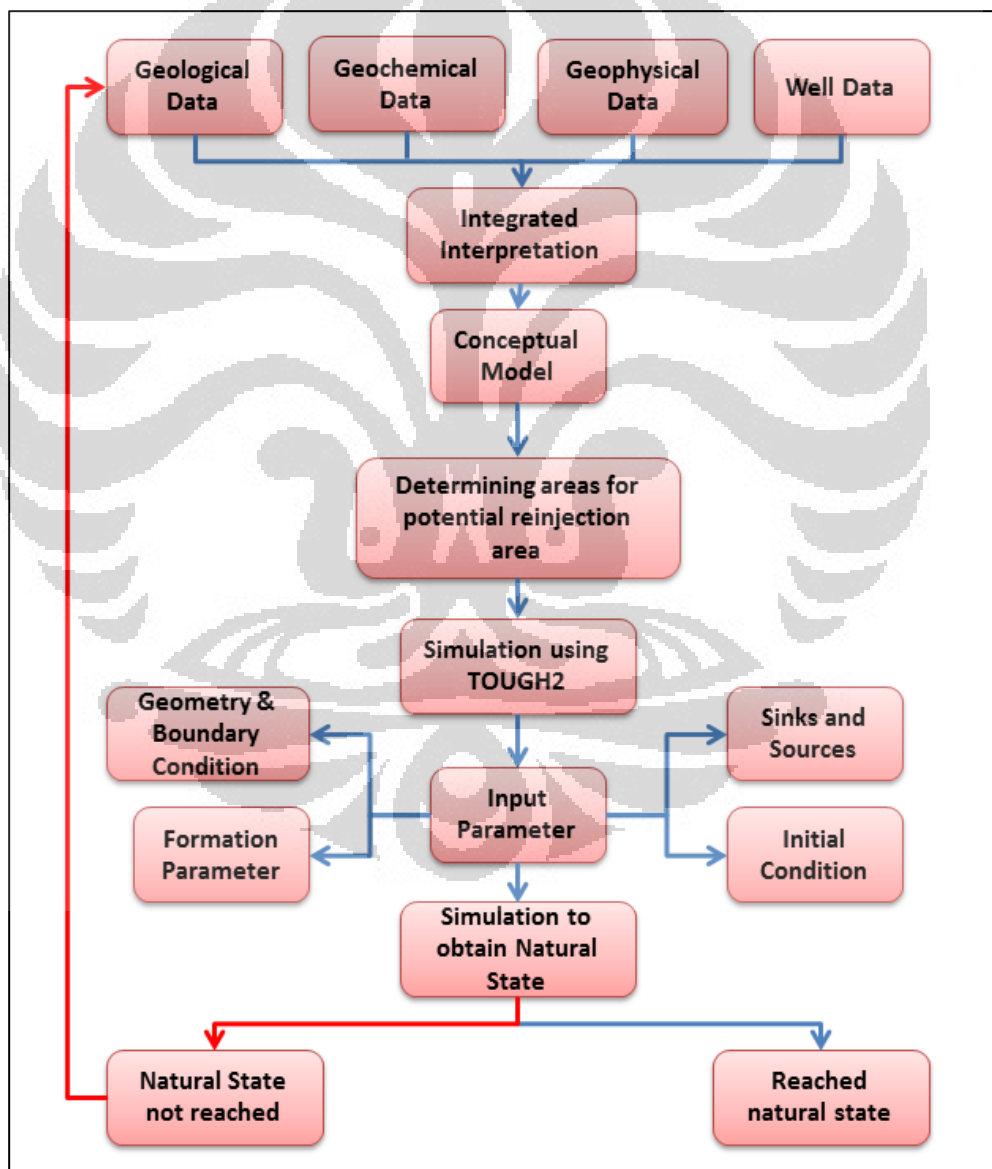


Figure 1.1 Workflow of research

1.5 Systematics of Writing

This thesis consists of 5 (five) chapter. On the first chapter, contains explanation on why modeling of the reservoir is done and the importance of it in production and developing a geothermal reservoir. In the subchapter consists of background, problem limitation, purpose of research, purpose of research, methodology used in the research, and systematic of writing.

The second chapter contains a literature review covering the basic concepts in making a model with explanations, mathematical equations, and parameters needed in the modeling such as permeability, porosity, water saturation, temperature, and pressure. Not forgetting an introduction of the software used in this research.

Third chapter contains a review of the research area. It looks at the area under study from the geological, geochemical, and geophysical analysis. From the three field of analysis, an integrated interpretation is made as the basic foundation in making the reservoir model (simulation). The geophysical data that are available are gravity and magnetotelluric (MT) method.

The fourth chapter contains explanation of existing well data and steps taken in creating the reservoir model (simulation) of the prospected area. It also has the explanation of the input data needed in making the model and finally creating a model of the reservoir that has achieved natural state condition.

Fifth chapter contains analytical result and discussion by the author of the model obtained and comparing the result of the simulation model with the well data (temperature). Until eventually it reached natural state condition that can be checked from the curve matching temperature profile from a couple of wells.

The last chapter contains the conclusion obtained from the geothermal reservoir simulation model and also suggestion for further study of the prospected area or other geothermal fields.

CHAPTER II

LITERATUR REVIEW

Geothermal reservoir is a geothermal system that contains fractured rocks so it is became permeable to allow fluid flow such as vapor or hot water from inside the reservoir. Even though most of the heat is trapped in the host rock, but fluid is the heat carrier to the surface making it able to be produced. The production of a geothermal reservoir depends on how the reservoirs are managed to find enough energy to utilize. If not managed properly, it could give “deadly” effect to the ability of the reservoir to produce large amount of energy where it was supposed to be a renewable source of energy that can be reused. This is why studying the physical and chemical properties of the reservoir is important, so we are able to maintain its condition in productive phase.

The monitoring of reservoir has to be done from the beginning of production and ongoing so we can study and compare the changes that occur during the production from the initial state. Besides that, by analyzing the physical and chemical properties of the reservoir, we are expected to know the permeability distribution which we know the exact location where the production and reinjection needs to be taken. The process of reinjection fluid into the reservoir needs to be monitored so the pressure remains constant on production and low – temperature fluid not entering the production well.

2.1 Types of Fluid Phase

Classification of types of fluid phase depends on the content of the fluid itself. There are two types of fluid phase, the one phase and two phase. Each type of phase has different characteristic and content of fluid. One phase system generally contains water of temperature $90^{\circ}\text{C} - 180^{\circ}\text{C}$ and boiling did not occur during exploitation. Meanwhile the two phase system consists of vapor dominated system and water dominated system.

2.1.1 Vapor Dominated System

Vapor dominated system is a closed system of a geothermal system. In this closed system, convection occurs causing homogenization of pressure and temperature. Thus, the result of temperature profile is constant towards depth. This is caused by the fluid inside the reservoir is located in the impermeable layer, so it isn't able to get out of the layer. It has a high temperature which mixed water and steam exist, and steam is the pressure controlling fluid phase. This type of system is well suited for production of electrical power generator.

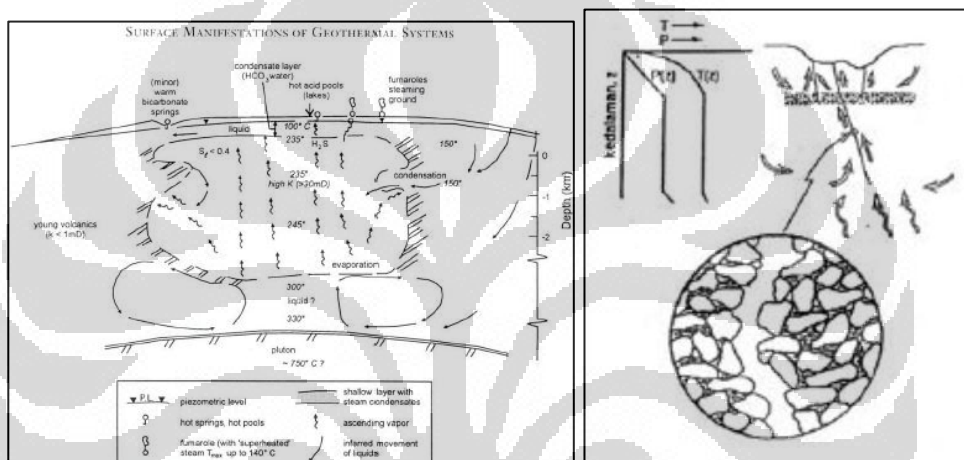


Figure 2.1 Vapor dominated system

(Sigurdsson, 2000)

2.1.2 Water Dominated System

Water or liquid dominated system is an open cycled of a geothermal system with indication of existing outflow in the geothermal field area. This is caused by the impermeable layer of the system is not closed perfectly so the hot fluids that is contained inside flows out.

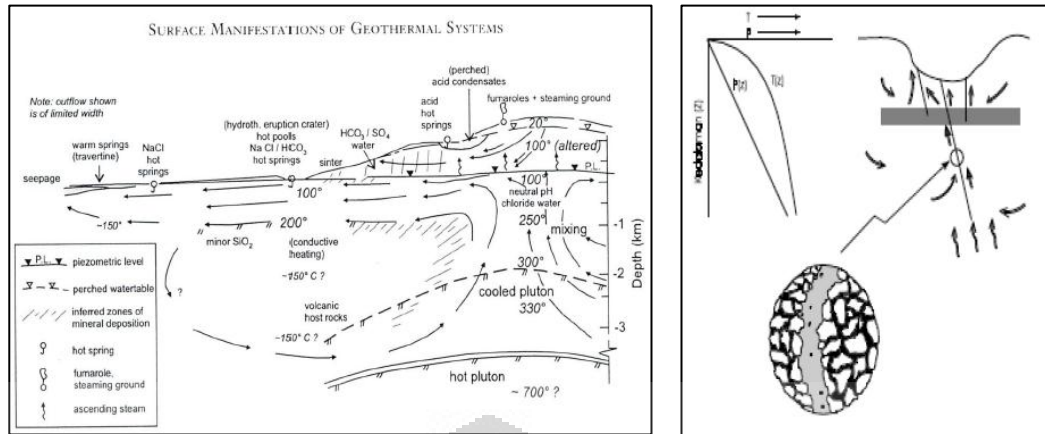


Figure 2.2 Water dominated system
(Sigurdsson, 2000)

2.2 Changes Caused by Production

During exploitation, there are several physical properties that changes, like:

1. Temperature changes vertically and laterally,
2. Changes in mass (gravity) due to loss of fluid in reservoir,
3. Ground subsidence due to pressure drop,

Effects of subsidence can be minimized by doing reinjection towards the reservoir to stabilize its pressure.

4. Changes in seismic activity,
5. And many others, we can see from the Figure below.

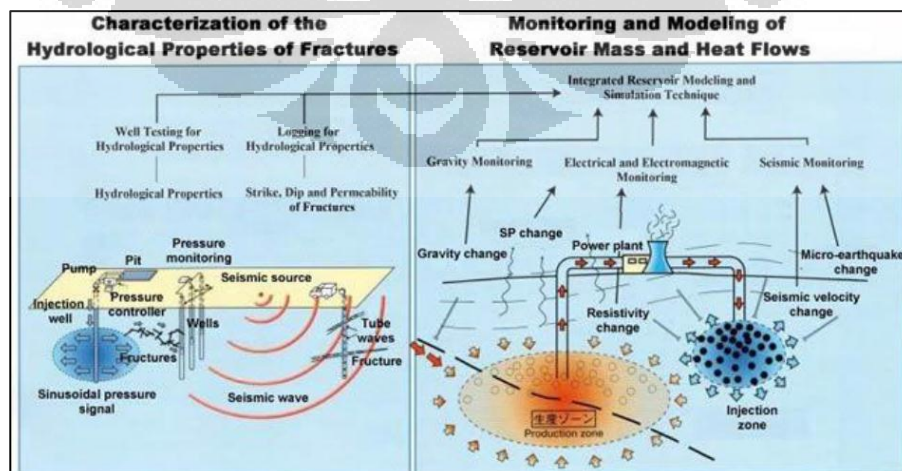


Figure 2.3 Physical changes after production

2.3 Fractures

As we know, the location of a geothermal reservoir is usually located in volcanic regions where the most likely source of natural heat is below the Earth's surface. Fractures that has become the connection path where fluid flow from reservoir to the surface, surely have high permeability. Usually drilling is done at the cross section of fractured zones where good permeability is to be found and proven by successful drilling.

Of course in addition of determining a good area to drill and become a good production well, we also need to find an area outside the reservoir that still connects to the reservoir. This area will be the recharge for the reservoir when productions occur. This reinjection area must be outside the production zone because as the author have said before, we have to keep the low – temperature fluid from reinjection wells is not also sucked into the production well. But it can act as a replacing fluid that has been taken out to be heated and fill pores that were empty so scaling doesn't occur. Because scaling which are deposition of minerals can close the connection path which will decrease the permeability of the reservoir and also the production.

2.4 Tracer Analysis

Tracers are inserted into the fractures that are potentially a reinjection well across the reservoir and appear on the production well. By calculating the time for the tracer to flow between the production and reinjection well, we can use this information to predict the fluid volume contained in the reservoir.

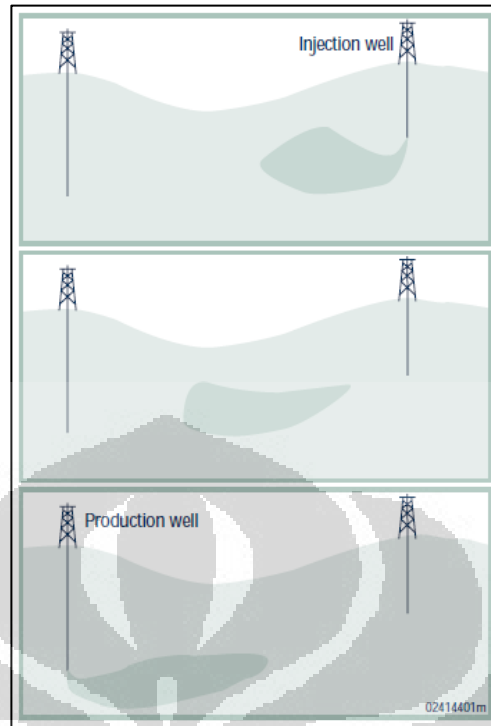


Figure 2.4 Use of tracers in monitoring a geothermal reservoir
(Natural Renewable Energy Laboratory, DOE. March 1998)

2.5 Fluid Flow

Fluid flowing causes a flowing force, based on an experiment done by Henri Darcy (1856). On the Figure below a change of pressure occur, so the fluid flows from pressure $P1+\Delta P$ to $P1$.

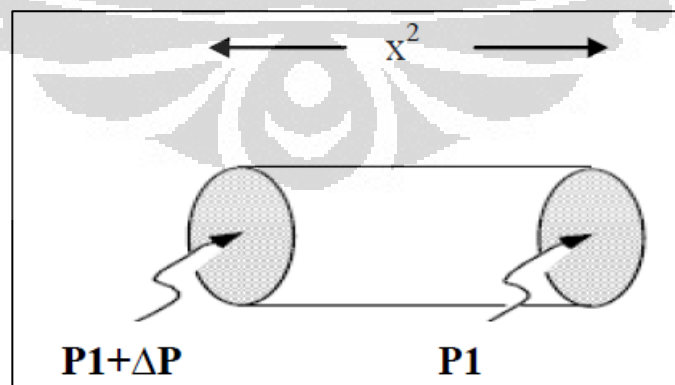


Figure 2.5 One – dimensional porous medium held between surfaces at constant pressure
(Pruess, 2002)

The velocity of flowing fluid is not based on the change of pressure, but based on the intensity of pressure change called pressure gradient ($\Delta P/\Delta x$). This experiment showed that the fluid mass flow rate (F) per unit cross – sectional area of the medium is proportional to the pressure gradient. The minus – sign in **Equation 2.1** occur because fluid flows from higher pressure to lower pressure, analogous to heat flowing from higher temperature to lower temperature (Pruess, 2002).

$$F = -k \left(\frac{\rho}{\mu} \right) \frac{\Delta P}{\Delta x} \quad (2.1)$$

where:

F = fluid mass flow rate per unit cross – sectional area per time ($\text{kg}/\text{m}^2\text{s}$)

k = permeability (m^2)

ρ = density (kg/m^3)

μ = viscosity (Pa.s)

ΔP = change of pressure (Pa)

Δx = maximum thickness of porous medium (m)

The pressure gradient has 3 (three) components (x, y, and z). Where the vertical component is called body-force cause of gravitational force. On **Equation 2.2** the vector notation (F_x, F_y, F_z) can be written out mathematically as **F**. SO the pressure gradient can be written out as ($\Delta P/\Delta x, \Delta P/\Delta y, \Delta p/\Delta z - \rho g$).

$$\begin{pmatrix} F_x \\ F_y \\ F_z \end{pmatrix} = -k \frac{\rho}{\mu} \begin{pmatrix} \Delta P/\Delta x \\ \Delta P/\Delta y \\ \Delta P/\Delta z - \rho g \end{pmatrix}$$

$$\mathbf{F} = -k \frac{\rho}{\mu} (\nabla P - \rho \mathbf{g}) \quad (2.2)$$

Where the vector **g** of the gravitational acceleration is given by the components (0, 0, g). The velocity of the fluid flow in a fluid density over some time is called volumetric flux (u).

$$\mathbf{u} = -\frac{k}{\mu} (\nabla P - \rho g) \quad (2.3)$$

In groundwater hydrology, volumetric flux can be written mathematically in form of head pressure $h = P/(\rho g)$, so we can obtain the mathematical equation as follow:

$$\mathbf{u} = -\mathbf{K} \nabla h \quad (2.4)$$

where:

$\mathbf{K} = k\rho g/\mu =$ hydrolic conductivity (m/s)

$h = P/(\rho g) + z =$ hydraulic head + rock permeability (m^2)

In geothermal reservoir we often find cases of a two phase fluid, liquid and gas. Each fluid of the two phase system flows beneath the pressure gradient. But for the one phase gradient permeability gradually decreases in every medium. This is caused by each of the fluid phase has a porous medium. So this effect is called the permeability reduction factors or relative permeability, symbolized by $k_{r\beta}$. β shows that the fluid is in a two phase, liquid and gas (Pruess, 2002).

$$\mathbf{F}_{\beta} = -k \frac{k_{r\beta} \rho_{\beta}}{\mu_{\beta}} (\nabla P_{\beta} - \rho_{\beta} g) \quad (2.5)$$

The $k_{r\beta}$ coefficient represents the reduction of permeability due to the fact that only a fraction of the pore space is occupied by phase (S_{β}). So the relative permeability is a function of S_{β} . k_{β} become $= k_{r\beta} (S_{\beta})$. Relative permeability as a function $k_{r\beta} (S_{\beta})$ depends on the geometry of the porous medium and the connectivity between pores.

2.6 Mass Balance

Determining whether the medium is porous or space free, the mass balance plays an important role. The change of fluid mass in a reservoir volume is given by the net inflow across the surface of the volume, added by the contributions from sinks (productions wells) and sources (injected wells).

$$\boxed{\begin{array}{c} \text{change in fluid} \\ \text{mass in volume} \\ V \end{array}} = \boxed{\begin{array}{c} \text{net fluid inflow across} \\ \text{surface of } V \end{array}} + \boxed{\begin{array}{c} \text{net gain of fluid from} \\ \text{sinks and sources} \end{array}}$$

Figure 2.6 General mass balance equation for any (sub-)volume of a reservoir, regardless its shape and size
(Pruess, 2002)

Mass balance contained in the system is determined by the amount of fluid flowing in the weak zone that has high permeability. In addition, the fluid volumes from the *sinks* (production well) and *sources* (injection well) affect the changes of mass fluid volumes or mass balance. If the volume of mass fluid is proportional to the fluid contained in the weak zone and from the production and reinjection well, then mass balance of fluid in the reservoir system will occur.

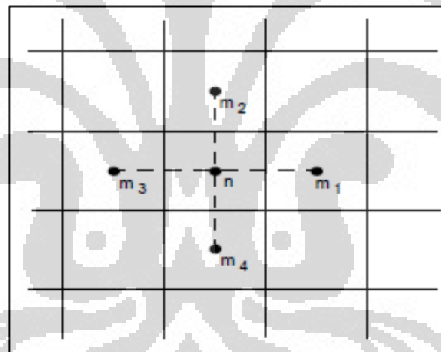


Figure 2.7 Grid n connected with m in two - dimension
(Pruess, 2002)

In reservoir simulation, the total volume of the reservoir consists of sub - volumes with smaller sizes and each grid is set up to reach mass balance. In a one phase system with only water acting as the fluid, mass balance occur on grid n. Fluid flow to grid n from grid m when the simulation is being done. The cross sectional area between grid m and grid n is written as A_{nm} and F_{nm} is the average mass flux across the interface. Mass flux will be counted positive if fluid flow from grid m to grid n. the change of total mass fluid flowing during time Δt .

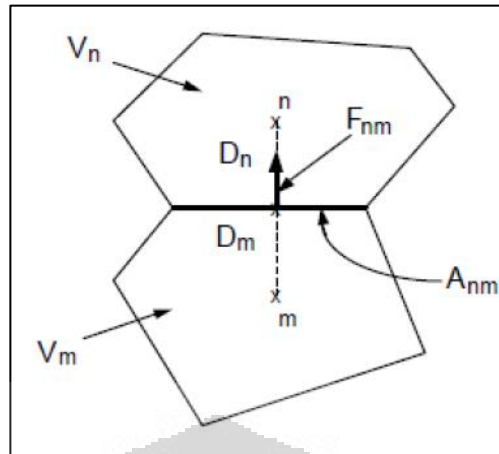


Figure 2.8 Geometry data in the integral finite difference method
(Pruess, 2002)

$$\Delta \mathcal{M}_n = V_n \Delta M_n = \Delta t \{ \sum_m A_{nm} F_{nm} + Q_n \} \quad (2.6)$$

where:

Q_n = Total net mass rate per time (kg/s)

V_n = Grid volume (m^3)

$\Delta \mathcal{M}_n$ = change of fluid mass in V_n (kg)

ΔM_n = change of fluid mass per unit volume during time Δt ($\text{kg}/\text{m}^3 \cdot \text{s}$)

Changes of mass fluid per unit volume are different in every condition. Whether it is a one phase one component, one phase with many components or two phase with many components.

single phase, single component $M = \phi \rho$

single phase, multi-component $M^k = \phi \rho X^k$

multi-phase, multi-component $M^k = \phi \sum_{\beta} S_{\beta} \rho_{\beta} X_{\beta}^k$

Average flux F_{nm} in a single phase system across the interface between grid blocks n and m can be written as:

$$F_{nm} = k_{nm} \left| \frac{\rho}{\mu} \right| \left[\frac{P_m - P_n}{D_{nm}} + \rho_{nm} g_{nm} \right] \quad (2.7)$$

Where the subscripts (nm) denote a suitable averaging at the interface between grid blocks n and m. P_n and P_m are the average pressure in two grid blocks. Meanwhile $D_{nm} = D_n + D_m$ is the distance between the nodal points n and m (Pruess, 2002).

2.7 Energy Balance

Energy balance follows the first Law of Thermodynamics:

$$\Delta U = G + W \quad (2.8)$$

where:

ΔU = internal energy of a system (Joule)

G = heat transfer (Joule)

W = mechanical work (Joule)

Here we consider both heat transfer and mechanical work as positive value when they are done to the system. For a finite (sub-) volume of a flow system, where fluids may exchange with the surroundings, the energy balance can be written as:

$$\begin{array}{|c|} \hline \text{change in} \\ \text{internal} \\ \text{energy in} \\ \text{volume V} \\ \hline \end{array} = \begin{array}{|c|} \hline \text{net} \\ \text{transfer of} \\ \text{energy by} \\ \text{fluid flow} \\ \hline \end{array} + \begin{array}{|c|} \hline \text{mechanical} \\ \text{work done} \\ \text{to volume V} \\ \hline \end{array} + \begin{array}{|c|} \hline \text{net heat} \\ \text{transfer by} \\ \text{conduction} \\ \hline \end{array} + \begin{array}{|c|} \hline \text{net energy} \\ \text{gain from} \\ \text{sinks and} \\ \text{sources} \\ \hline \end{array}$$

Figure 2.9 Energy balance equation where fluid also exchange with surroundings (Pruess, 2002)

The internal energy per unit volume in a general multiphase system is given by:

$$M^h = \Phi \sum_{\beta} S_{\beta} \rho_{\beta} u_{\beta} + (1 - \Phi) \rho_R C_R T \quad (2.9)$$

where:

M^h = Internal energy per unit volume (J/m^3)

ρ_R = Grain density (kg/m^3)

C_R = Specific heat of the rock ($J/kg \cdot ^\circ C$)

T = Temperature ($^\circ C$)

u_{β} = Specific internal energy in phase β (J/kg)

ϕ = Porosity

2.8 Water

Water may exist as a single phase liquid, a single phase gas called vapor or steam, or as a two phase mixture of both water and steam. At any given temperature, there is a saturated vapor pressure denoted as $P_{\text{sat}}(T)$ where both vapor and liquid may exist. At pressure bigger than P_{sat} , there will only be a single phase liquid and at pressure below P_{sat} , we have only single phase vapor. At increasing temperature, the properties of vapor and liquid become similar and the differences between the two phases vanish at the critical point $(T_{\text{crit}}, P_{\text{crit}}) = (375.15^{\circ}\text{C}, 221.2 \text{ bars})$. Above the critical point, there would only be a single supercritical phase of water.

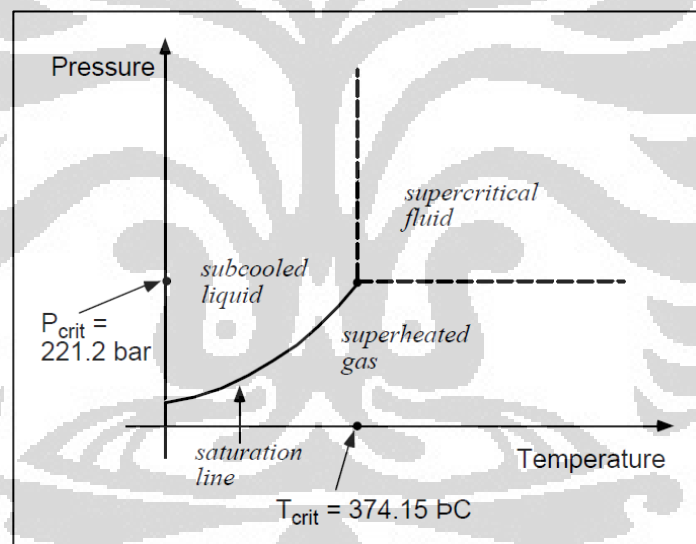


Figure 2.10 Schematic temperature – pressure diagram of the phase states of pure water

(Pruess, 2002)

The relationship of $P_{\text{sat}}(T)$ with properties such as densities, specific enthalpy of liquid and vapor, and viscosities has been studied through experimental observations and theoretical analysis with mathematical correlations known as steam tables (Keenan et al., 1969). Steam tables are now

being calculated by software made from the ChemicalLogic Corporation. It makes it easier to use rather than reading the long – list table itself.

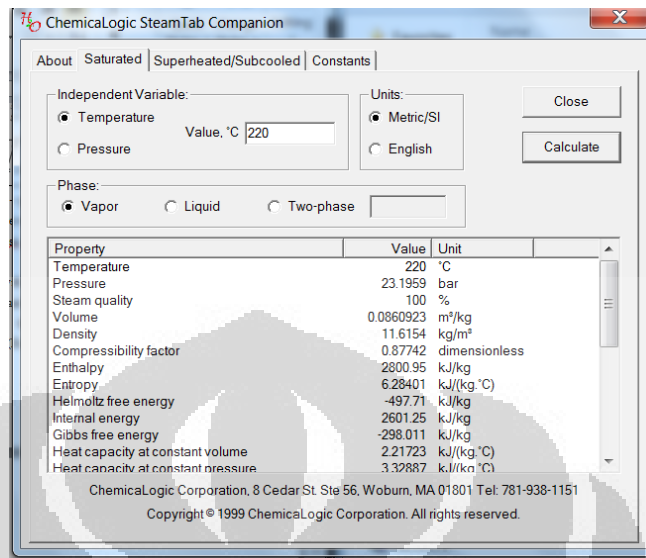


Figure 2.11 Steam Tab

2.9 Reservoir Simulation

Reservoir simulation is one of the methods used to determine the reservoir characteristics and also to know the potential that it has. The making of geometry of the model and reservoir characteristics is made by using TOUGH2 simulator. The simulation model is created by making grid that forms the geometrical shape of the reservoir also the boundary condition which we obtained from geophysical data, gravity and magnetotelluric (MT) method. The conceptual model gained from the gravity and MT data is critical in making the grid model used for the simulation. In addition, other supporting data such as geology, geochemistry is also needed to support the geophysical data. The boundary of geometry and number of grids will affect the final result of the geothermal reservoir model simulation (Dewi, N. K., 2010).

Rocks physical parameter inputted into the TOUGH2 simulator consists of rock density, porosity, permeability, thermal conductivity, also specific heat capacity. The thickness and depth of rocks at the field is gained from well data. Temperature and also the mass production is also obtained from well data.

BAB III

REVIEW OF REGIONAL AREA

3.1 Regional Geology

Field “X” is one of the potential geothermal field located at Walawi area, province of West Java, Indonesia with elevation of 1280 masl – 2341 masl. This field is part of the stratovolcanic andesite of the Sundanese Volcanic Basin. The Sundanese Basin formed as a result of subduction between the Indian – Australian plate with the Eurasia plate. The subduction heading to the North is creating maximum horizontal stress, making strike – slip faults facing towards North - Northeast, that will provide important structural control on the distribution of heat source and permeability for the geothermal system in the area (*Mandala Nusantara Ltd, 1997 op cit Unocal Geothermal of Indonesia, 2002*).

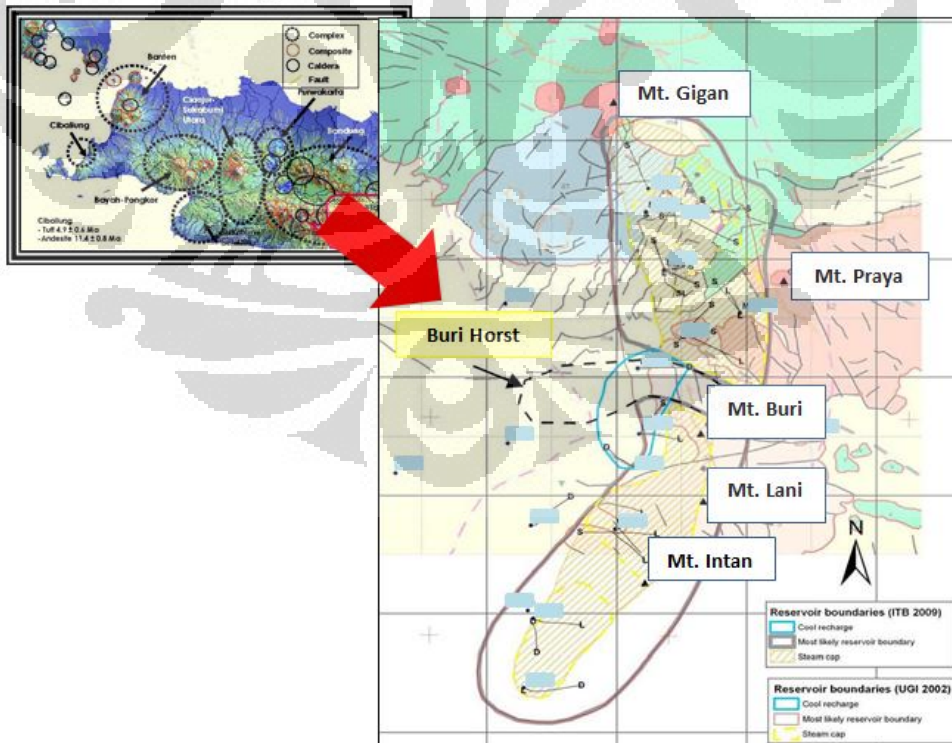


Figure 3.1 Location of Geothermal Field “X”
(Star Energy, 2012, pers. comm.)

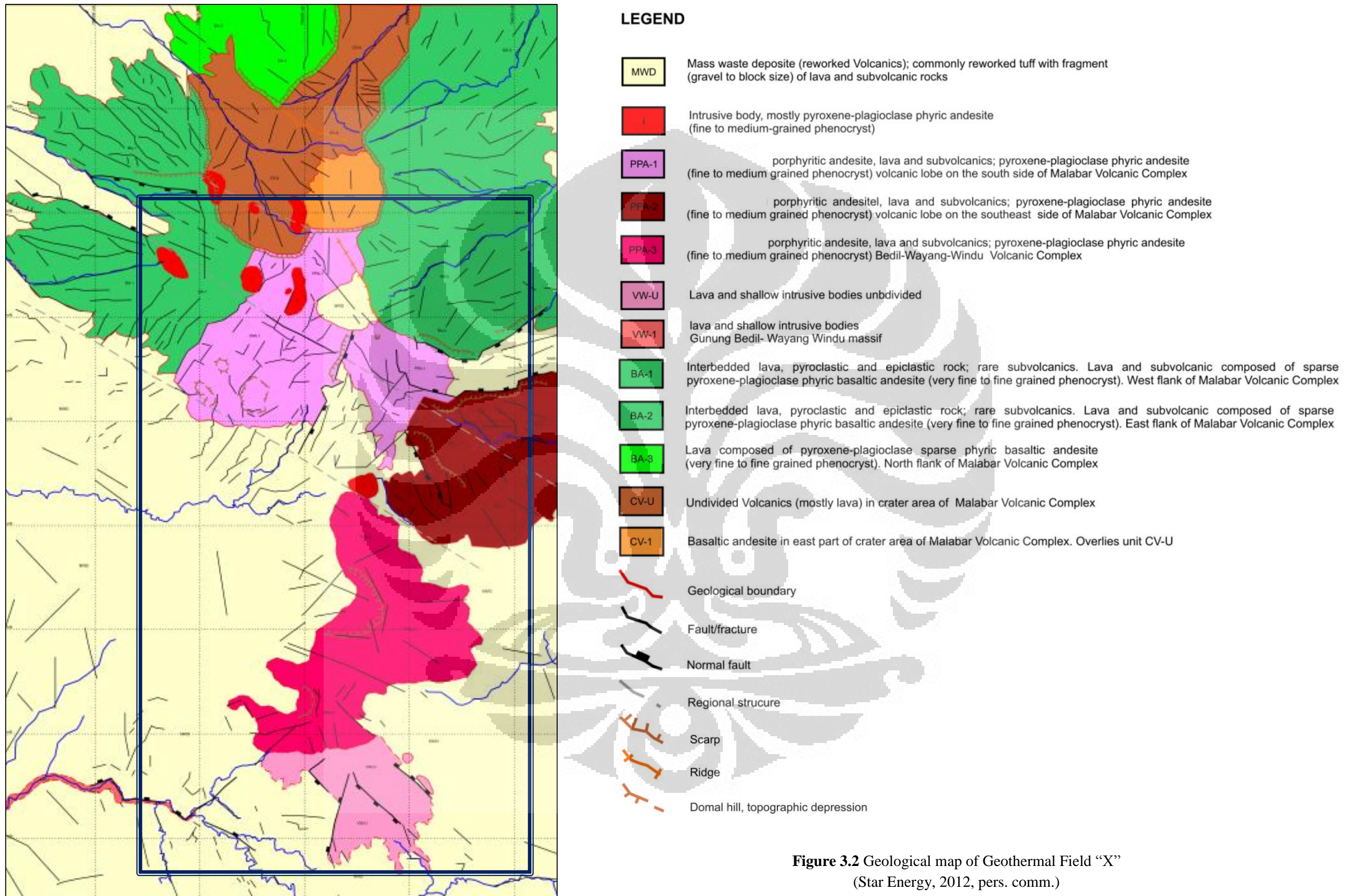


Figure 3.2 Geological map of Geothermal Field “X”
(Star Energy, 2012, pers. comm.)

Geothermal system “X” is interpreted as a transition between a vapor – dominated system with a liquid – dominated system. With the North sector producing fluid from vapor – dominated system, meanwhile the South sector is producing fluid from a liquid – dominated system. The field consists of 4 (four) upwelling centers and are increasingly younger towards the south. Manifestations in this field are fumarole, steaming and altered ground, acid – sulfate springs (Bogie et. al., 2008).

There are 5 (five) rock types in the Melebar region, when sorted by age of the youngest to the oldest age of rocks (Bogie et. al., 2008):

a. Volcanic Deposit Pakpakan

Located along the southern part of the Walawi caldera up to the Pakpakan Basin. Consists of sorted tuff, andesite, basalt, and pyroclastic. While the top part consists of pyroclastic rocks and laharic breccia called as mass waste deposit.

b. Old Walawi Volcanic

Spread almost all over the edge of the Walawi caldera, Consists of andesitic rocks and interspersed with volcanic breccia.

c. Young Walawi Volcanic

Distributed in the Walawi caldera that contains pyroclastic breccia, andesite, and volcanic breccia.

d. Two units of intrusive rocks (old and young aged)

Characterized by a dome that is mostly andesitic rocks.

Geological structure in the Walawi region are brecciation, fault zone, normal fault, and strike – slip fault.

3.1.1 Physiography

From its physiography, there are 3 (three) geomorphological units in the Geothermal Field “X”, they are:

a. Mount Walawi volcanic complex on the North sector

b. Mount Intan – Lani – Buri *massif* on the South – East sector

c. Pakpakan intermountain plateau, which unite Mount Walawi with the Southern area and Mount Intan – Lani – Buri with the West area.

There are two eruption centers, the Northern eruptive center that consists of Mount Walawi and Mount Gigan, meanwhile the Eastern eruptive center consists of Mount Intan and Mount Lani.

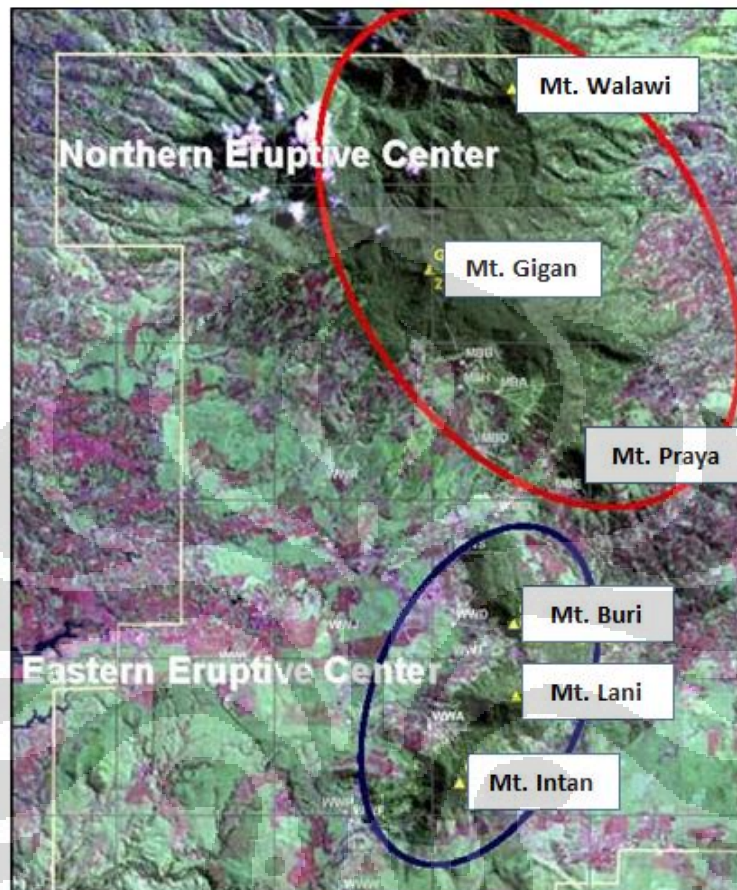


Figure 3.3 Volcanic Eruption Center Geothermal Field “X”

3.1.2 Fault Distribution

The main fault on the South is facing towards North – East and North – Northeast. Meanwhile on the North the fault is facing towards Northwest – Southeast. There are also faults facing towards Northwest – Southeast that is believed to represent minor horst and graben that disrupt the fault facing North – East. This horst indicates the possibility of block with low permeability, separating the reservoir into several smaller reservoirs (*Mandala Nusantara Ltd, 1997*).

3.1.3 Surface Manifestation

Digo crater (in the Northern area) and Intan crater (in the Southern area) are fumaroles that indicate that the steam is from the inside of the reservoir. Altered ground spreading across the East until the Northern sector of the Geothermal Field "X". Fumarole is an indication of an upflow zone, meanwhile steaming and altered ground, also acid - sulfate springs are indication of outflow zones. The absence of chloride water is indication of steam or vapor dominating the reservoir at geothermal Field "X"

3.1.4 Stratigraphy

Rocks that lie beneath the geothermal Field "X" are rocks results of andesitic stratovolcanoes, which contain lava flows, flow breccias, lahars, and several pyroclastic rocks in form of tuffaceous breccias, massive lapilli, and crystal tuffs. In the reservoir, there are indications of intrusive rocks in form of microdiorite and dolorite dikes.

Based on the regional study, the Jambang formation consists of tuffaceous sandstone, pumice tuff, clay stone, conglomerate, and lignite. They are the regional basement rocks of the reservoir aged Tertiary. It is then intruded by Tertiary aged quartz diorite. Meanwhile the reservoir rock consists of Waringin formation volcanic complex and/or Pakpakan formation aged between Pliocene until early Quarternary. On the Northern part, the rocks of the reservoir and Walawi formation are the same age. The stratigraphic cross - section of Field "X" can be seen in **Figure 3.4**.

Volcanic rocks are generally very complex and are not easy to correlate form one well data to another. So the interpretation is best done by classifying the rocks into the same origin of facies. To correlate the rocks at the subsurface of the andesites stratovolcano structure, Bogie & McKenzie (1998) facies model is used.

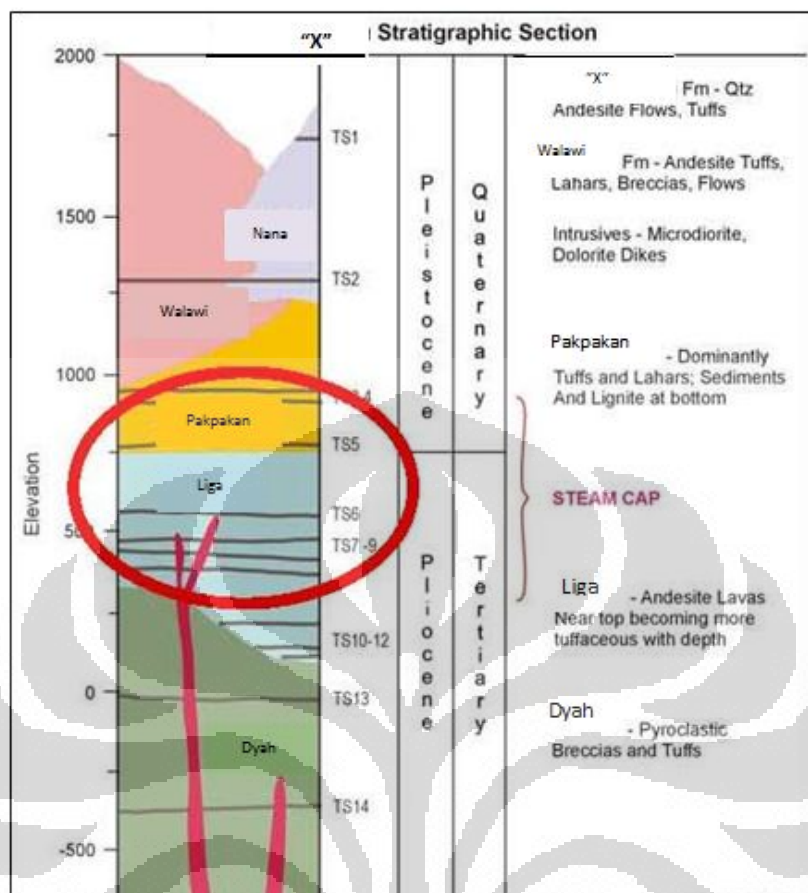


Figure 3.4 Stratigraphic cross – section of Geothermal Field “X”

3.1.5 Alteration

Rock alterations found on the drilling data are in form of argillic at a relatively shallow depth and overlaying prophylic. On the Northern part, the Southern part of Mount Gigan, epidote has a temperature above 240°C . Meanwhile on the South, the Western part of Mount Intan – Lani – Buri, epidote found has a temperature approximately 270°C . this is because the Southern part is warmed up or because of the high content of gas in the reservoir.

Alteration of rocks that become into argillic are a collection of smectite mineral, mixture of smectite – illite, and mixture of smectite – chlorite together with calcite, chalcedony, quartz, and pyrite. It overlies the reservoir acting as the cap rock to the reservoir because of its low permeability.

3.1.6 Porosity of Reservoir Rock

Geothermal Field “X” has average lava porosity of 1%, meanwhile the average porosity of lapilli tuff 7.5%. Tuffaceous rock is a kind of reservoir rock that is dominant and distributed evenly besides the amount of neither lava flows nor brecciated lavas.

3.1.7 Permeability of Reservoir Rock

The permeability of moderate to high is located at depth between – 250 mbsl until -500 mbsl. The permeability is a result combination from fractures and also permeability near intrusive rocks. On the South – East (Intan – Lani – Buri) there is a clear connection between the distribution of domes and the geothermal potential located here.

3.2 Geophysics

3.2.1 Result of Gravity Method

The use of the gravity method is to identify the depth of the basement, major fault structures, and depth location of the intrusive bodies. The result of this method can be seen on **Figure 3.5** where there are two gravity anomalies with positive value or high density at the geothermal Field “X”.

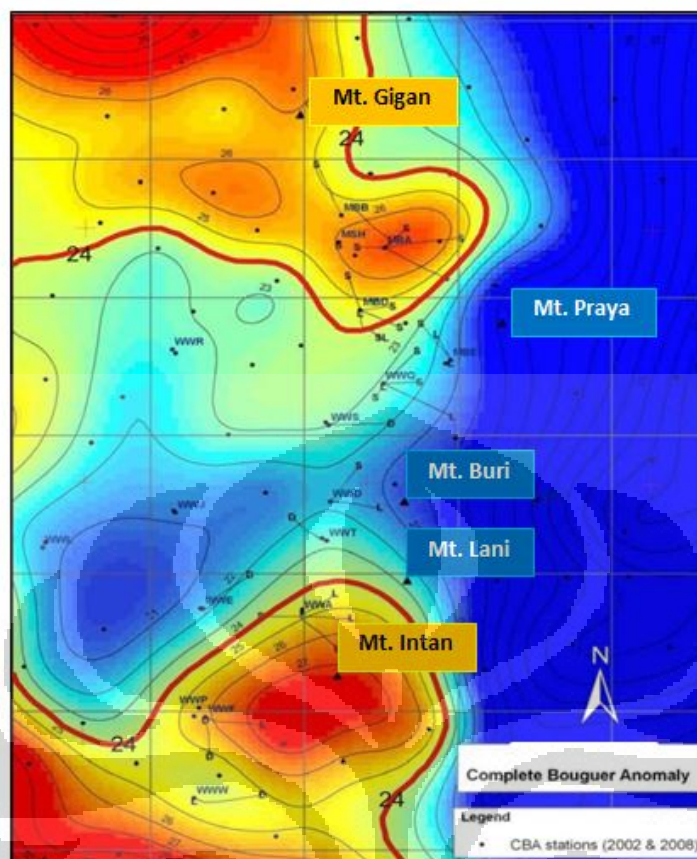


Figure 3.5 Anomaly Bouguer contour of Geothermal Field “X”

The first anomaly covers the area of Mount Walawi until Mount Gigan is constantly lengthwise until Mount Praya where geologically is the same or in accordance with the Walawi volcanic complex. Meanwhile for the second anomaly covers Mount Intan – Lani – Buri where geologically fitted with the Intan – Lani – Buri massif. The transition between the two anomalies is located on the Northern part of Mount Buri.

From here we can see the two geothermal systems are separated by a low anomaly gravity structure near Mount Buri which is then called Buri horst. Horst is a self - sealing low permeability body, at first it has moderate to high permeability, but as time goes because of hydrothermal process there are accumulation of mineral deposits that are able to drop the permeability value of this area.

3.2.2 Result of Magnetotelluric (MT) Method

Low resistivity model ($< 5 \Omega\text{m}$) shows high distribution of hydrated smectite clay formed by low – temperature hydrothermal alteration along the reservoir boundary. Fluid causing these alterations comes from ground waters of the geothermal system that contains gas.

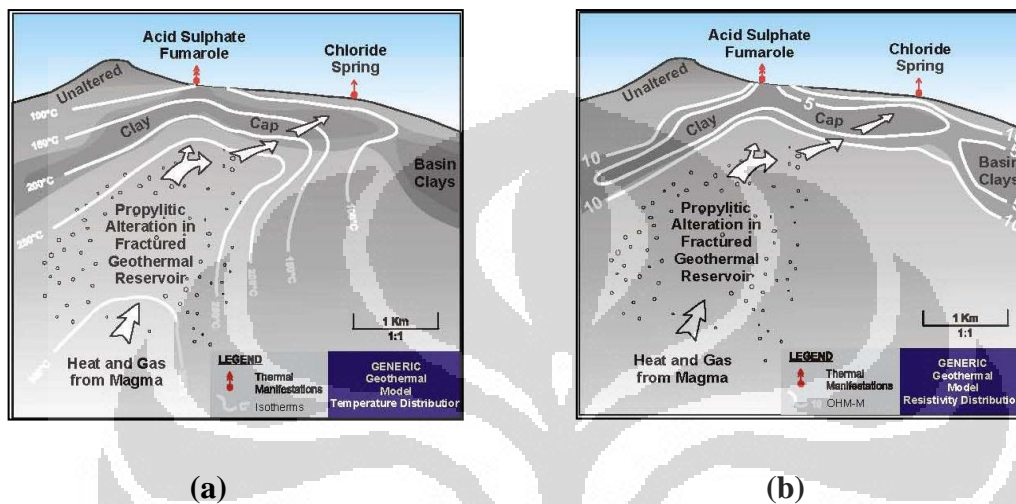


Figure 3.6 Illustration (a) Temperature distributin, clay alteration, and thermal Features on Geothermal System; (b) Conceptual element used on the Integrated Interpretations of MT-TDEM Resistivity, Geology, and Geochemistry (Star Energy, 2012, pers. comm.)

Magnetotelluric (MT) survey is the only method that can effectively plot the variation of resistivity value distributed in a geothermal field from near the surface until depth of thousand meters beneath. The resistivity value is influenced by formation parameter such as lithology, alteration, content and type of fluid, and temperature. At geothermal Field “X”, it is a type of system located in a volcanic area where the reservoir has high temperature (convective) characterized by prophyllitic alteration and has high resistivity compared to the cap rock who is characterized argillic alteration.

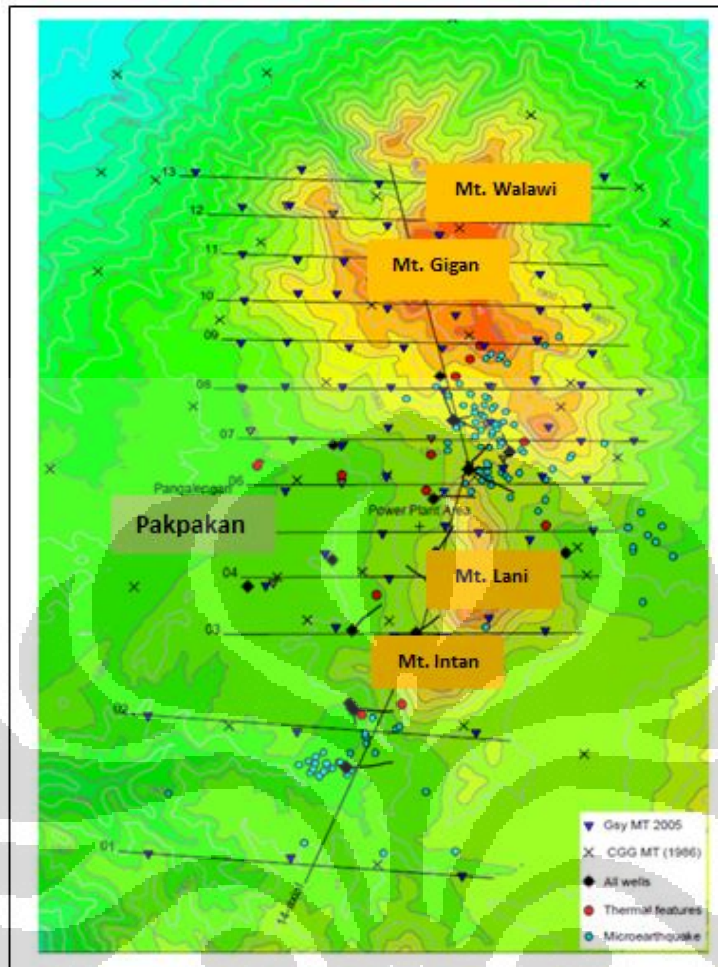
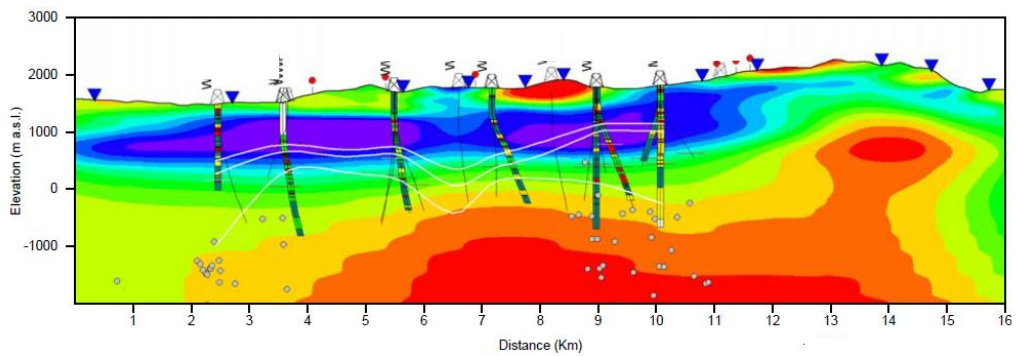
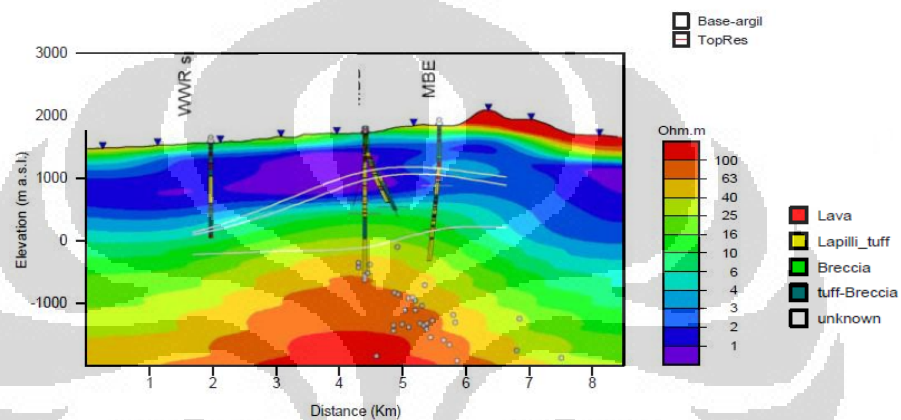


Figure 3.7 Distribution of MT stations on topographic map of Geothermal Field “X”
(Star Energy, 2012, pers. comm.)

From the modeling, we obtain that the reservoir of geothermal Field “X” has a symmetrical form seen from the vertical slicing East – West with conductive layer distributed on the West and East side, thickening towards the North. The base of the high resistivity zone is predicted to be at depth less than 12 km.



(a)



(b)

Figure 3.8 Resistivity cross - section: **(a)** North – South, **(b)** East – West profile 7. With isotherm 225, 250, dan 275^oC (White coloured contour)
(Star Energy, 2012, pers. comm.)

Low resistivity layer as shown on **Figure 3.9** consists of 3 (three) anomaly area located at high elevations, Mount Gigan toward the North, Mount Praya towards Northwest, and Mount Lani – Buri towards the West. These areas are interpreted as the upwelling thermal fluid at shallow depth (Bogie, 2008) which is acting as the cap rock of geothermal Field “X”.

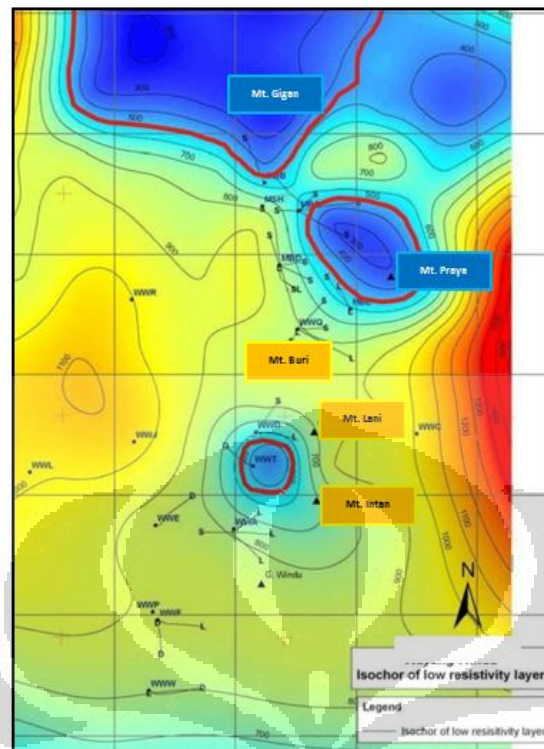


Figure 3.9 Cap rock marked by red line
(Star Energy, 2012, pers. comm.)

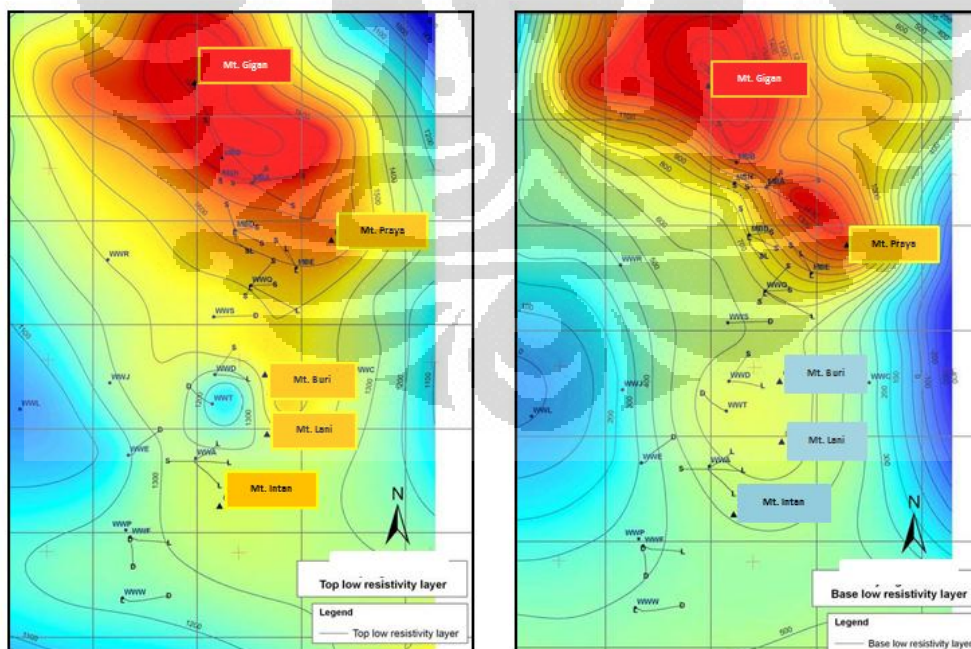


Figure 3.10 (a) Top Elevation and (b) Base Elevation of Low Resistivity Layer
Geothermal Field “X”
(Star Energy, 2012, pers. comm.)

3.3 Geochemistry

From the geochemical analysis from the existing surface manifestation, we can conclude that:

- a. Not many surface alterations are found on the geothermal Field “X”.
- b. Surface manifestations are dominated by steam condensate spring dan fumarole.
- c. Geothermometer shows the temperature of reservoir is not more than 210°C.
- d. Cilayu spring is the only surface manifestation that has neutral pH.
- e. Stable isotope compositions are stable at the springs indicates that the thermal waters are in form of meteoric water with addition of magmatic water and magmatic vapor.

Meanwhile from geochemical analysis of borehole data, we can conclude that:

- a. Plotting of enthalpy towards chloride indicates upflow exist beneath well pad ME and well pad WA and the fluid will change phase into steam at well pad WQ and MD.
- b. Calculation from geothermometer indicates that the reservoir has temperature around 220°C at well pad ME and WQ, but has low temperature at well pad WA.
- c. Ratio of B/Cl at well pad WQ and ME are the same (0.04 – 0.2), different from the fluid from well pad WA (B/Cl = 1.2) and well pad MD (B/Cl = 11.2). These 3 (three) values indicate the existence of three thermal fluid systems.
- d. Plotting of CO₂, CH₄, and H₂S as shown of **Figure 3.11** indicates boiling occur when fluid flows from well pad ME towards well pad MD and WQ. These shows the wells at WQ pad, WD pad, and WA pad are at the marginal of the system. In addition, input of magmatic fluids is from the WQ well pad.

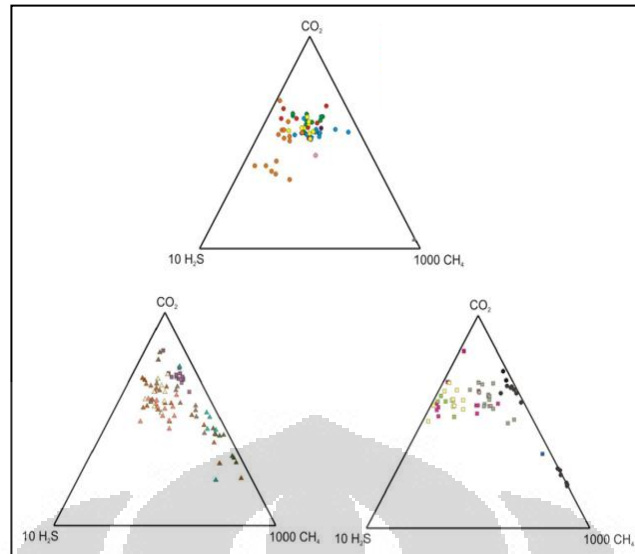


Figure 3.11 Plotting of CO_2 - CH_4 - H_2S from a several wells at Geothermal Field “X”

From the result of geochemical analysis of altered rocks, we can conclude that:

- a. There are 2 (two) geothermal system indicated by alteration model occurring on geothermal Field “X”. On the Southern part, dominated alterations are in form of clay who is acting as the cap rock and that there is epidote domination at the reservoir. Meanwhile, on the Northern part clay mineral is associated with calcite that also acts as the cap rock. Calc silicates (actinolite) which are found with epidote at the reservoir indicate content of CO_2 in the thermal fluids heading north.
- b. Mineral geothermometer shows the reservoir having temperature of 250°C . On the Northern part, the temperature of the reservoir is relatively higher.

3.4 Conceptual Model

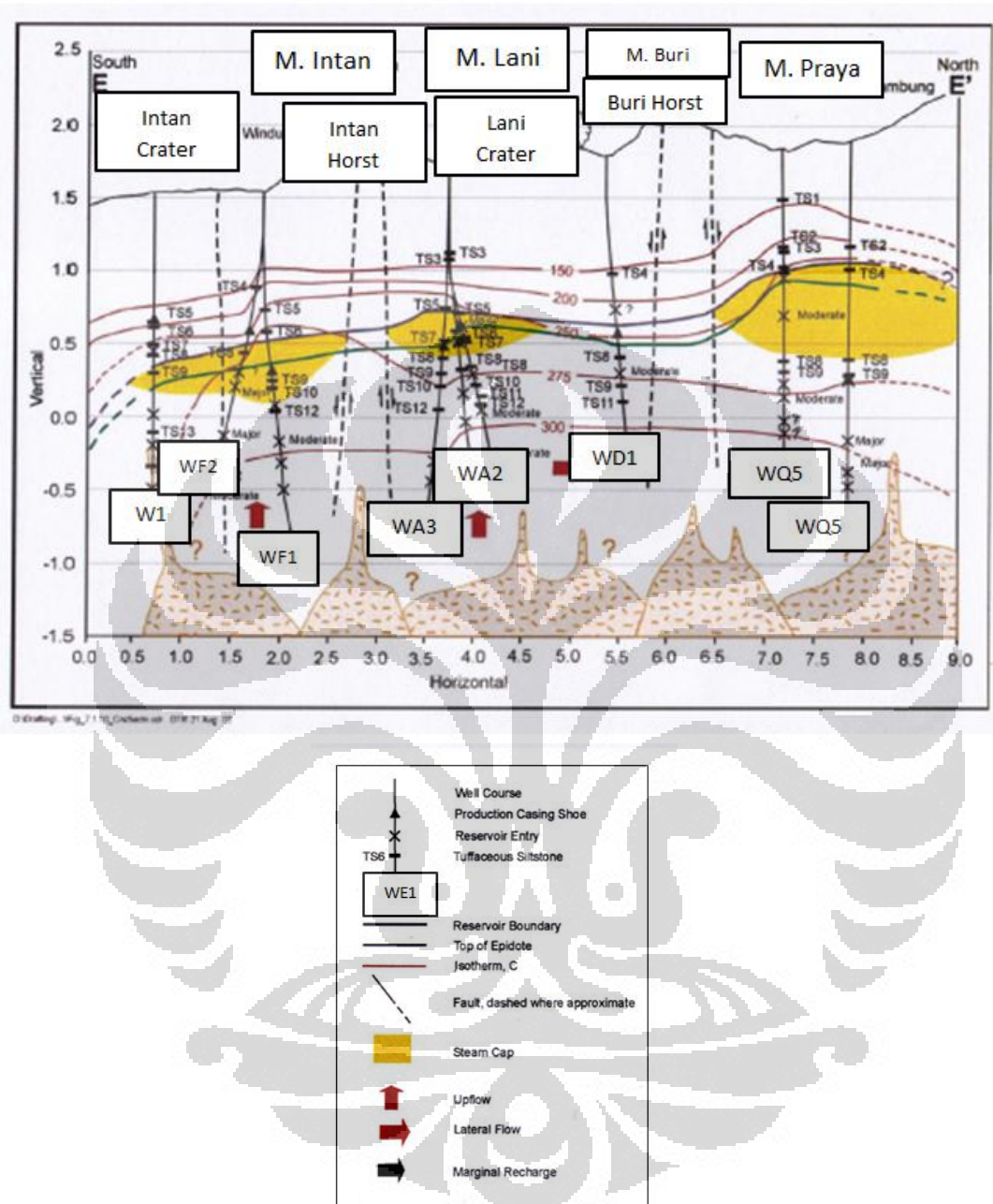


Figure 3.12 Conceptual Model of Geothermal Field “X”

3.4.1 The Cap Rock Layer

The strata on top of the two - phase layer are the cap rock (layer). The layer varies in thickness between approximately 1200 m in the southern sector and approximately 800 m in the northern sector. A thick low resistivity

layer ($< 2 \Omega\text{m}$) can be found in the lower half. It also contains thin layers of tuffaceous siltstones which vary in thickness between a few and several tens of meters. These layers can form the base of perched and leaky aquifers which are separated by undersaturated layers.

Chemical data of samples from the two-phase layer (tritium and non-equilibrated Mg values, for example) indicate that minor water of meteoric origin can enter the two-phase layer. However, since all the known occurrences of this minor meteoric water are found in the vicinity of wells with overly shallow set or damaged casing no wide spatial configuration can be given for the inferred perched aquifers but a current numerical model should allow for some permeability throughout the whole 'cap rock'.

The area of this top layer could be extended to cover most of the area with the low resistivity ($< 2 \Omega\text{m}$) layer. Blocks defining the margin of the 'cap-rock' structure could be designed as inactive blocks. Some changes in permeability structure with depth will probably be required to obtain acceptable calibration matches. To reproduce some minor recharge by surface waters, the inferred setting of stacked perched and leaky aquifers (separated by desaturated layers) could be modeled by using a horizontal permeability around 1.10^{-15} m^2 with an order of magnitude lower value for the vertical permeability.

3.4.2 The Two Phase Layer

The lateral extent of the layer will increase slightly to the west in the north and central sectors. However, its thickness will decrease, probably attaining a wedge - shaped (cross-sectional) structure towards the Western boundary. A wedge - shaped boundary could also restrict this layer to the east of the northern sector. The western extent of the west-lobe in the micro-gravity map is difficult to reconcile with any mass withdrawal from a vapor layer which may not exist in that area.

3.4.3 The Brine Layer

The brine layer can now be redefined as the layer of variable thickness saturated with hot, high density brine which lies between the bottom of the two-phase layer (or bottom of the cap-rock layer where the two-phase layer has not been developed) and the top of hot, but probably cooling crustal intrusive which are associated with the deeply seated, almost N-S elongated high resistivity structure that is recognizable in all MT soundings. This layer exhibits some permeability as indicated by the capacity of slugs of injected, cool condensates to move downwards into this layer and the deeper heat source rocks.

The rather high permeability of $50 \times 10^{-15} \text{ m}^2$ as used in model 1 for this layer could be retained but allowing also for the actual density of the hot brine (containing up to 30 g/kg dissolved solids) which affects buoyancy. The brine layer could be extended laterally beyond the adopted boundary of the cap-rock layer. Matching of temperature-pressure profiles of wells standing in the brine layer but located outside the 'vapor' layer could provide control for the heat and mass transfer parameters of this layer.

3.4.4 The Heat Source

The likely extent of the deep heat source is inferred from deep MT resistivity data consisting of the area enclosed by the $> 50 \text{ } \Omega\text{m}$ contour at 2 km depth below sea level. A wide-spread low ($< 2 \text{ } \Omega\text{m}$) resistivity layer between 0.6 to 1 km depth (the 'conductor') covers large parts of the "X" field prospect although it did not develop (or has been modified in response to the system boiling off) fully beneath the M. Lani, M. Gigan, and M. Walawi areas. The 'vapor-layer' is sandwiched between the low resistivity conductor containing highly conductive, thermal alteration (clay) minerals and a deeper, brine-saturated substratum which exhibits resistivities that increase with depth, also called the 'resistor'. The substratum is saturated with hot brine with $T > 300^\circ\text{C}$ at approximately 2 km depth and contains up to approximately 30 g/kg dissolved solids (TDS) in deep wells standing in the central sector of the field. Boiling of brines near the top of the substratum

produced in the vapour which accumulated in the 'two-phase layer'. Boiling over long periods increased the TDS content of the deep brines which have attained 'brine' characteristics.

The bottom level of the heat source structure is not known but to satisfy proportional constraints, it could be assumed to occur at -3 to -4 km depth below sea level with its ridge reaching - 1 km depth. Beneath G. Malabar the top might occur at sea level. The permeability of the structure has to be low to stop convective flow within the structure and to transfer most of the heat at the top by conduction into the 'brine'-layer. The value of approximately $0.2 \times 10^{-15} \text{ m}^2$ as used in model 1 appears to be a good estimate although the inferred conductivity of 2 W/m.K appears to be too low and the inferred porosity (0.07) too high but both parameters have little effect on the dominantly conductive heat transfer at the top of the heat source structure which should be able to transfer up to 1 MWth/km^2 at the top. Whether the pressure at the bottom level has to be kept constant to maintain convection in the brine layer and boiling at its top has to be assessed by trial and error. A set of inactive blocks could be put around the heat source.

CHAPTER IV

WELL DATA AND RESERVOIR SIMULATION

4.1 Well Data

Geothermal system at Field “X” has 19 well pads distributed across the field from North to South. But only 4 well pads are used in curve matching, they are ME, WA, MD, and WF. In this well cross – section on **Picture 4.1** only 6 well data are available to see, MB - 1, MA - 4, MD - 4, ME - 1, WQ - 5, and WQ - 1. Well pad MB only has one well to its pad, MB - 1, with elevation around 2,000 masl. Well pad MA consists of 4 wells with elevation of 1,924 masl. Well pad MD also has 4 wells at elevation of 1,841 masl. Well pad WQ has 4 wells at elevation of 1,789 masl. Well pad ME has 2 wells at elevation of 1,850 masl.

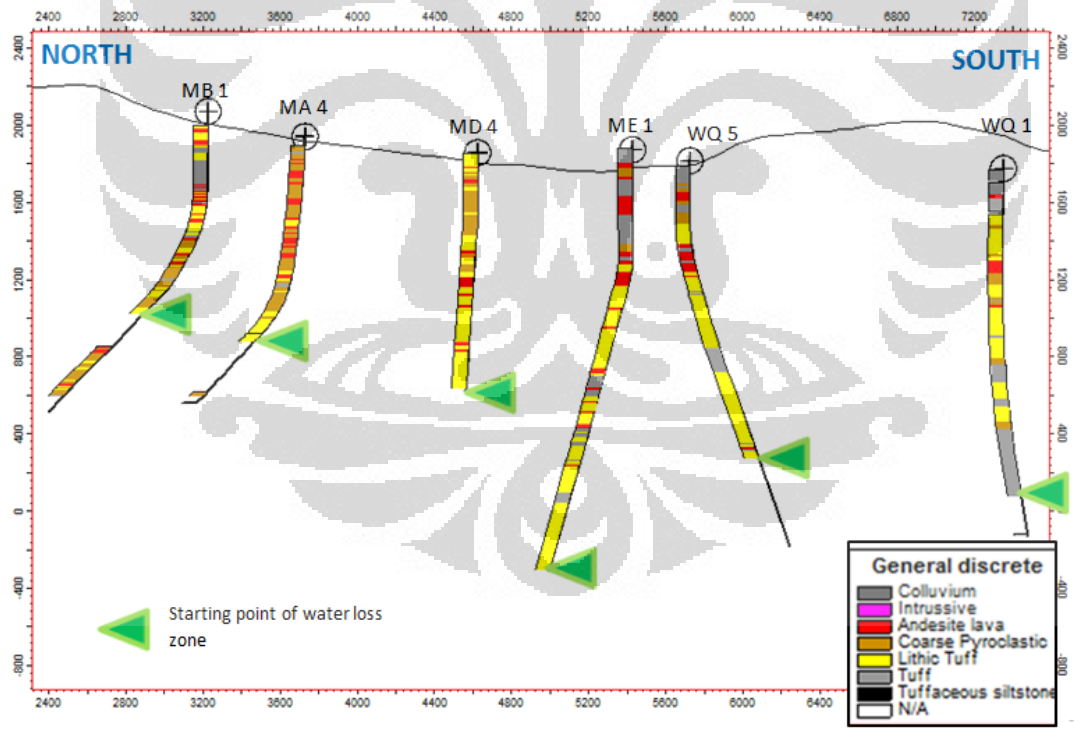


Figure 4.1 Distribution of lithology and location of water loss zones at geothermal Field “X”
(Star Energy, 2012, pers. comm.)

Based on the well data from **Figure 4.1** we can indicate that the lithology of area “X” consists mainly of volcanic rocks and only colluvium is a sedimentary rock that has been deposited. This can be said coming from the Pakpakan formation, where it is the only formation containing sedimentary rock. Volcanic rocks in this area are andesite lava, lithic tuff, tuff, tuffaceous siltstone.

Water loss zones are shown in the Figure where there is no lithology data obtain from the well. This is because at the water loss zone, the permeability is high so when drilling of the well with fluid, the fluid is transported into the layer of the zone. The lithology information is flushed out by the high permeability filled with drilling fluid. There are two types of water loss zones, partially and total loss zones. Partial loss zone means that even though the drilling fluid are caught inside the zone, by giving the well a certain amount of pressure fluid can circulate its way up of the drilling well again. For the total loss zone, the drilling fluid is still trapped in the zone even though added pressure is given into the well. This is an indication that the permeability of the zone in the subsurface has high permeability and can be a good path for fluid to flow through.

4.2 TOUGH2

TOUGH2 is a modified version the TOUGH2 (*Transport of Unsaturated Groundwater and Heat*) simulation program created by Lawrence Berkeley Laboratory.

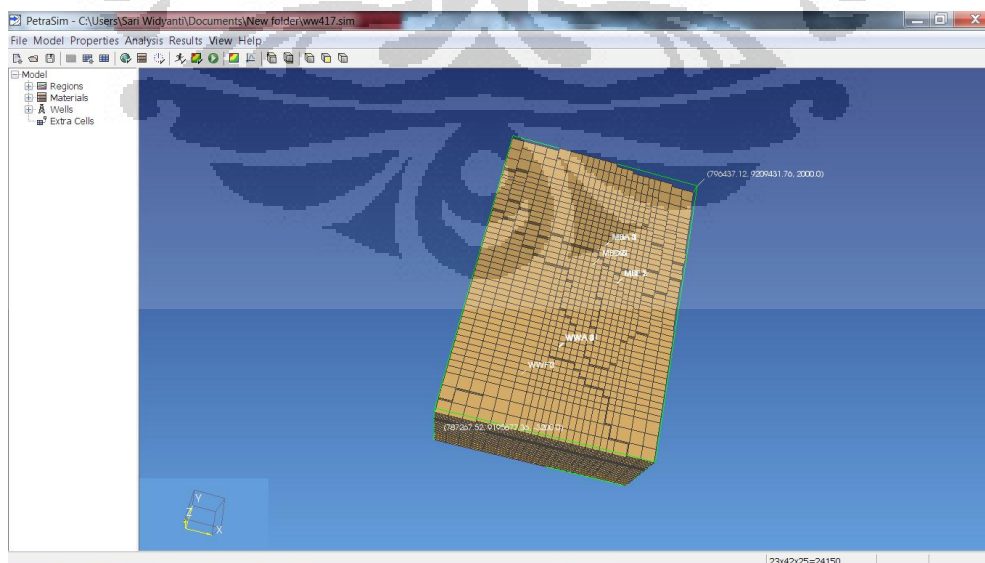


Figure 4.2 Main window TOUGH2

4.3 Simulation Process to Obtain Natural State of Reservoir

The simulation to obtain the natural state model of a reservoir needs to be done over and over again to fit with data geophysics, geology, geochemistry, and well data of the area. The simulation is being carried out by changing position and how big the enthalpy of the heat source, distribution of rock permeability, recharge area, and finally results of the simulation is matched with the well data.

The making of the model is based on the existing conceptual model. It uses distributed parameter approach where the system is being divided into several grids correlating to each other. Interaction of grids will affect the variation value of permeability, porosity, and fluid saturation in the reservoir, also the type of fluid contained.

Validation of the simulation process is done based on curve fitting of simulation results with well data from the field. The parameter to be matched here can be temperature towards depth, pressure towards depth, enthalpy towards depth, or production towards time. In this thesis, the author only does curve matching of temperature towards depth. Because the data available to be fitted with model is limited. Natural state of the model here is calibrated by curve fitting of 11 well data.

4.3.1 Boundary & Initial Condition

Boundary condition is defined in the simulation of the reservoir system. Base of the reservoir is located at depth of 1200 mbsl (layer 7). Heat source is considered to have constant temperature and pressure of 320°C and 160 bar located beneath the reservoir zone with large volume blocks. Boundary at the bottom layer is impermeable that has several blocks acting as the fluid recharge with high temperature. The system of the model is considered as a closed system because impermeable layer is surrounding the reservoir making it has a high temperature and high enthalpy system.

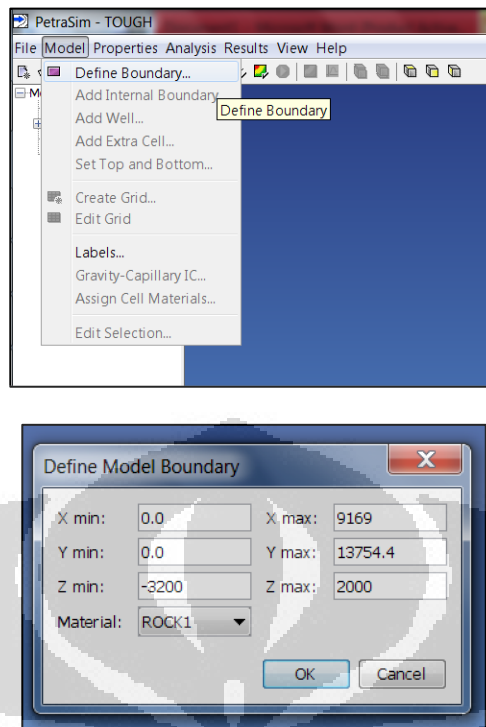


Figure 4.3 Boundary coordinates of the simulated system

Initial condition is assumed at initial hydrostatic pressure where natural heat source hadn't occurred. Input data of the initial condition will be saved in disc file SAVE and the process of calculation saved in disc file INCON.

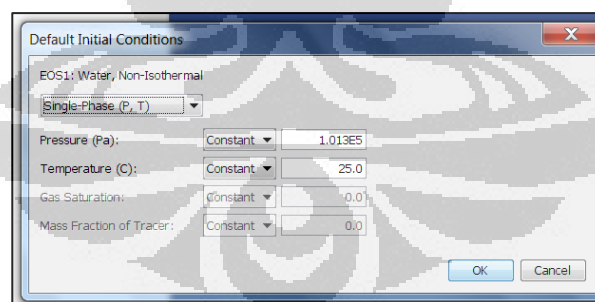


Figure 4.4 Initial condition

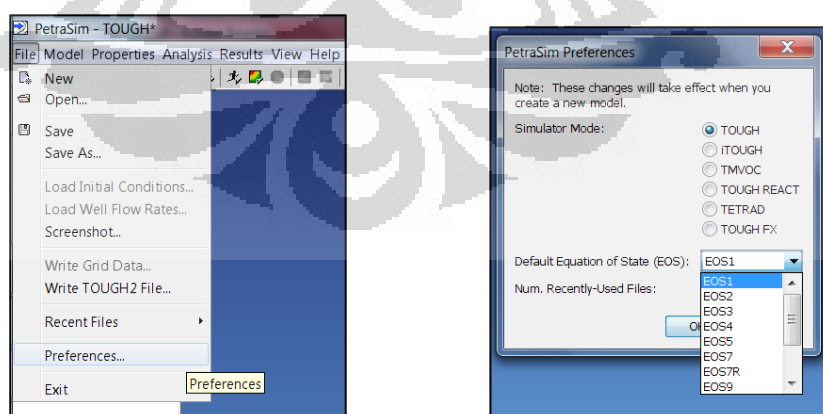
4.3.2 Equation of State (EOS)

There are several types of geothermal reservoir system, they depend on the condition of each phase also the variables affecting the reservoir such as pressure, temperature, mass fraction.

Table 4.1 Module EOS fluid (Atmojo, 2001)

Type of EOS	Explanation
EOS1*	water
EOS2	water, CO ₂
EOS3*	water, air
EOS4	water, air, low vapor pressure
EOS5*	water, hydrogen
EOS7*	water, <i>brine</i> , air
EOS7R*	water, brine, air, parent – daughter radionuclides
EOS8*	water, “dead” oil, NCG
EOS9	saturated isothermal flow variables based on Richard’s equation
EWASG*	water, NaCl, NCG
ECO2	water, CO ₂ , NaCl
T2VOC	water, air, volatile organic compound
TOUGH-FX	hydrates
TMVOC	water, air, volatile organic compound until it reach 19

*applies only on constant temperature state (Atmojo, 2001)

**Figure 4.5** Selecting EOS

4.3.3 Making the Grid

The geothermal system is modeled by the size of 9.17 km x 13.8 km x 5.2 km. It consists of 25 layers with varied thickness. The position and grid size is adjusted with existing conceptual model. The size of the grid will affect the result obtained from the simulation. The smaller the size of the grid, the more accurate the modeled area will be. The size of the grid is based on the position of the reservoir and fractures distributed in the area.

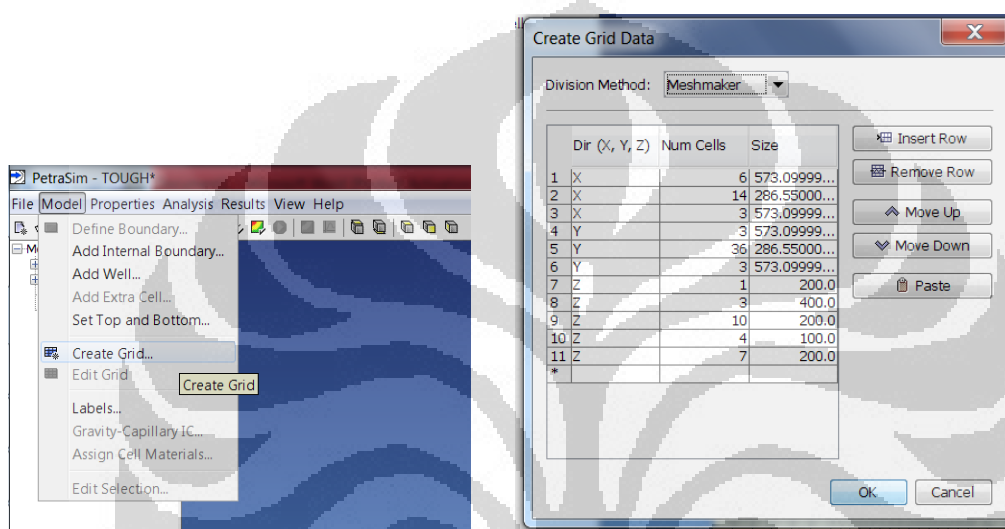


Figure 4.6 Making the grid with meshmaker method

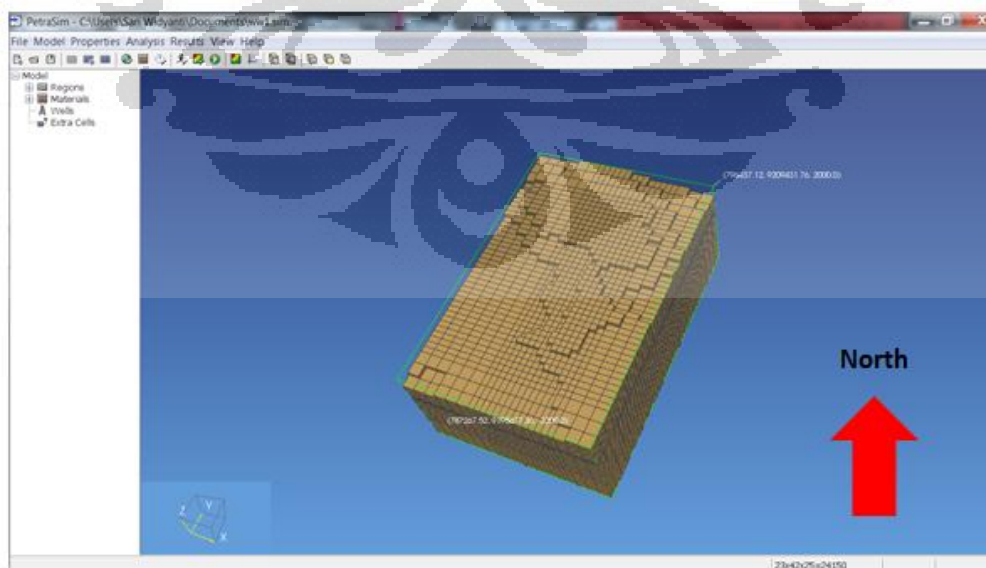


Figure 4.7 A grid view that has been made

4.3.4 Physical Parameters of Rocks

This simulation that has been done using TOUGH2 simulator has 17 types of rock materials as seen on **Table 4.2**. Each of these rocks has different characteristics that describe the location and condition of each grid. These material and their physical properties are obtained from laboratory analysis of core sampling from drilling wells.

Table 4.2 Rock type with each of their parameter for the simulation

Material Type	Rock Density (kg/m ³)	Porosity	Permeability (x 10 ⁻¹⁵ m ²)			Heat Conductivity (W/m ⁰ C)	Rock Specific Heat (J/kg/ ⁰ C)
			X	Y	Z		
Caprock	2500	0.05	0.001	0.001	0.001	2.0	1000
Formasi Walawi	2600	0.07	100	100	50	3.0	1000
Formasi Pakpakan	2600	0.01	80	80	30	3.0	1000
Formasi Liga	2600	0.1	20	20	5	2.0	1000
Formasi Dyah	2600	0.1	5	5	3	2.0	1000
AAA01	2600	0.07	1	1	0.5	2.0	1000
AAA02	2600	0.05	0.5	0.5	0.25	2.0	1000
AAA03	2600	0.05	0.1	0.1	0.06	2.0	1000
Buri Horst	2600	0.05	0.001	0.001	0.001	2.0	1000
BBB01	2600	0.05	50	50	50	3.0	1000
Heat Source	2600	0.07	0.2	0.2	0.1	2.0	1000
XX	2600	0.07	0.1	0.1	0.1	2.0	1000
FLT09	2600	0.07	10	10	5	2.0	1000
FLT01	2600	0.07	10	10	5	2.0	1000
FLT02	2600	0.07	0.1	0.1	0.1	2.0	1000
WQ	2600	0.07	10	10	2	2.0	1000
MWB	2600	0.07	20	20	10	3.0	1000

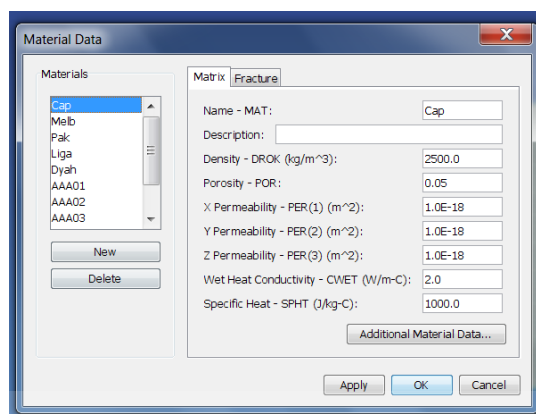


Figure 4.8 Input physical parameter of each material

4.3.5 Edit Grid

Here each grid is determined by what material is filled in based on the conceptual model that has been made before by integrating geological, geophysical, geochemical, and tied with well data.

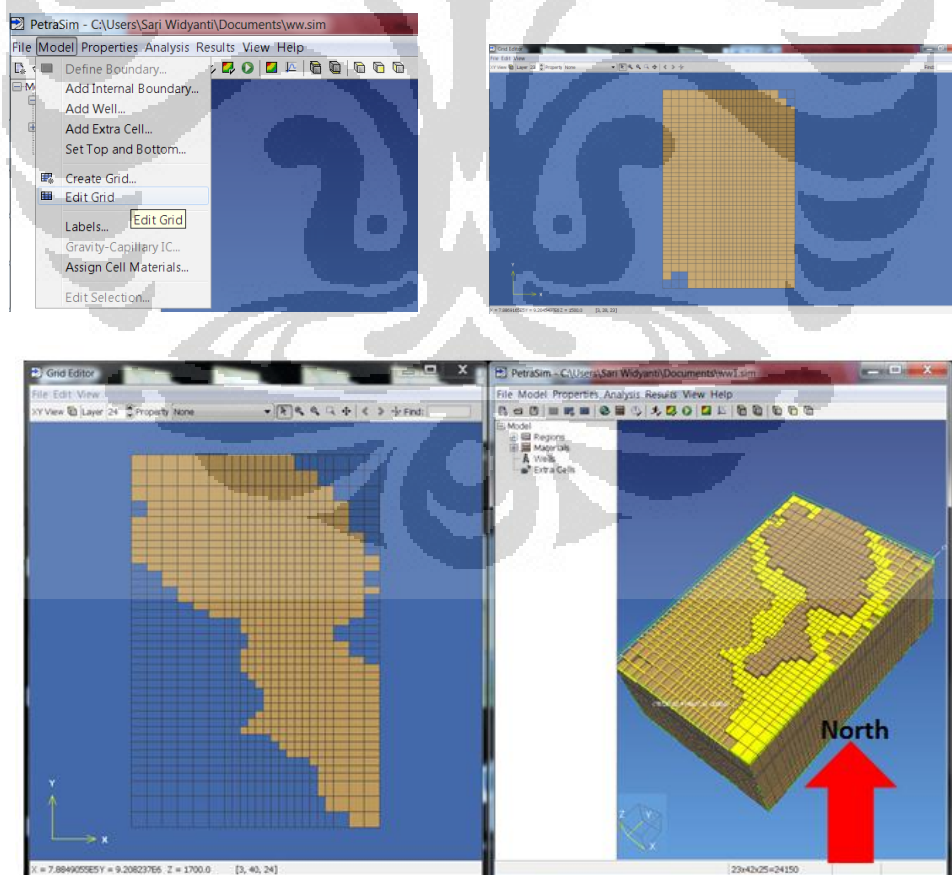


Figure 4.9 Edit of grid on each layer

4.4 Result of the simulation

Based on the result of the simulation, it is then plotted with temperature data from well to see if it has fitted or not. Comparing the simulated and well data will obtain RMS error for each curve fitting. Besides curve of temperature profile, we can also see layout block and vertical slicing to see the distribution of several parameters, such as temperature, material, pressure, gas saturation, rock density, permeability, wet conductivity, and specific heat.

4.4.1 Layout Block

Layout block can show the distribution of parameters that we wish to see on each layer. We can change the content depending on what physical parameter is to be shown.

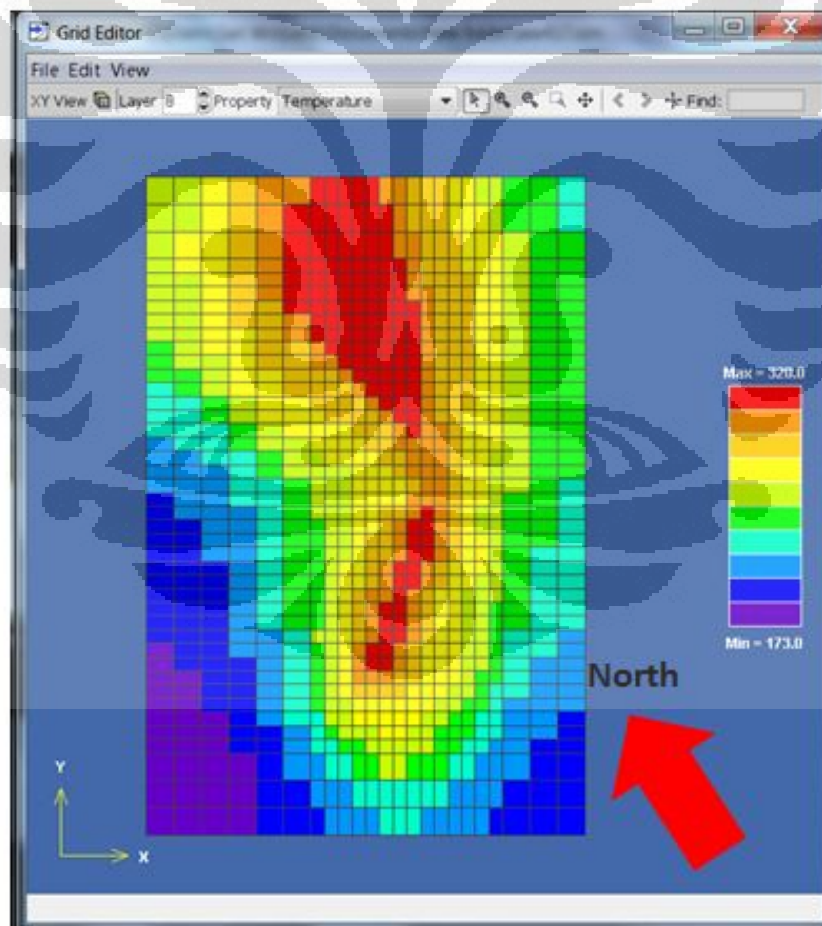


Figure 4.10 Distribution of temperature at Layer 8

4.4.2 Vertical Slice

On TOUGH2 we can also see vertical slicing or cross sectional part of the field, as shown on **Figure 4.11** we can see the distribution of temperature divided into two different reservoir, where the Northern part has higher temperature an closer to the surface, and the southern reservoir has more or less the same temperature but has lower depth to the surface. From the distribution of temperature we can already see the form of the reservoir being divided by low temperature which we can say it indicates the present of Buri horst.

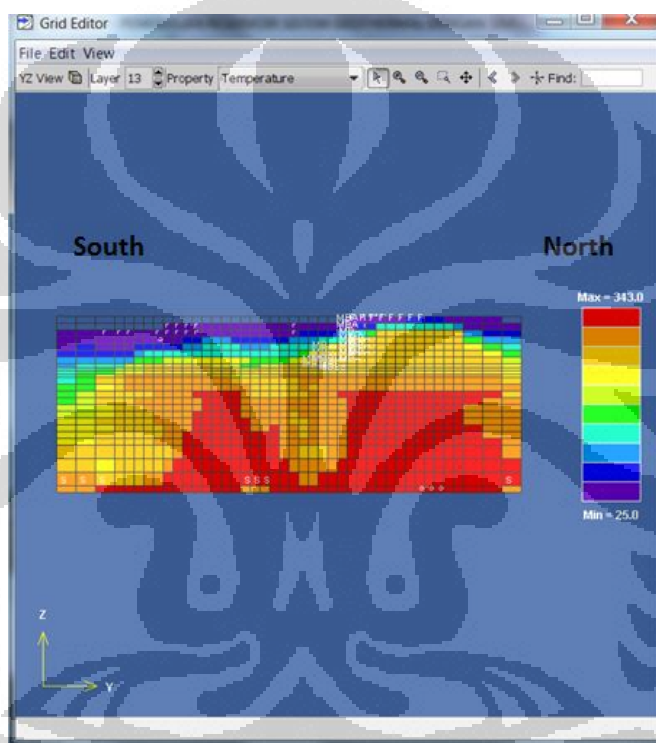
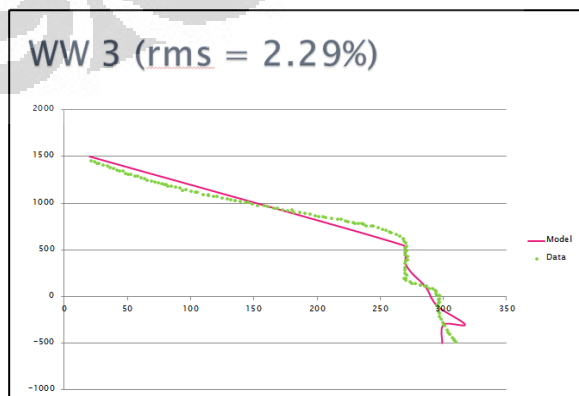
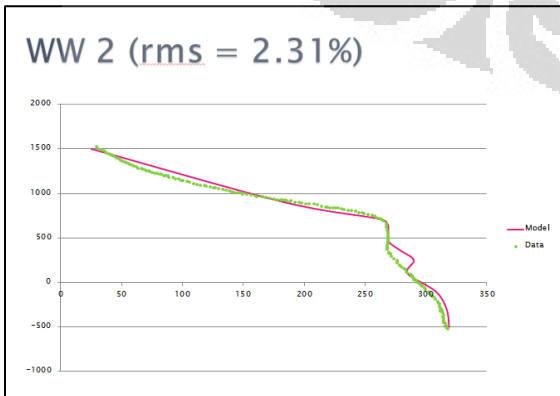
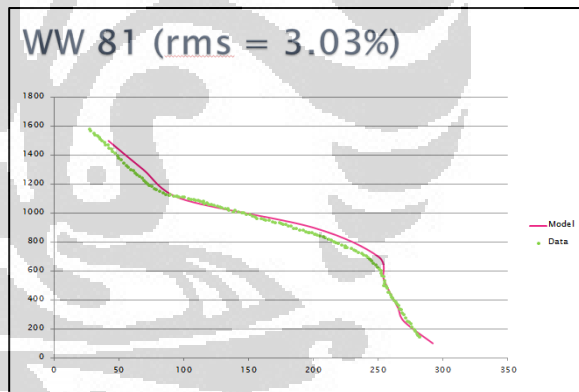
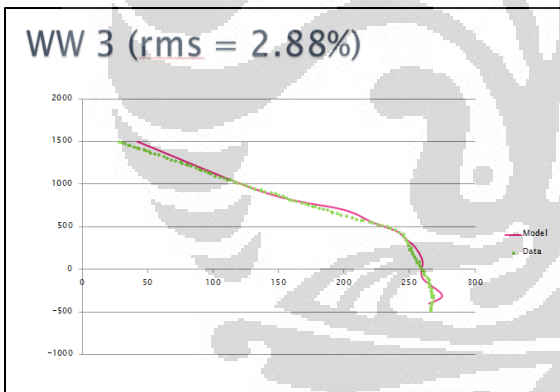
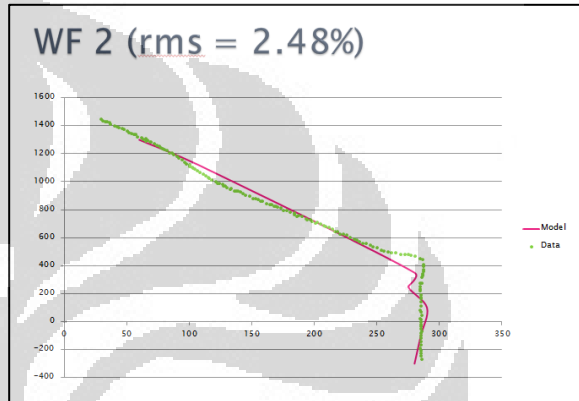
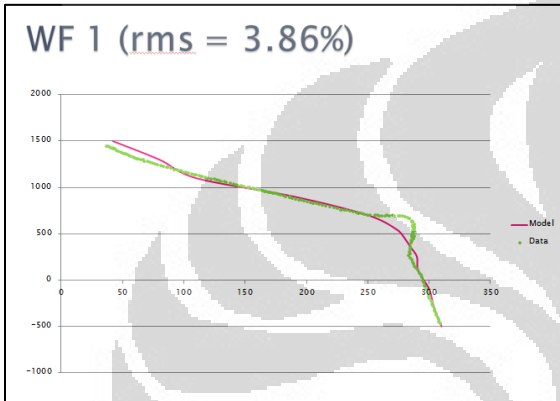
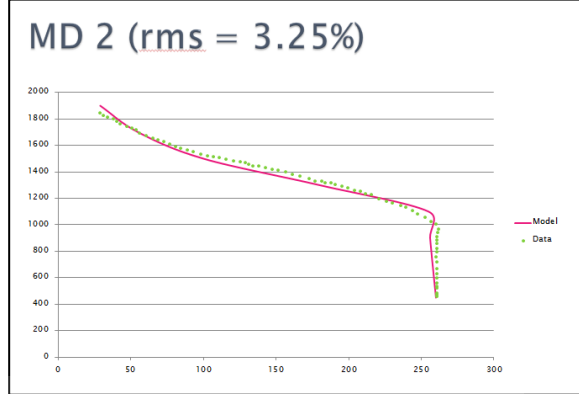
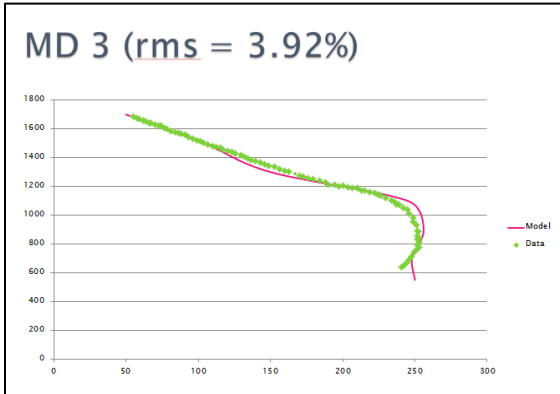


Figure 4.11 Distribution of temperature vertical slice view at Line 13

4.4.3 Temperature vs Depth Curve

The curve obtained from the simulation has the same trend of curve at **Figure 2.1** that shows that the geothermal system at Field “X” is a vapor – dominated system at the North sector. We can see from the trend of well curve MD – 4 and ME – 2 that is located in the west side of Mount Gigan. The closed system is making convection occur, sign of homogeneity of temperature towards depth. This is caused by the fluid inside the system is surrounded by impermeable rocks so no fluid can get out of the system.



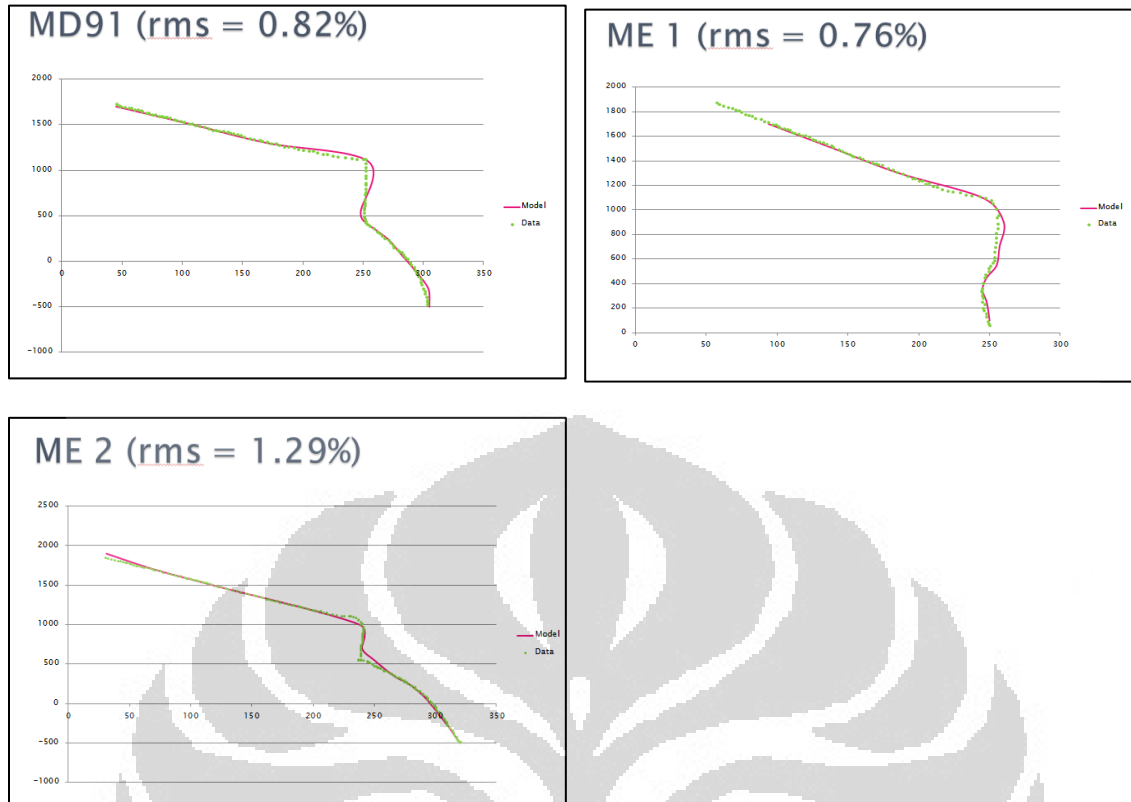


Figure 4.12 Curve matching temperature at natural state

CHAPTER V

RESULT AND DISCUSSION

5.1 Integrated Interpretation

The reservoir modeling is integrated with geological, geochemical, and geophysical data available, not to forget also cross – matching these data with well data. There is a difference between the geothermal system at Field “X” with the general andesitic stratovolcano geothermal system. The geothermal system at Field “X” consists of a few upwelling centers and the reservoir has two – phase. There are 3 (three) upwelling centers/convective cells near wellpad ME (Burung Crater), WA (most South area near Intan Crater), and WF (central or eastern area near Intan Crater) with the age of rocks becoming younger as we head into the South sector. Related to the shallow two – phase reservoir, even though geologically separated by Buri Horst structure, hydraulically they are permeable or connected as indicated from tracer results. The most southern part of the reservoir contains high gas saturation and called as the gas – vapor dominated *reservoir*.

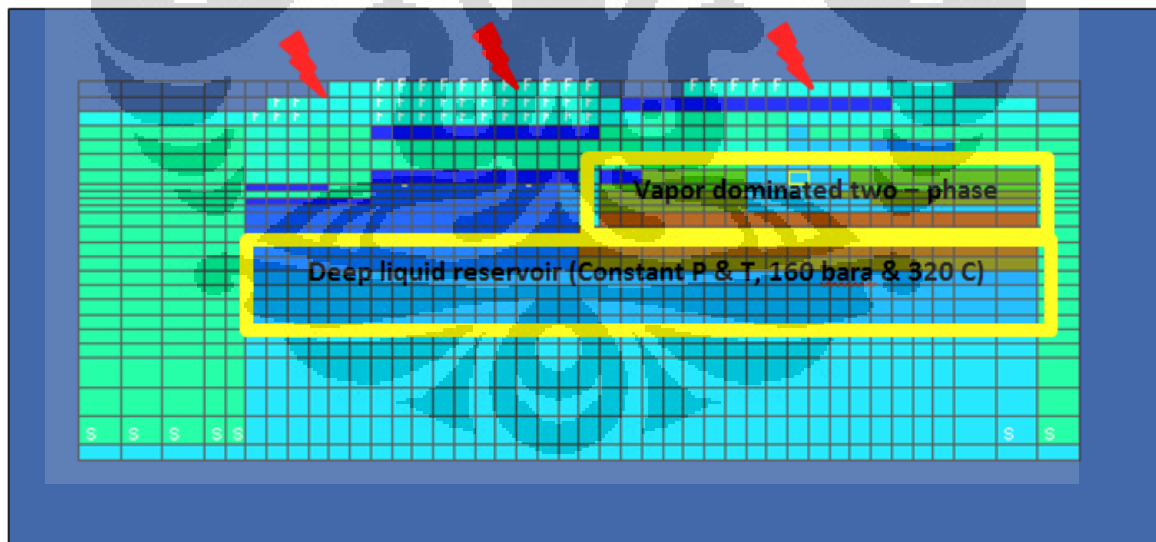


Figure 5.1 Geothermal Field “X” modeling description

Due to the increase thickness of the hydrothermal clay, the reservoir is closed tightly and has lateral permeability barriers as shown on **Figure 5.2**. The result of this is that the reservoir is isolated from recharge of meteoric fluid and has high temperature. Limits of recharging system means there are no convective cycle at shallow depths. From the mineral and chemical content of fluid shows fluid has boiled as decreasing of depth.

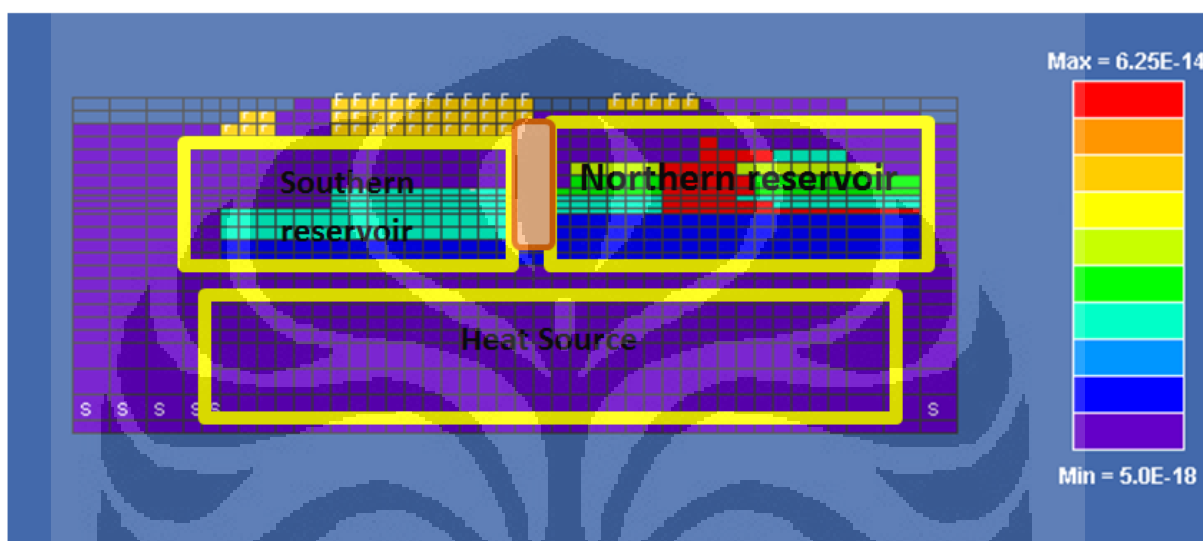


Figure 5.2 Reservoir surrounded by permeability barriers

From the distribution of permeability at **Figure 5.3**, high permeability is distributed at Mount Gigan until Mount Intan (colored red – orange), but is separated precisely on the location of where Buri horst exist separating the North and South reservoir at around the area of Mount Lani. The permeability of the reservoir is relatively high with range of 31 mD (millidarcy) up to 100 mD. If we are to extent and develop the reservoir, it is advisable to continue to the Northern part of Melebar area. This is advised is also supported by available microgravity data and shows there is ground subsidence occurring on the Northern sector. The reservoir itself is surrounded by low permeability rocks causing it as a closed system so heat and fluid is accumulated in the reservoir.

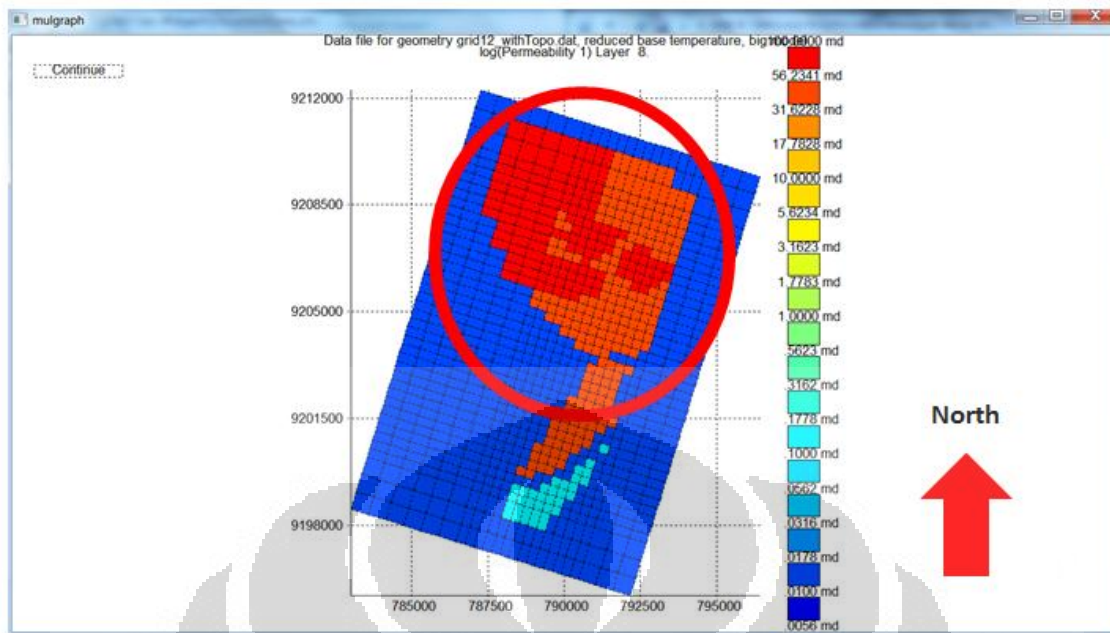


Figure 5.3 Distribution of rock permeability at Layer 8 using mulgraph

5.2 Vertical Distribution of Layers

5.2.1 Cap rock

Thickness is estimated to be around 1200m for the south reservoir and 800m for the north reservoir. This layer has low resistivity ($< 2 \Omega\text{m}$) and contains tuffaceous siltstones. In the model it is represented by material type AAA01 with permeability of $1 \times 10^{-15} \text{ m}^2$.

5.2.2 Two – phase Layer

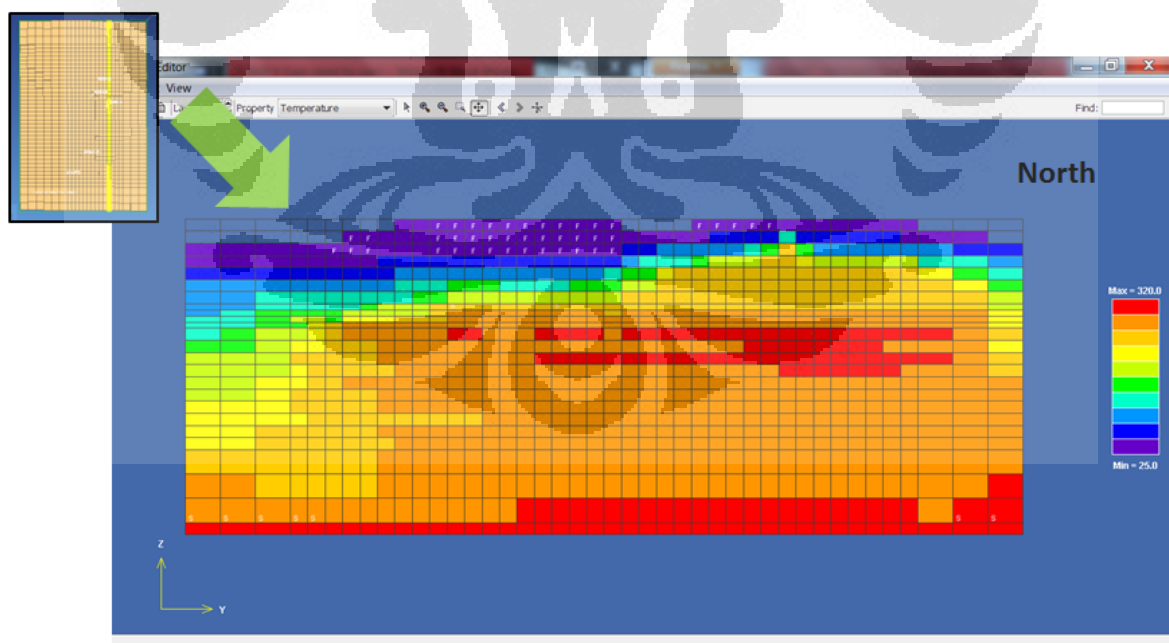
The lateral distribution of this layer is heading towards the west on the northern sector with their upwelling centers. The thickness of this layer decreases as the boundary at the west and also the east side of the northern sector. In the model it is represented by material type HIPER with permeability of around $1.25 \times 10^{-13} \text{ m}^2$.

5.2.3 Brine Layer

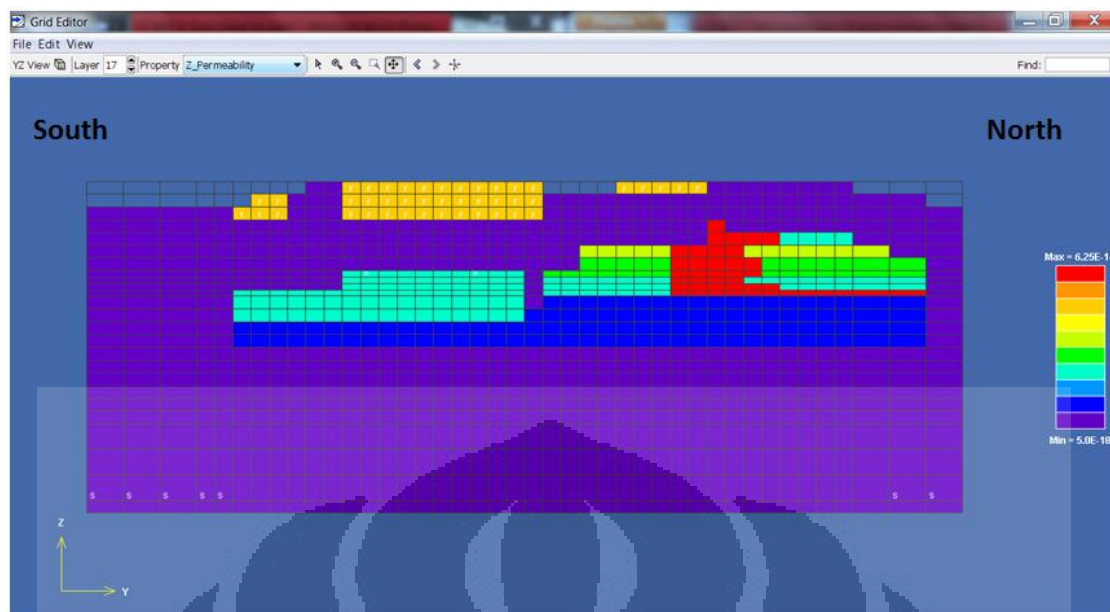
This layer is located between the cap rock and the two – phase layer. It is spread from North to South from the MT data. Has high permeability value ($50 \times 10^{-15} \text{ m}^2$) and the extension of this area is bigger than the extension of the caprock itself. But there needs to be other curve matching to be done outside the vapor layer so we can control the heat and mass transfer on this layer.

5.2.4 Heat Source

From MT data results we obtain that the heat source is surrounded by a resistivity contour of $> 50 \Omega\text{m}$ at depth of 2000 mbsl. It is predicted to have thickness of more or less 1 km at Mount Walawi area, and the top part of the heat source is above sea level depths. The permeability of the structure must have low value to be able to stop the possibility of convection flow and heat flow of conduction until it reaches the brine layer. The estimated permeability is around $0.2 \times 10^{-15} \text{ m}^2$. In the area of Digo Crater, we can say that this crater is connected directly to the heat source without any cap rock coverage.



(a)



(b)

Figure 5.4 Vertical Slice (a) Temperature & (b) Permeability North – South

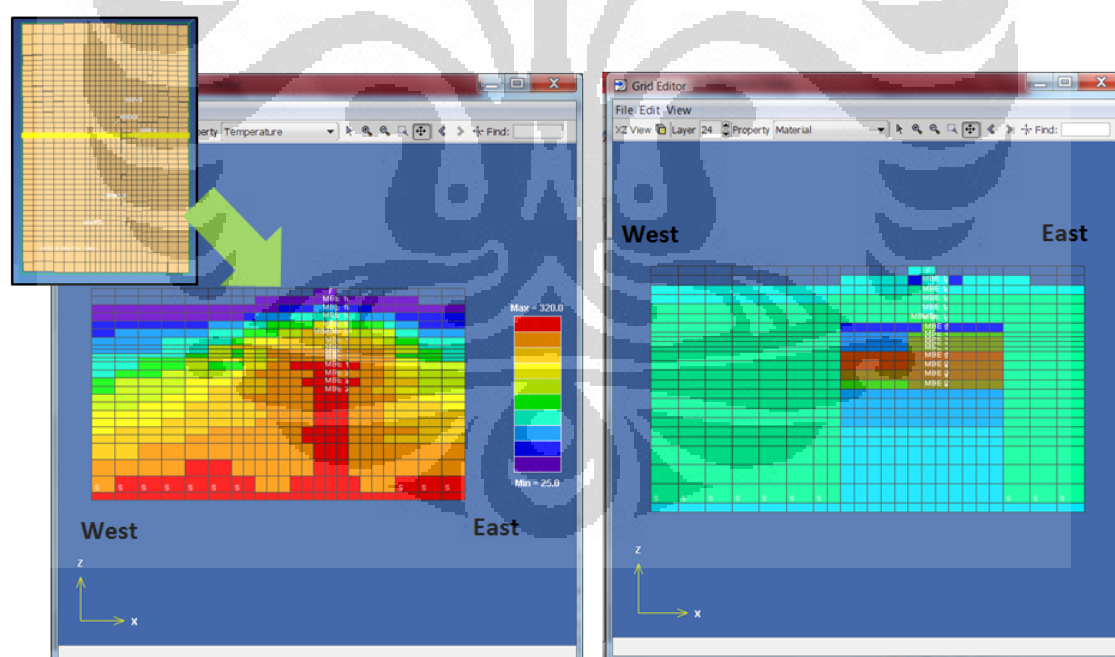


Figure 5.5 Vertical Slice Temperature & Permeability East - West

BAB VI

CONCLUSION AND SUGGESTION

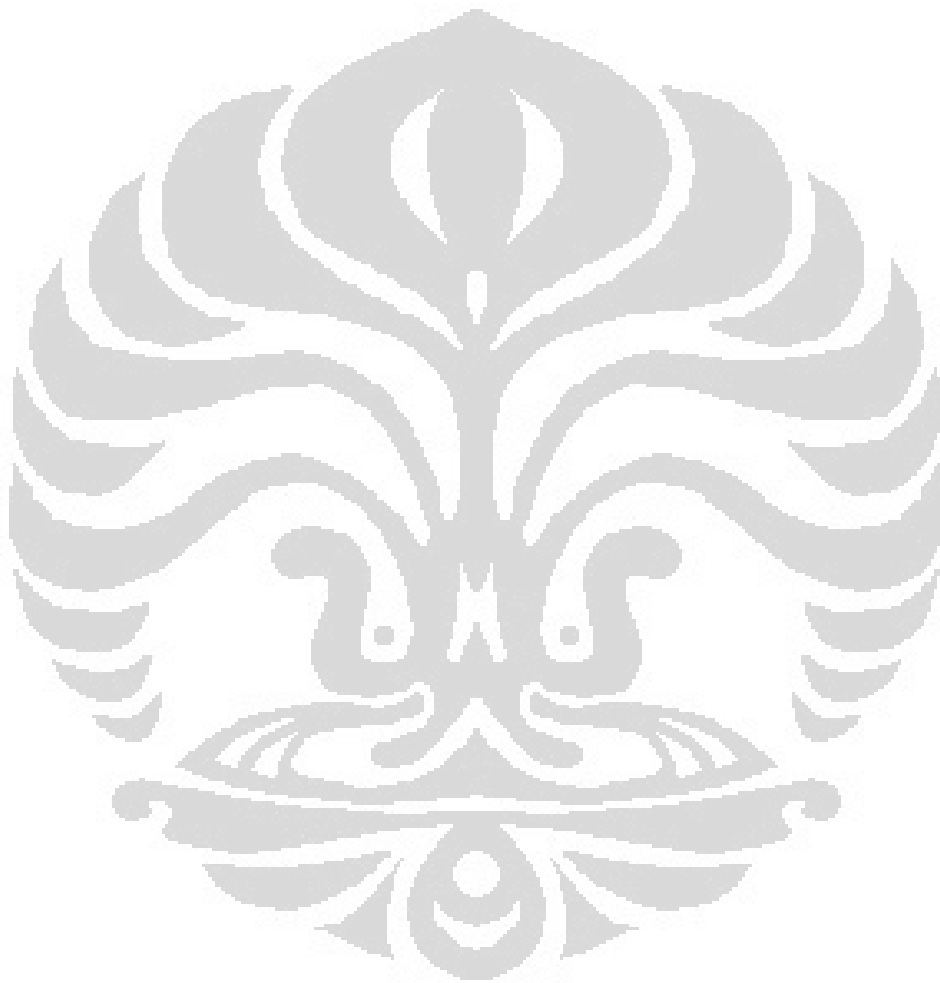
6.1 Conclusion

Based on the results of the research that has been done to obtain reservoir model of geothermal system, using simulator TOUGH2 and supported by geological, geochemical, geophysical, and also well data, it can be concluded that:

- ① Geothermal field “X” has reservoir with a transition from vapor – dominated in the northern sector (around Mount Gigan and Mount Praya) into liquid dominated system in the southern sector (around Mount Intan and Mount Lani).
- ① Heat source is to be found at depth of 2000 mbsl with a resistivity of $> 50 \Omega\text{m}$ available from MT data. Located around Mount Gigan and continuously to Mount Intan at elevation of 1500 mbsl. The center of the heat source is located under Mount Gigan and also between Mount Lani and Mount Intan.
- ① The geothermal Field “X” has 4 upwelling centers/convective cells. The indication of these upwelling centers are from the surface manifestation of fumarole.
- ① Hydrogeological of the system is upflow is known to appear around Mount Gigan, Mount Lani, and Mount Intan with manifestation form of fumarole and solfatara . meanwhile on the outflow manifestation appear in form of hot spring with bicarbonate sulfate in the east and South east sector.
- ① The geothermal system of field “X” has high permeability in the Northern sector around Mount Gigan and cut off by the Buri horst. High permeability is also found on the southern sector beneath Mount Lani and Mount Intan. The geothermal system is surrounded by a formation of low permeability acting as the boundary, making it a closed system.
- ① The heat source is located beneath the reservoir with temperature of 320°C and the average temperature of the reservoir is 257°C with extensive area of 40km^2 .

6.2 Suggestion

Development plan of the geothermal potential Field “X” better be focused on the northern area, above Mount Gigan where a two – phase reservoir is found above the brine layer. Besides that, ground subsidence occurring on the northern sector indicates the extension of the two phase layer. Temperature and production is good on the well MB – 1 (well located in the northern – most) is a good foundation of reservoir expansion up to Mount Walawi.



REFERENCE

- Bogie, I., Kusumah, Y.I., dan Wisnandary, M.C. (2008). *Overview of the Wayang Windu Geothermal Field, West Java, Indonesia*. *Geothermics* 37:347-365.
- Daud, Yunus. (2011). *Lecture Notes: Geophysical Monitoring*. Laboratorium Geofisika, F.MIPA Universitas Indonesia.
- Dewi, N. K. (2010). *Pemodelan Reservoir Sistem Geothermal dengan Simulasi Reservoir TOUGH2*. Skripsi. Universitas Indonesia, Depok.
- Finsterle, S., G. Bjornsson, K. Pruess, and A. Battistelli. (2000). *Evaluation of Geothermal Behaviour Using Inverse Modeling*, in B. Faybishenko, P.A. Witherspoon, S.M. Benson (ed.), *Dynamics of Fluids in Fractured Rock*, Geophysical Monograph 122, pp. 377 – 387, American Geophysical Union, Washington, DC.
- Keenan, J.B., Keyes, F.G., Bill, P.G. and Moore, J.G. (1969). *Steam Tables - thermodynamic properties of water including vapor, liquid, and solid phases* (International Edition - metric units): pp. 162. Wiley, New York.
- Mulyadi, Ashat A. (2011). *Reservoir Modeling of the Northern Vapor – Dominated Two – Phase Zone of the Wayang Windu Geothermal Field, Java, Indonesia*. PROCEEDINGS, Thirty – Sixth Workshop on Geothermal Reservoir Engineering, Stanford University, Standford, California, January 31 – February 2, 2011.
- Natural Renewable Energy Laboratory, DOE. Maret 1998.
- Newson, J., Mannington W., Sepulveda F., Lane R., Pascoe R., Clearwater E., O’Sullivan M.J. (2012). *Application of 3D Modeling and Visualization Software to Reservoir Simulation: Leapfrog Geothermal and TOUGH2*. *Thirty – Seventh Workshop on Geothermal Reservoir Engineering: SGP – TR – 194*. California: Stanford University.

Pruess, Karsten. (2002). *Mathematical Modeling of Fluid Flow and Heat Transfer Geothermal Systems – An Introduction in Five Lectures*. Lawrence Berkeley National Laboratory, University of California.

Ramey, H.J. Jr. (1977). *Petroleum Engineering Well Test Analysis – State of the Art*. Lawrence Berkeley National Laboratory, University of California.

Sigurdsson, Haraldur., et al. (2000). *Encyclopedia of Volcanoes*. Academic Press. A Harcourt Science and Technology Company.

Singarimbun, A., Irsamukhti, R., dan Bujung, C.A. (2011). Estimasi Distribusi Temperatur, Entalpi, dan Tekanan dalam Reservoar Panasbumi. *Material dan Energi Indonesia* 01: 31 – 39. Universitas Padjadjaran.

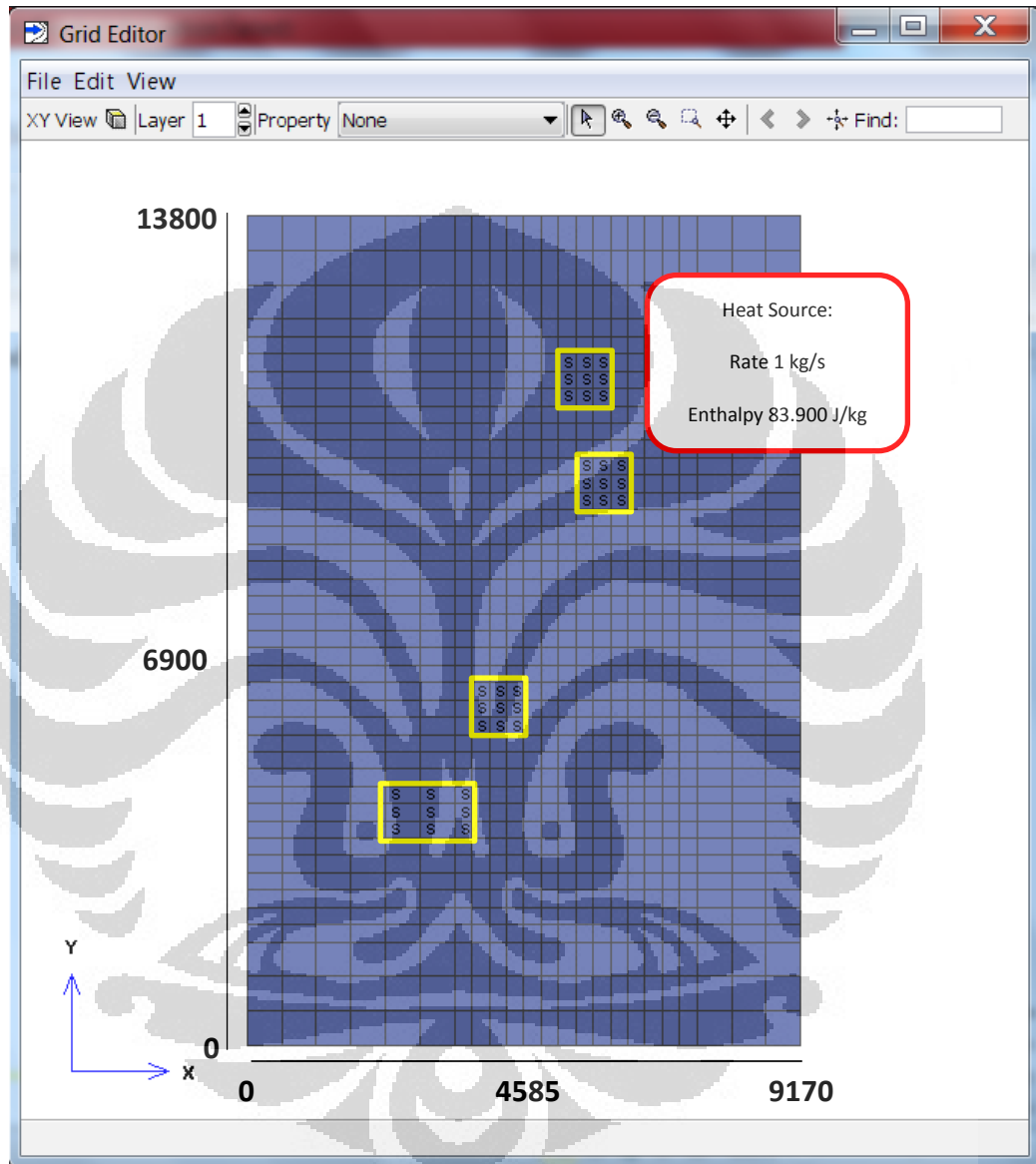
Susanto, A., Suparka, E., Tsuchiya, N., Hirano, N., Kishita, A., Kusumah, Y.I. (2011). *Hydrothermal Alteration Study in Malabar Area, Northern Part of the Wayang Windu Geothermal Field, Indonesia*. Proceeding of the 9th Asian Geothermal Symposium, 7 – 9 November 2011.

The University of Auckland, Faculty of Engineering. Mei 1, 2012.

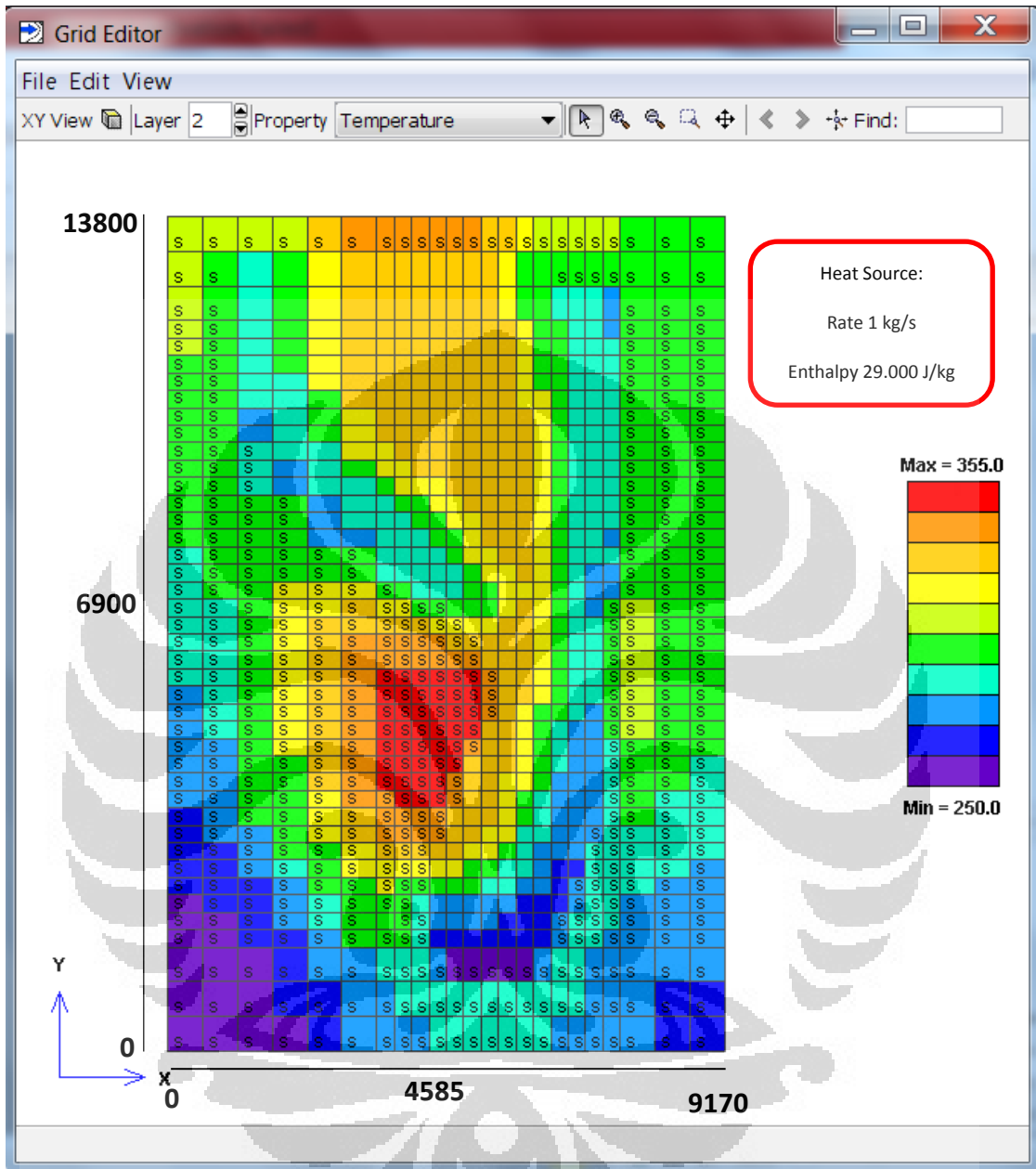
<http://www2.esc.auckland.ac.nz/research/geothermal-research-group/software/mulgraph>

APPENDICES

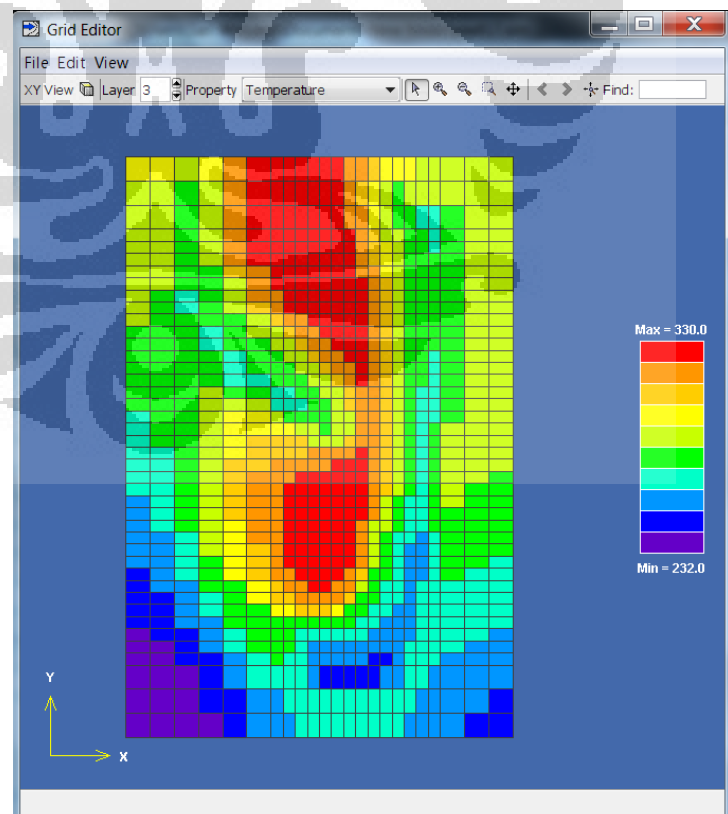
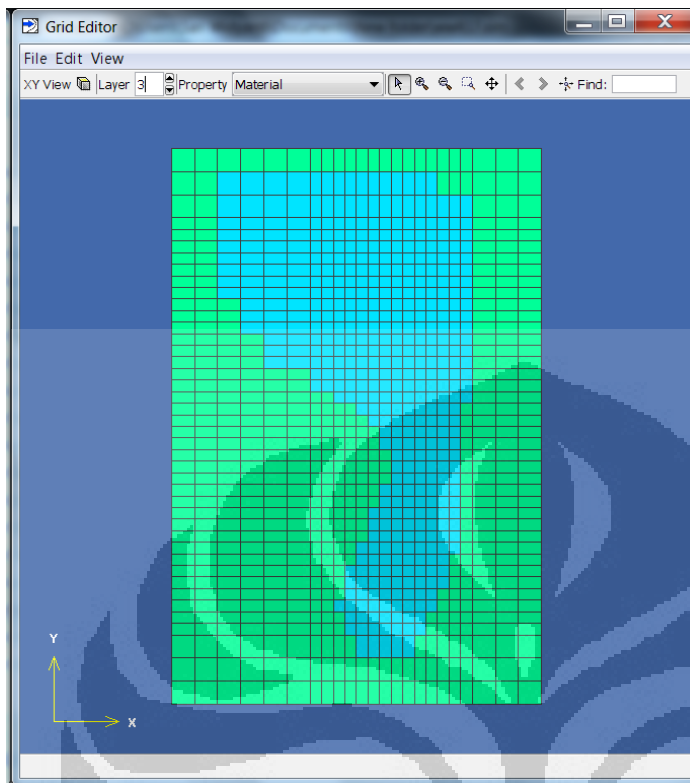
Appendix 1: Horizontal slicing of model simulation at Layer 1



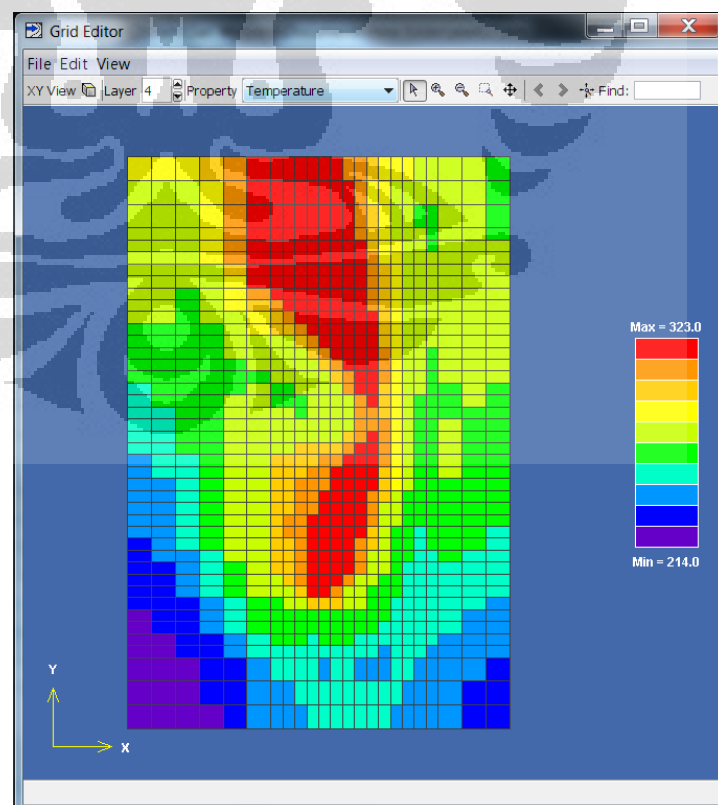
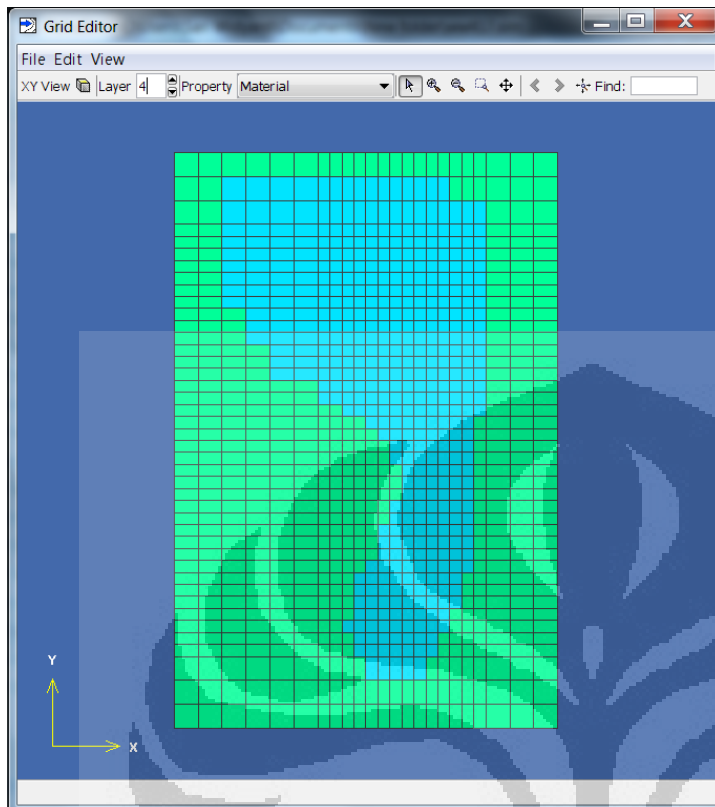
Appendix 2: Horizontal slicing of model simulation at Layer 2



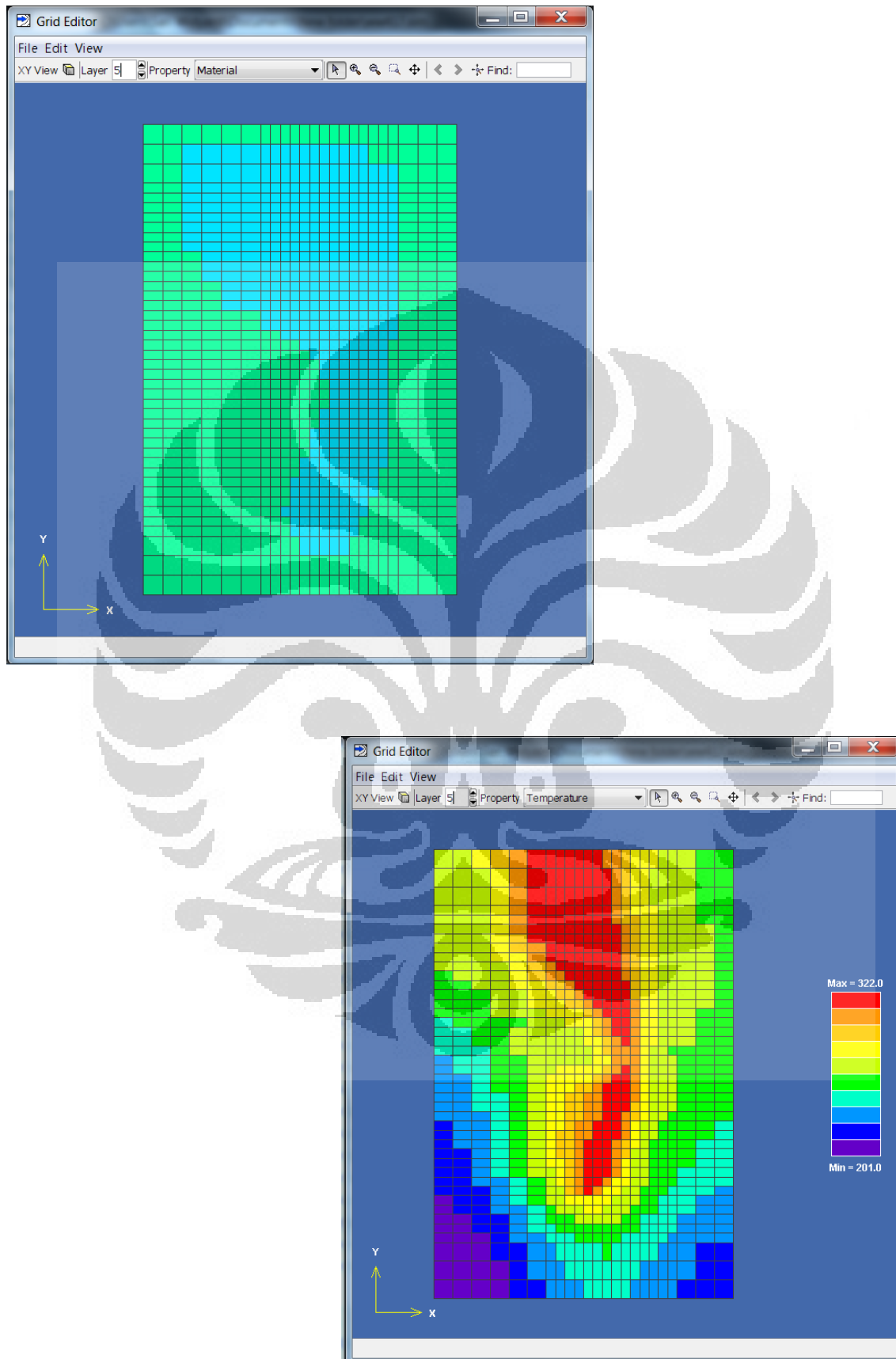
Appendix 3: Horizontal slicing of model simulation at Layer 3



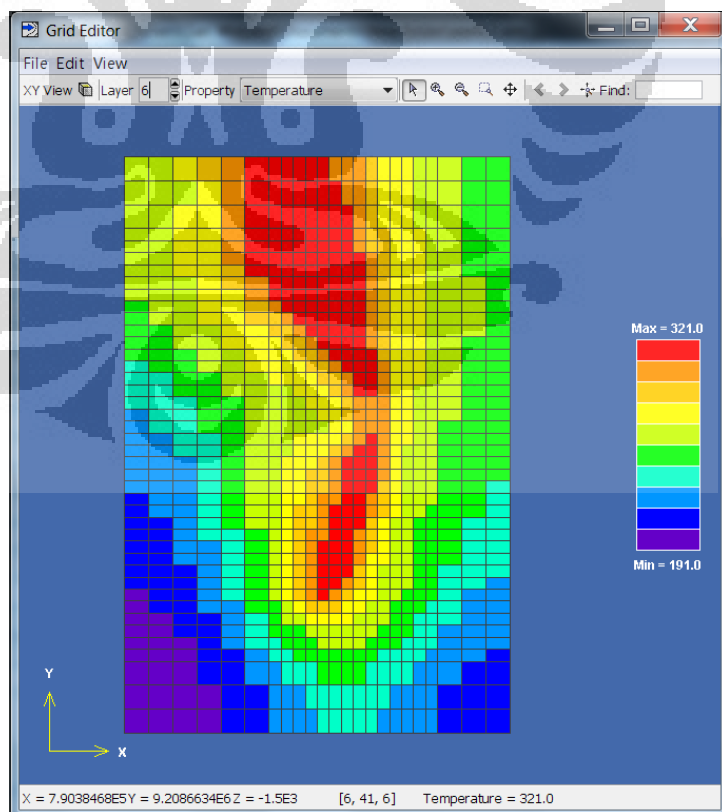
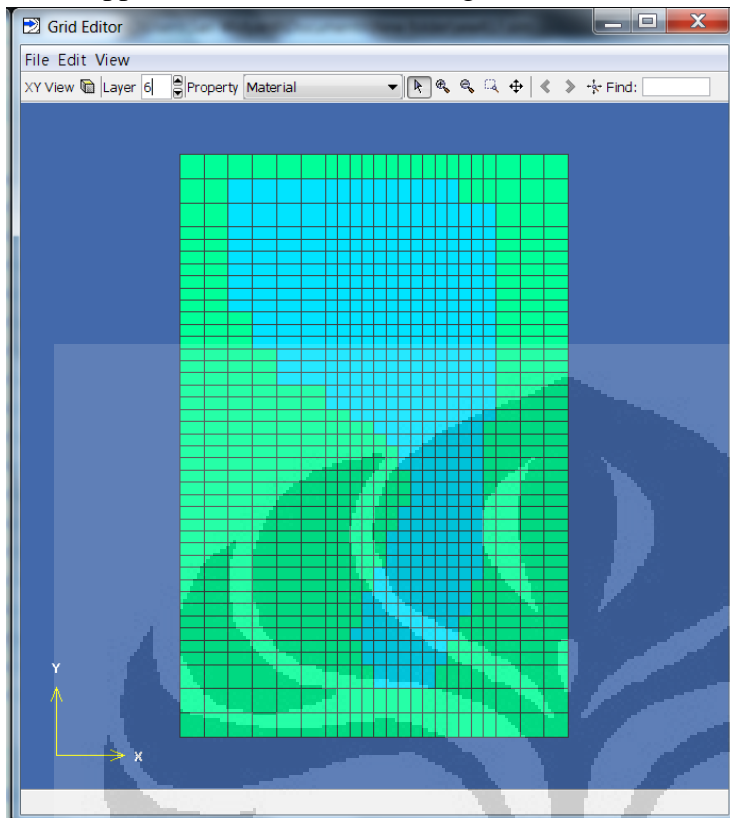
Appendix 4: Horizontal slicing of model simulation at Layer 4



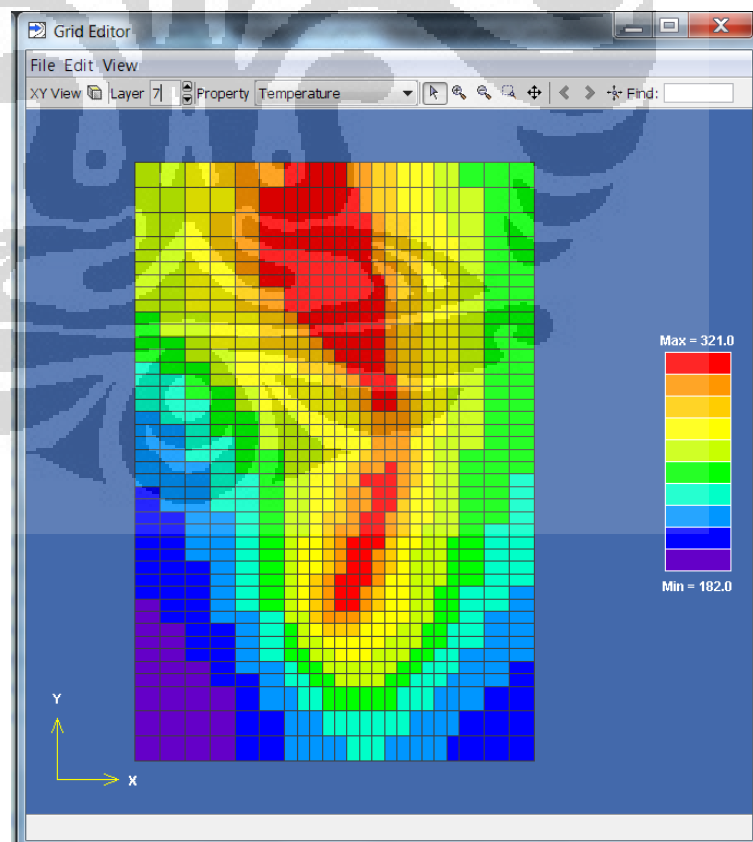
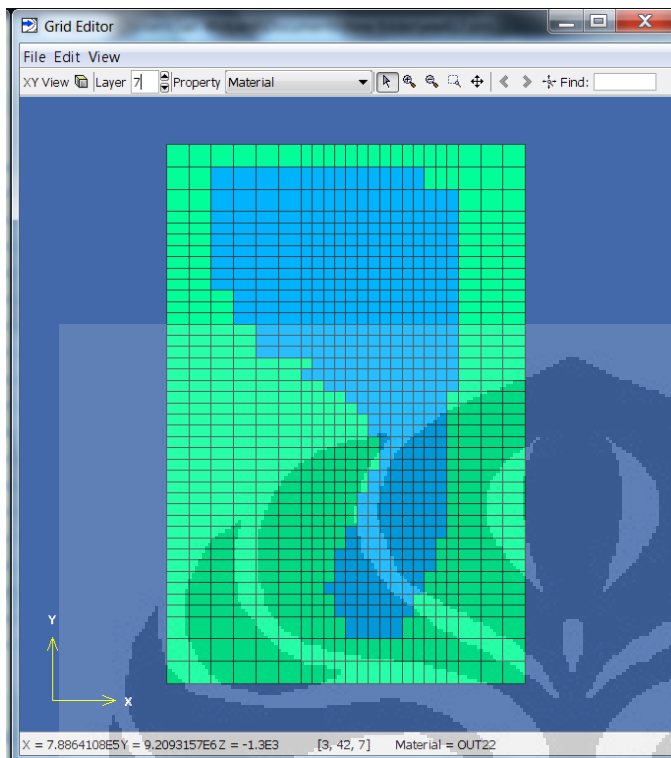
Appendix 5: Horizontal slicing of model simulation at Layer 5



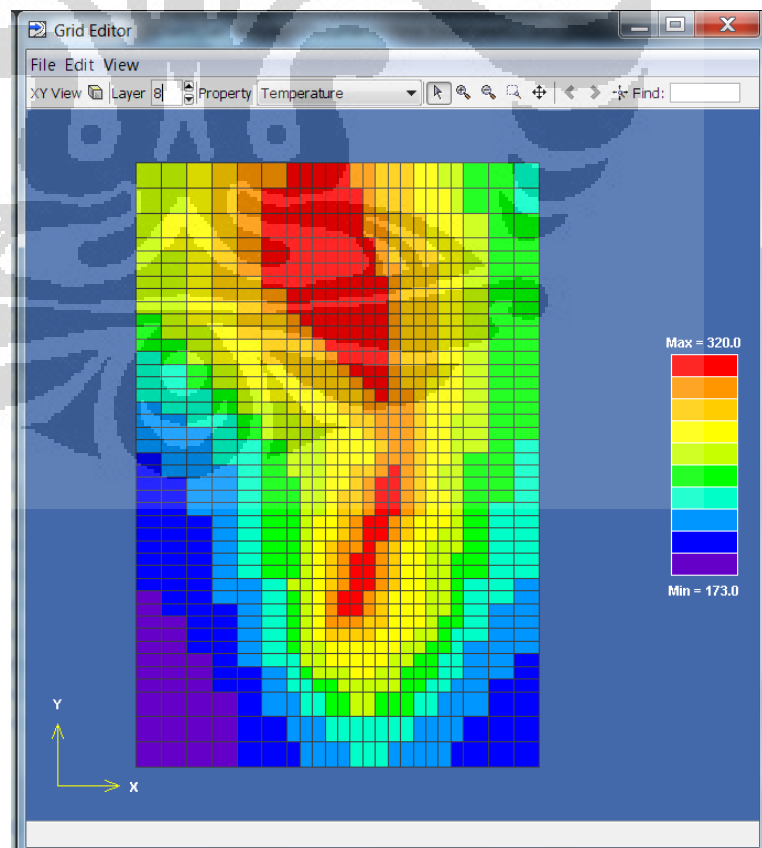
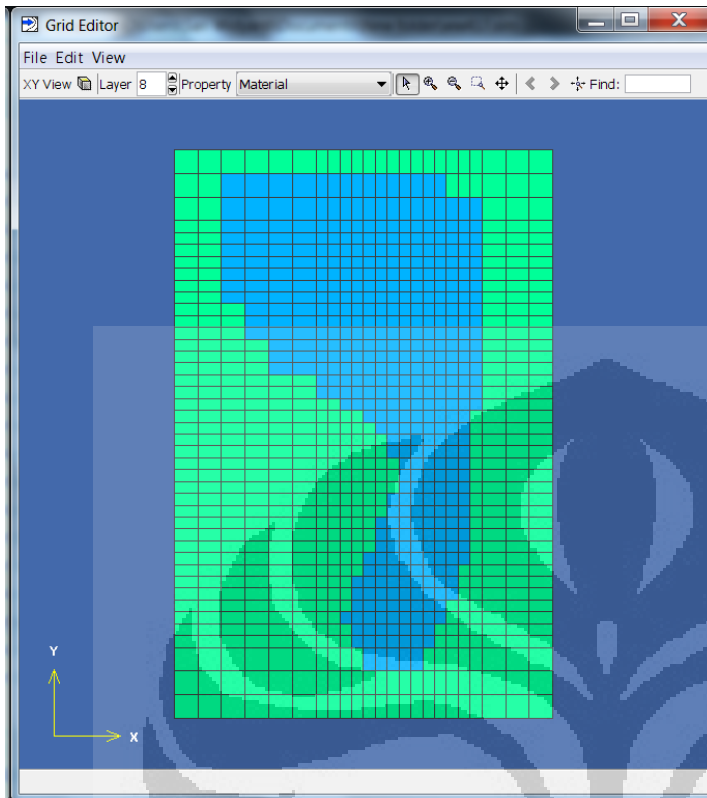
Appendix 6: Horizontal slicing of model simulation at Layer 6



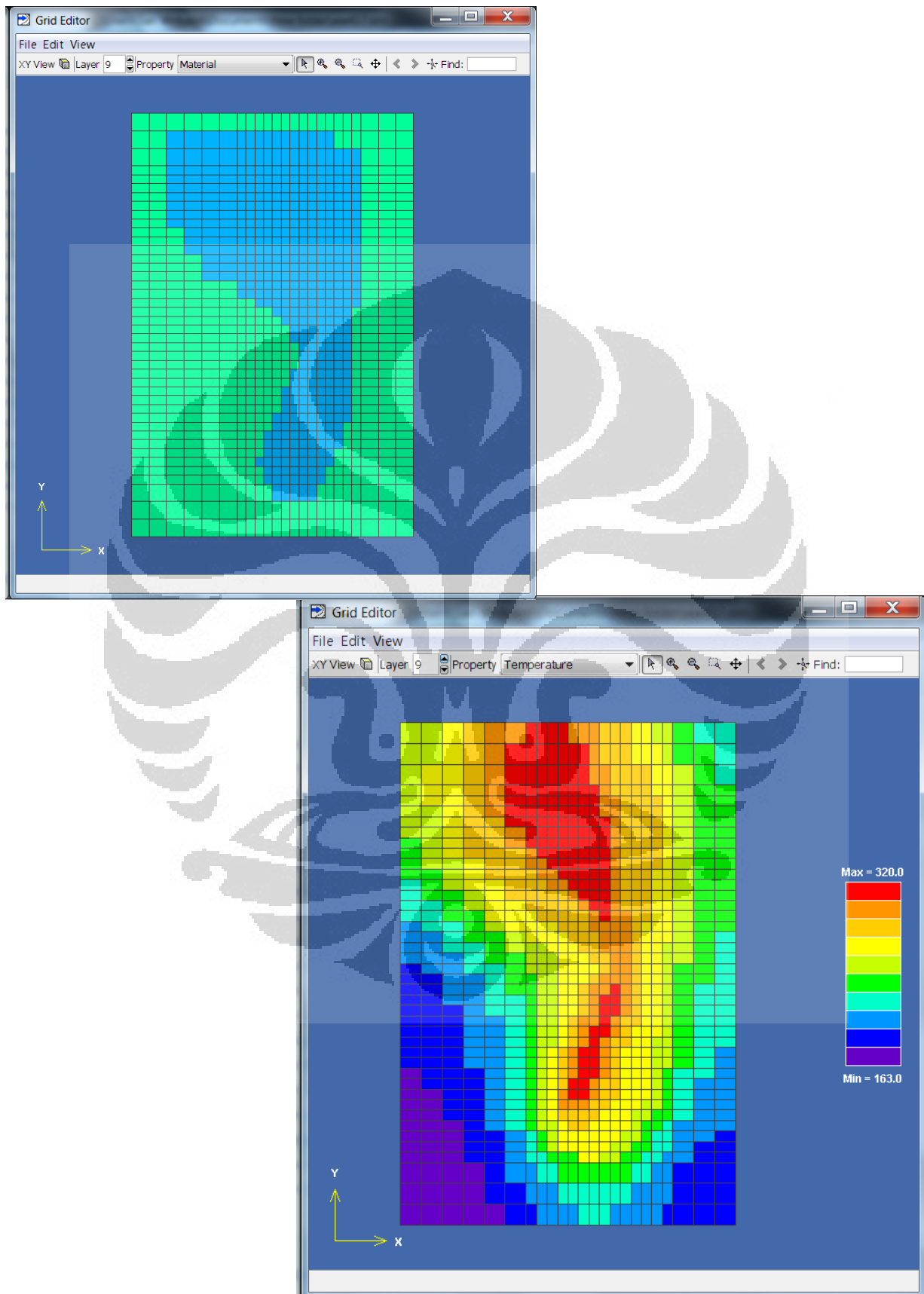
Appendix 7: Horizontal slicing of model simulation at Layer 7



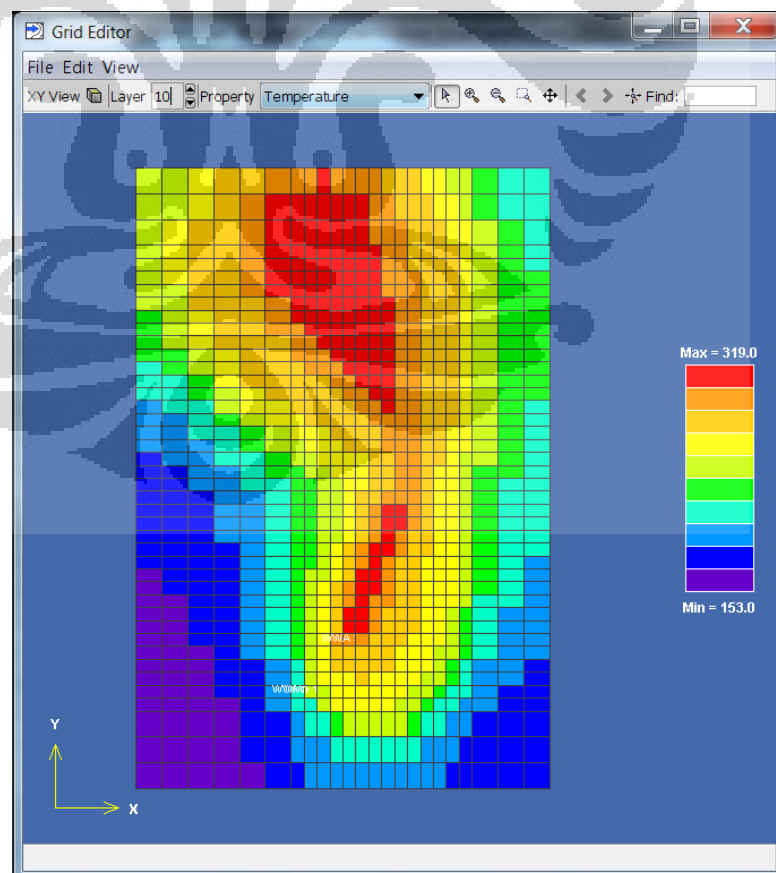
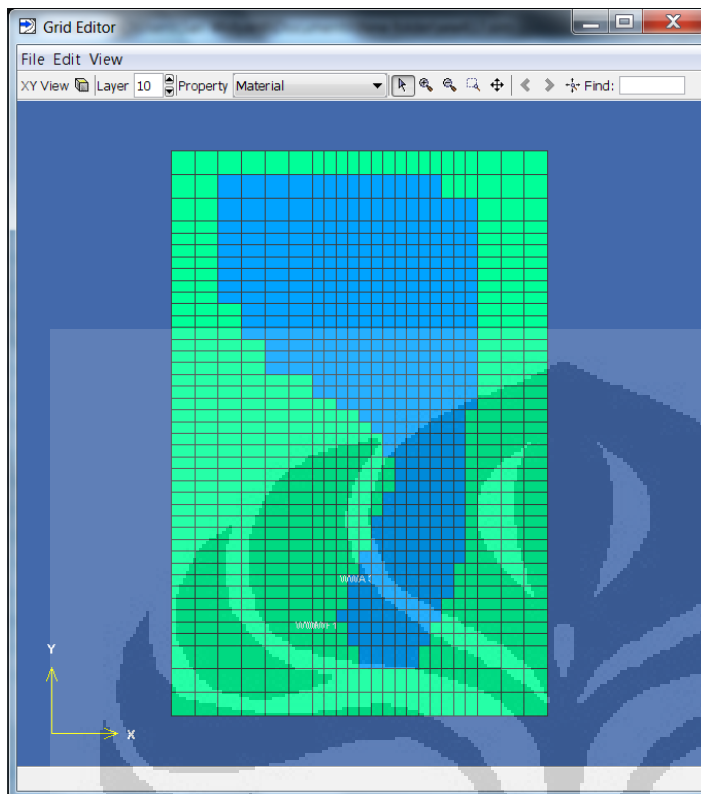
Appendix 8: Horizontal slicing of model simulation at Layer 8



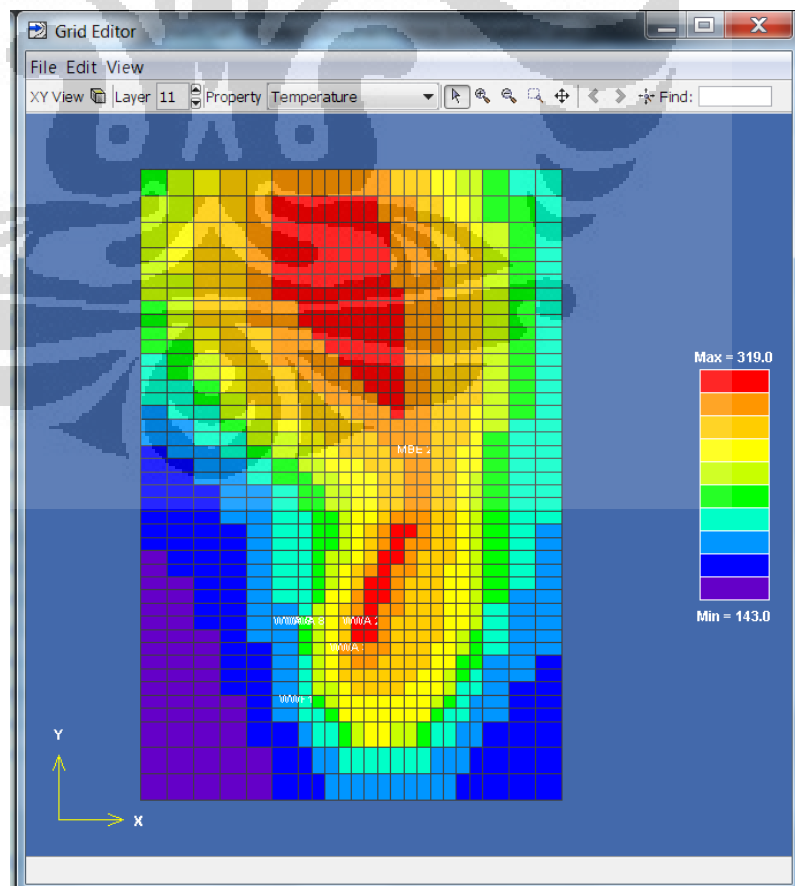
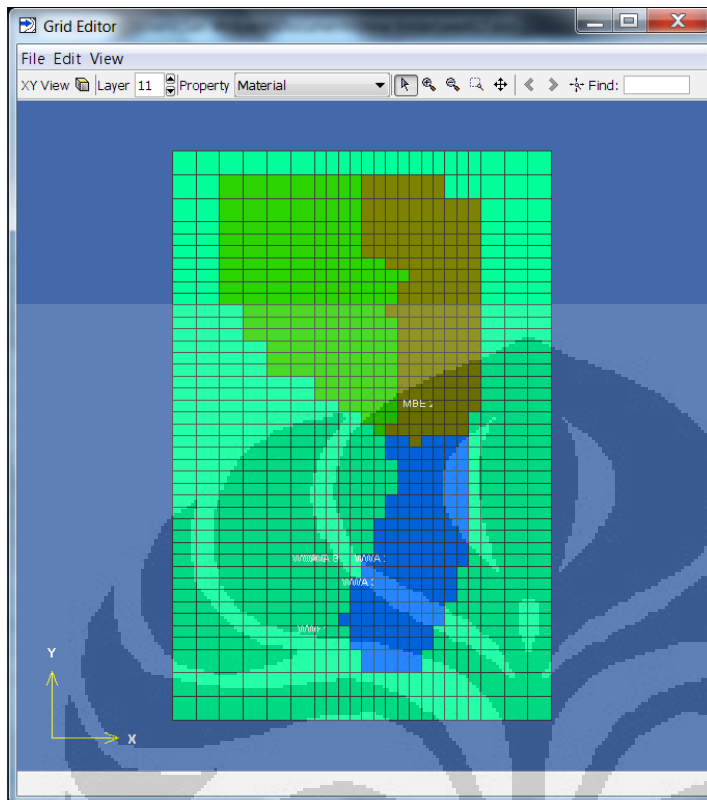
Appendix 9: Horizontal slicing of model simulation at Layer 9



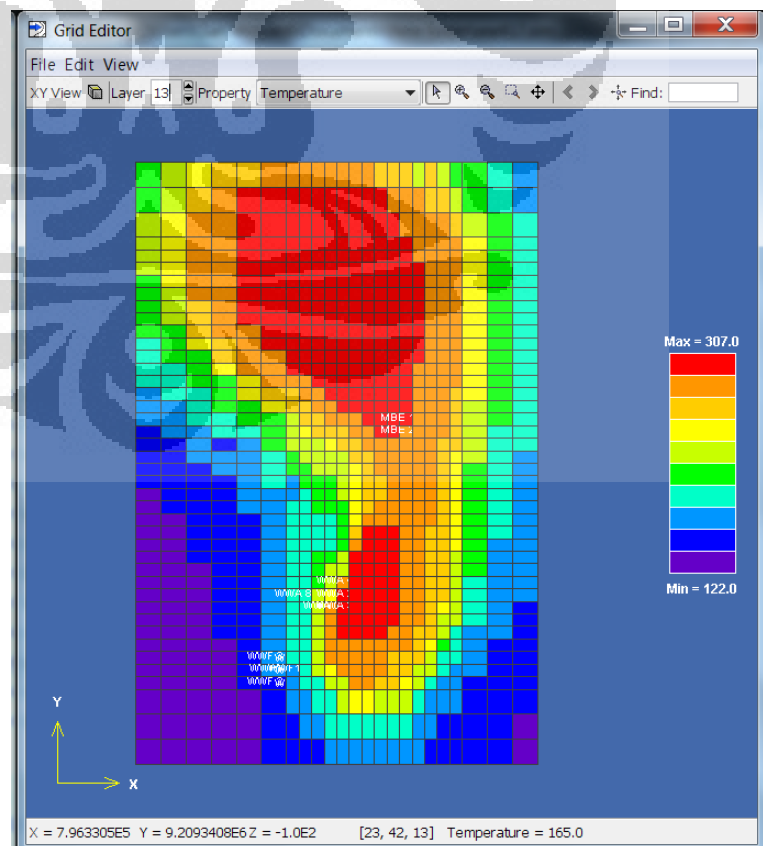
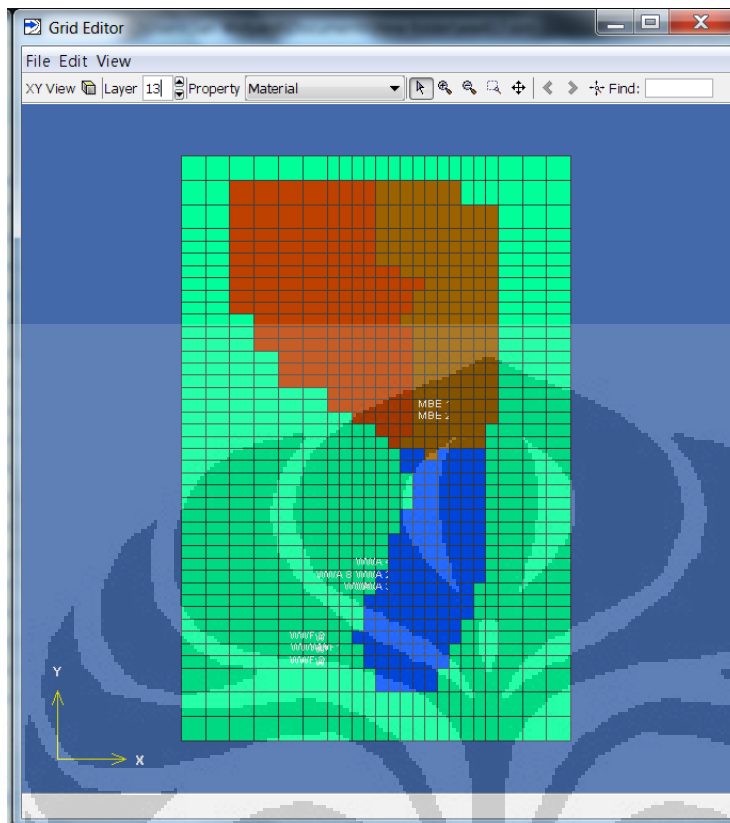
Appendix 10: Horizontal slicing of model simulation at Layer 10



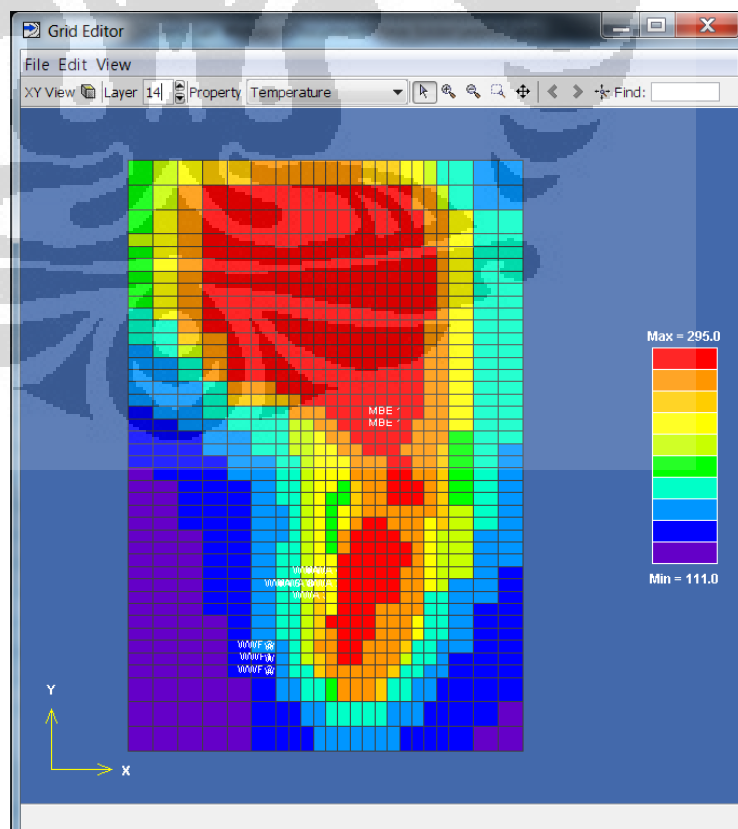
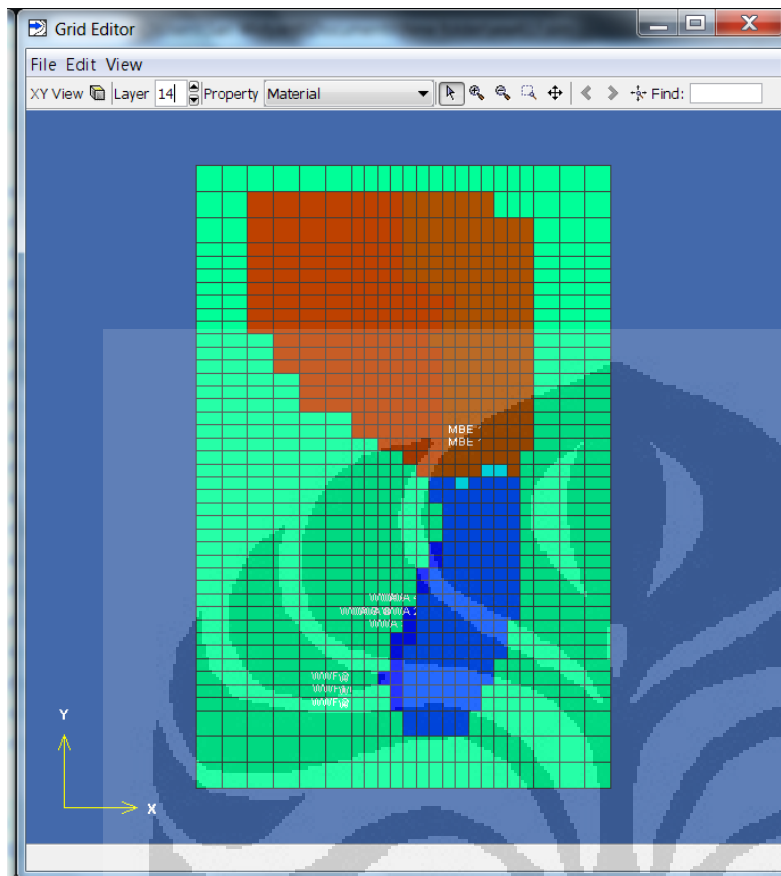
Appendix 11: Horizontal slicing of model simulation at Layer 11



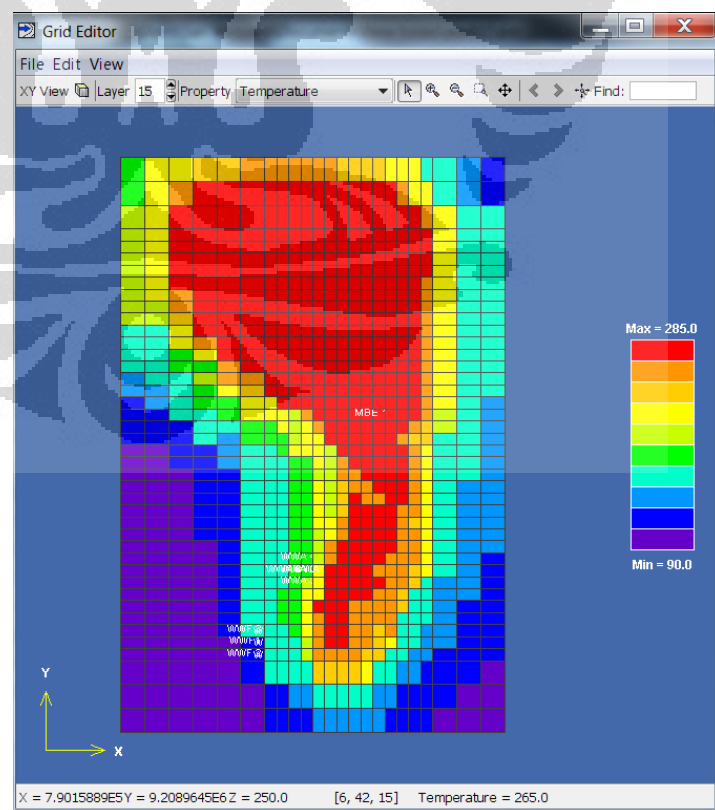
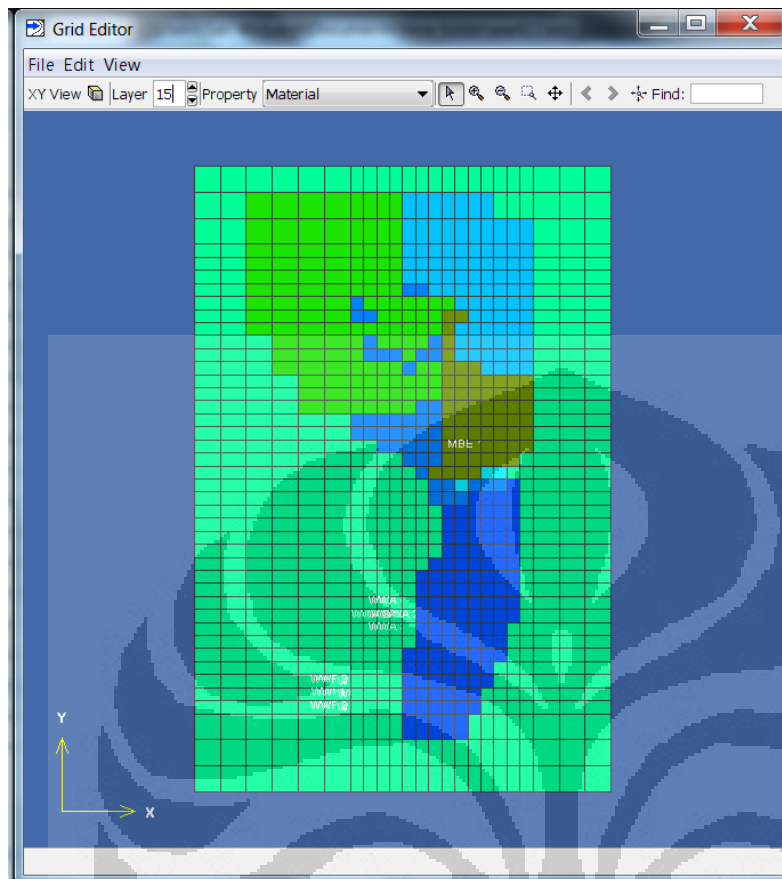
Appendix 13: Horizontal slicing of model simulation at Layer 13



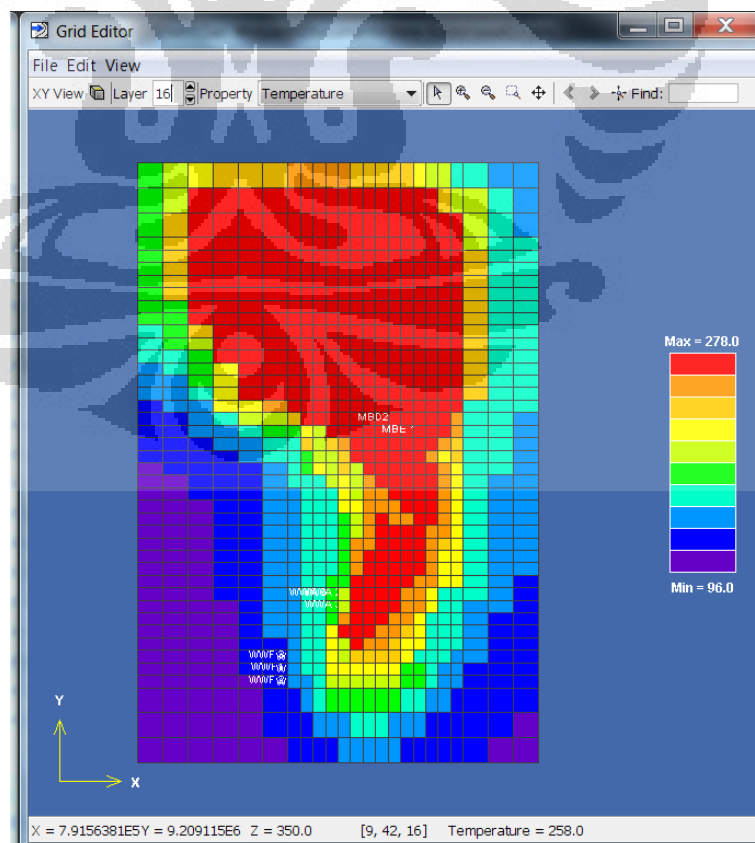
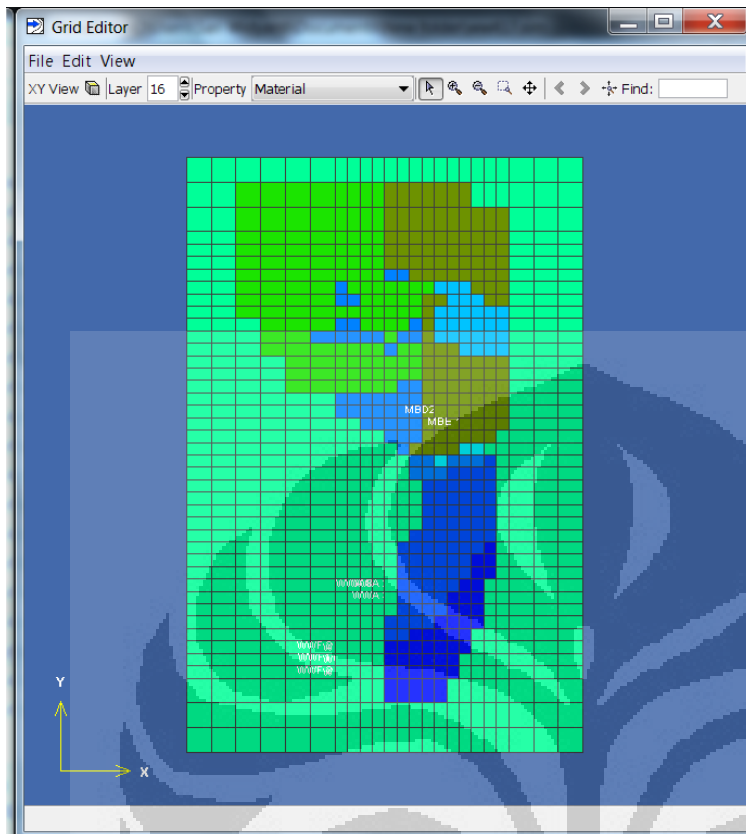
Appendix 14: Horizontal slicing of model simulation at Layer 14



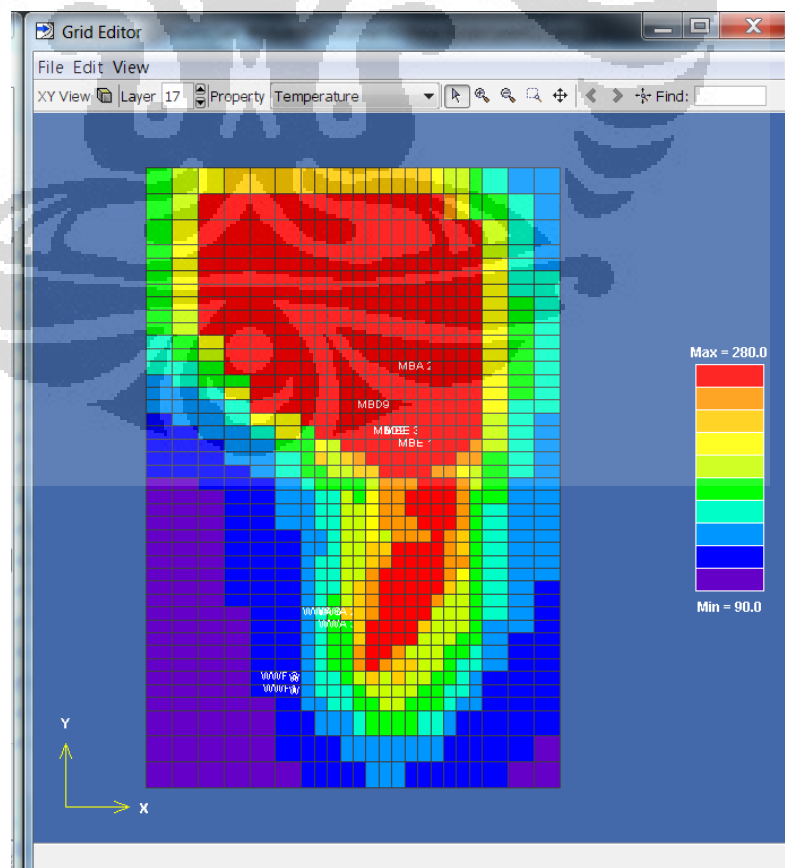
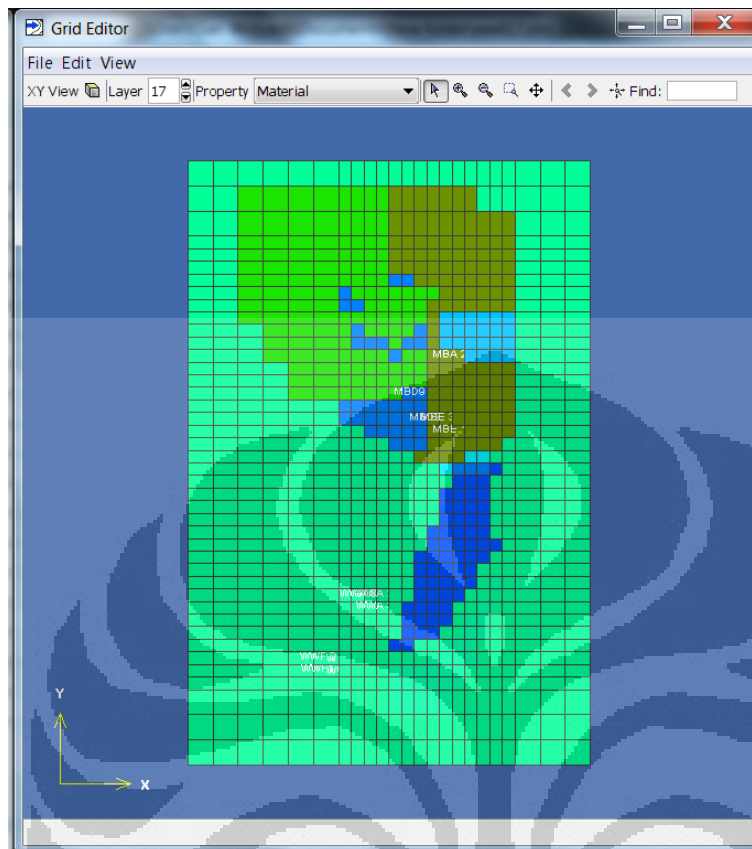
Appendix 15: Horizontal slicing of model simulation at Layer 15



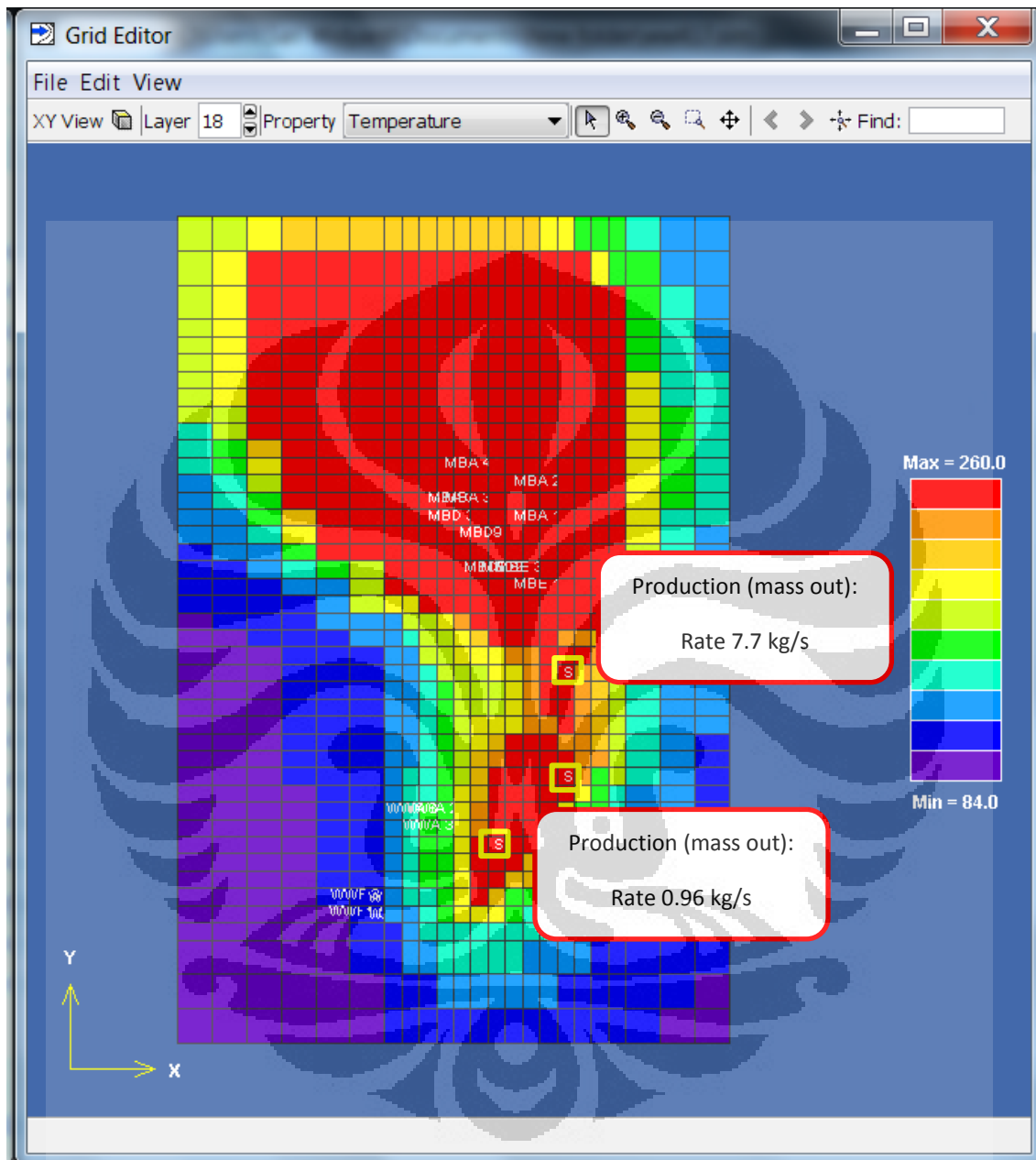
Appendix 16: Horizontal slicing of model simulation at Layer 16



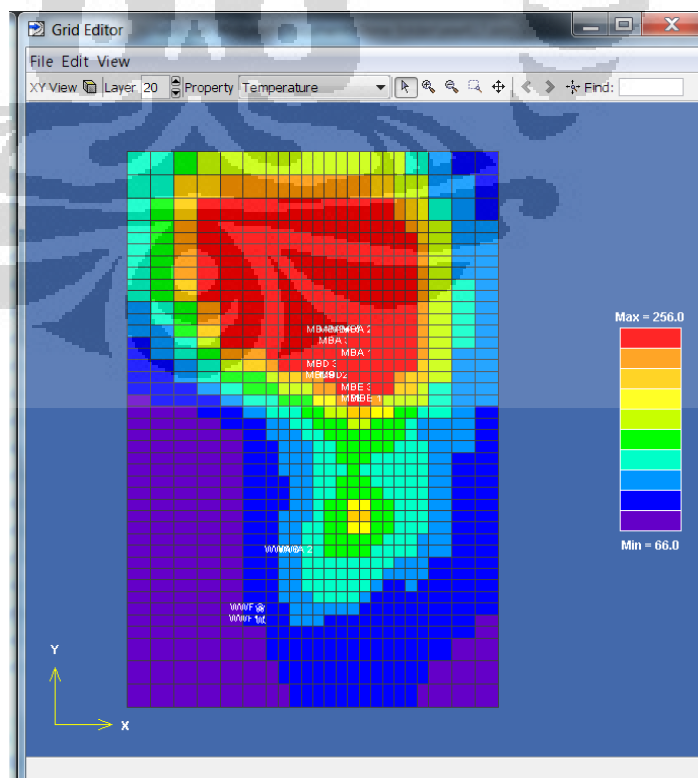
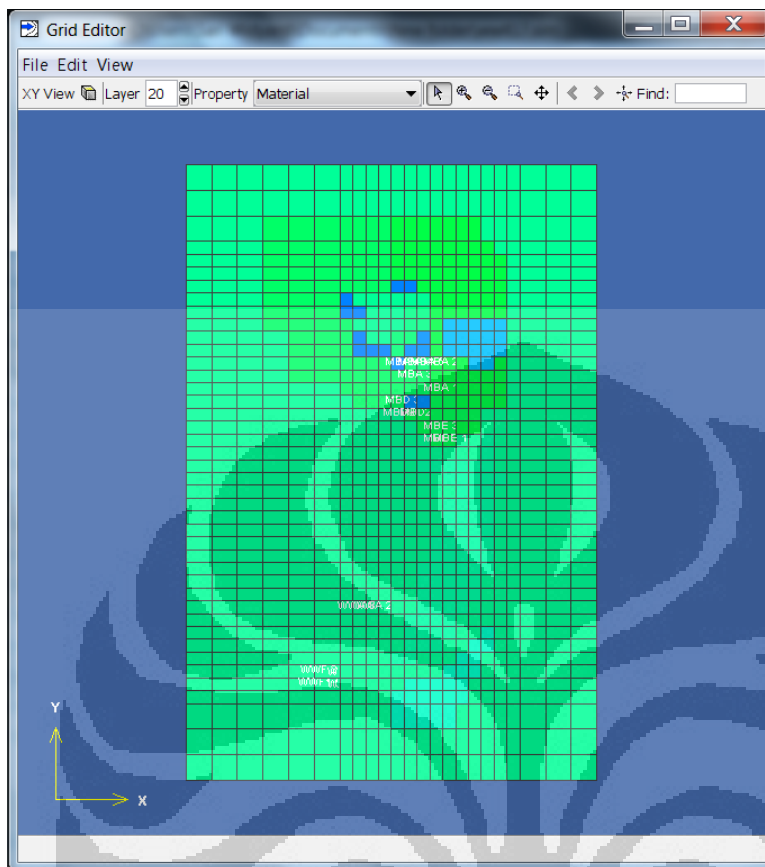
Appendix 17: Horizontal slicing of model simulation at Layer 17



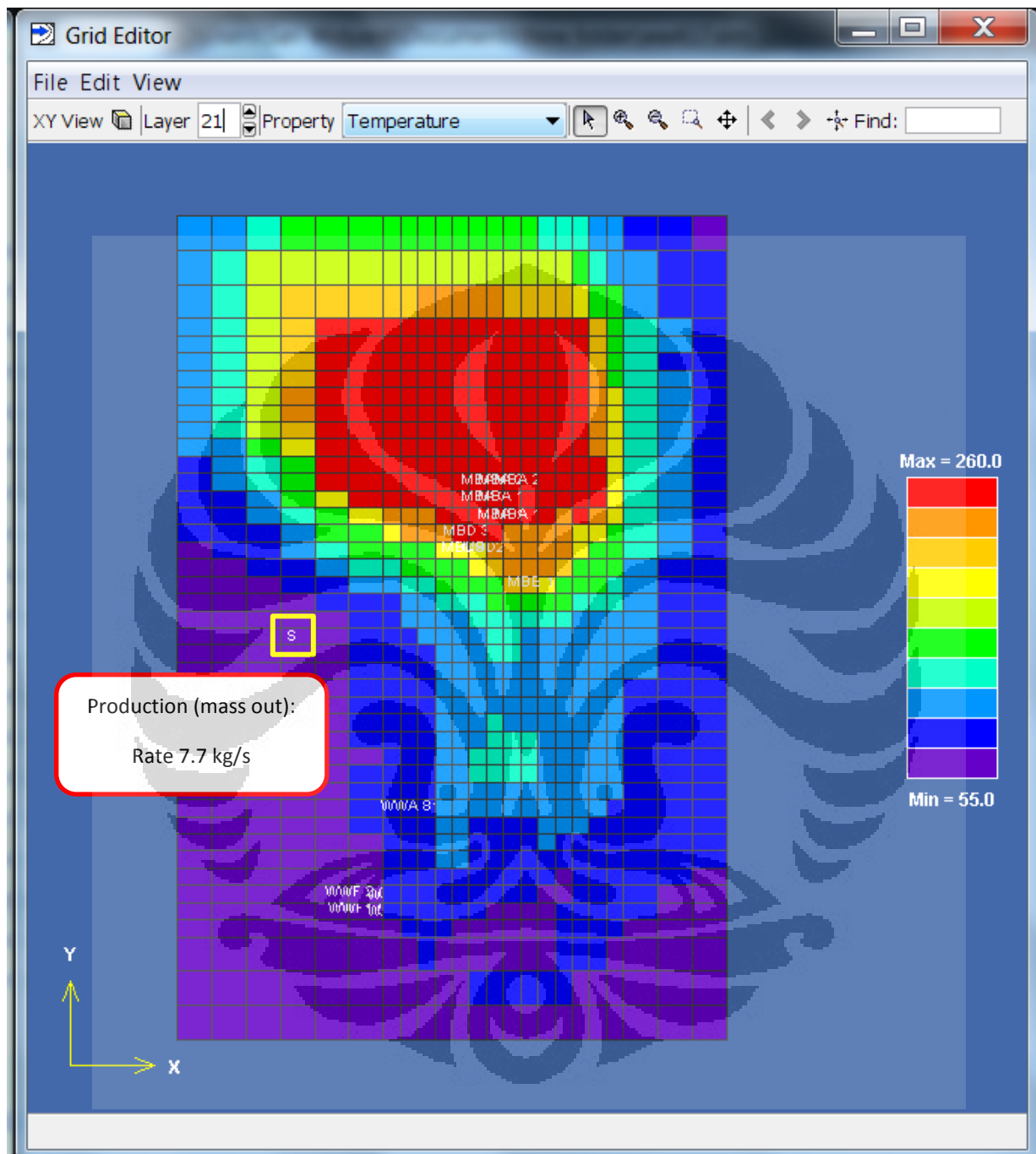
Appendix 18: Horizontal slicing of model simulation at Layer 18



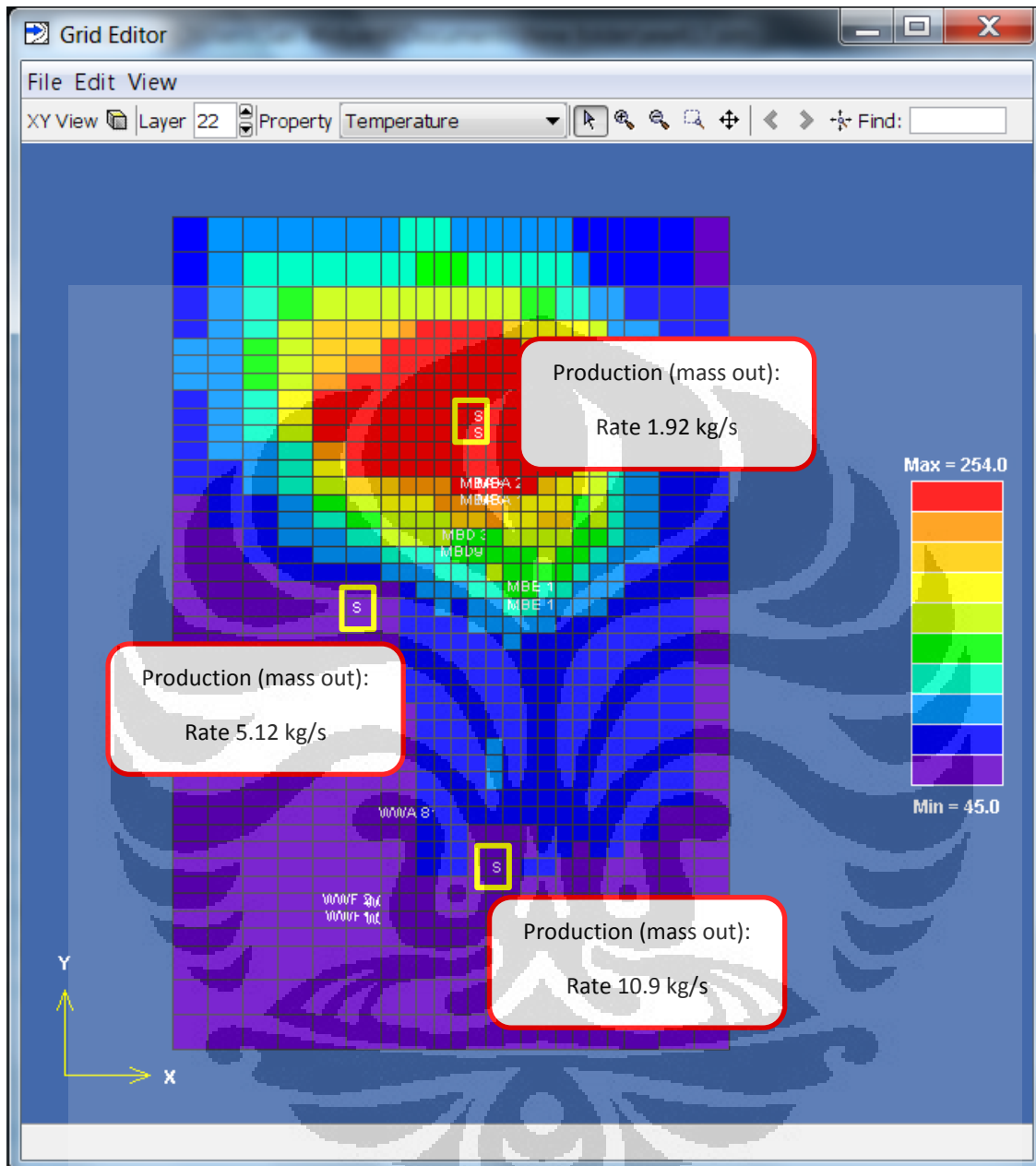
Appendix 20: Horizontal slicing of model simulation at Layer 20



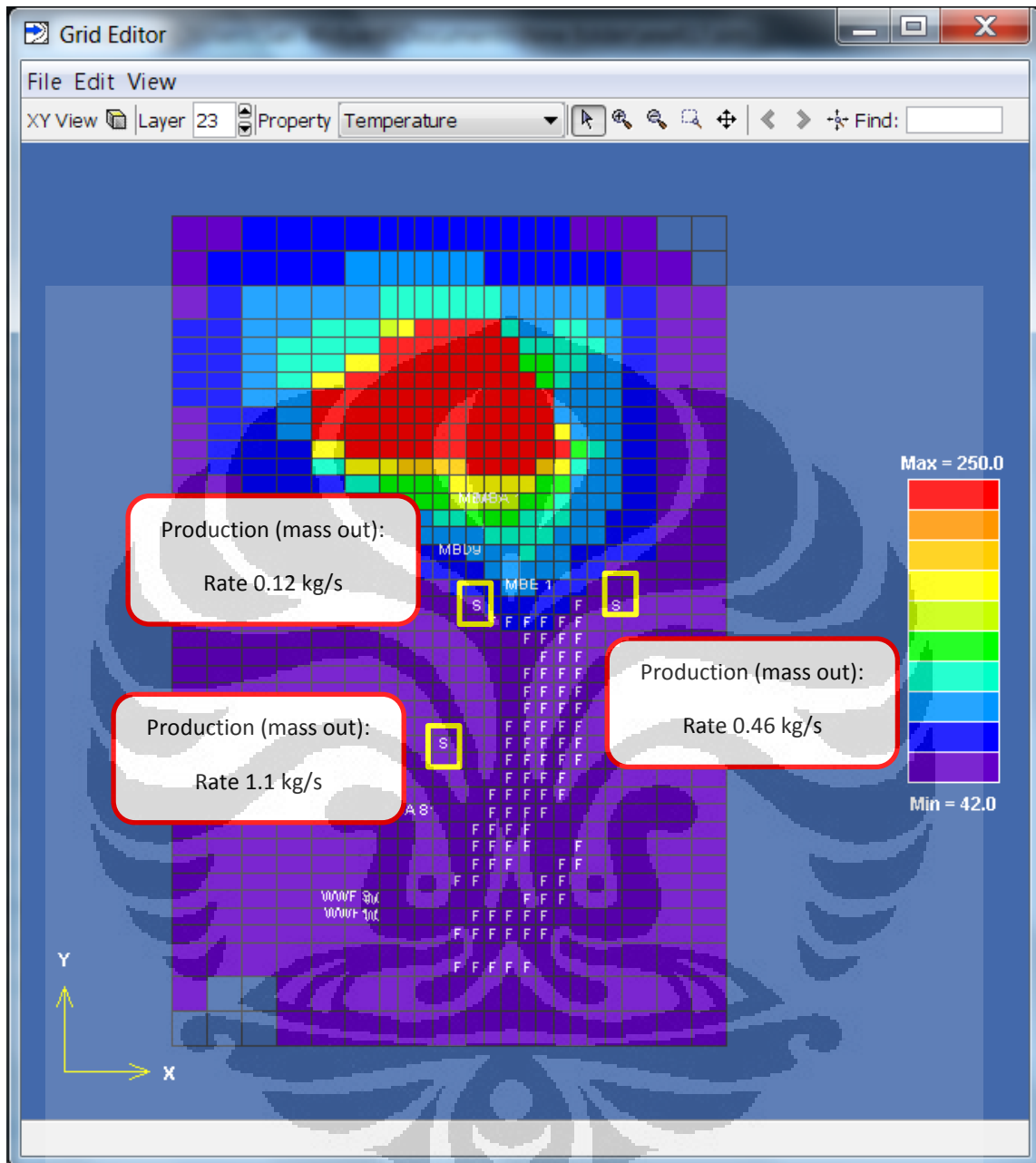
Appendix 21: Horizontal slicing of model simulation at Layer 21



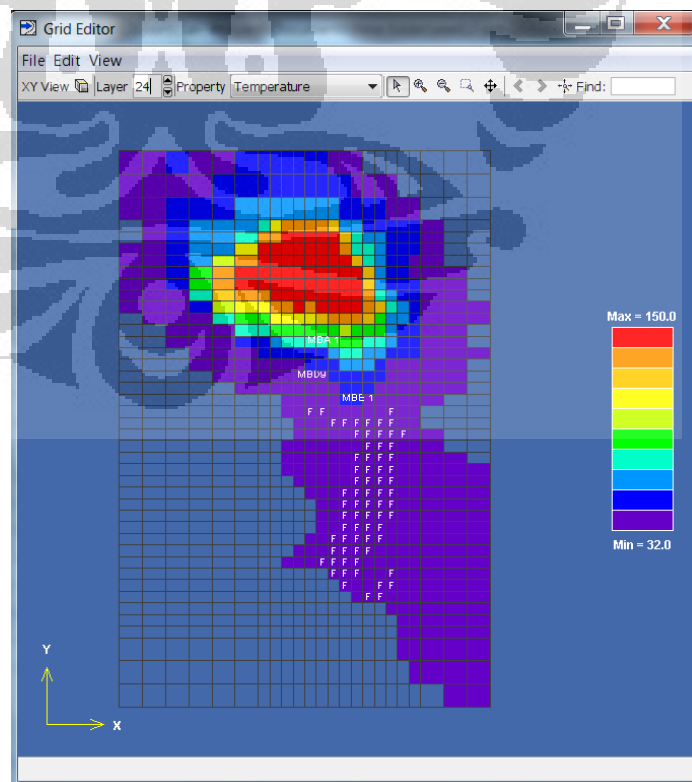
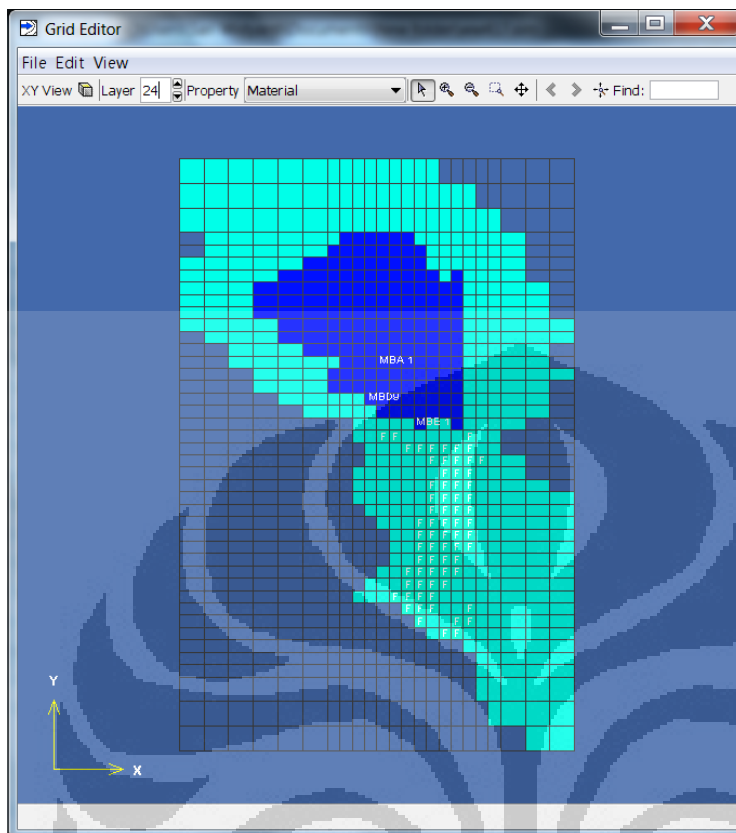
Appendix 22: Horizontal slicing of model simulation at Layer 22



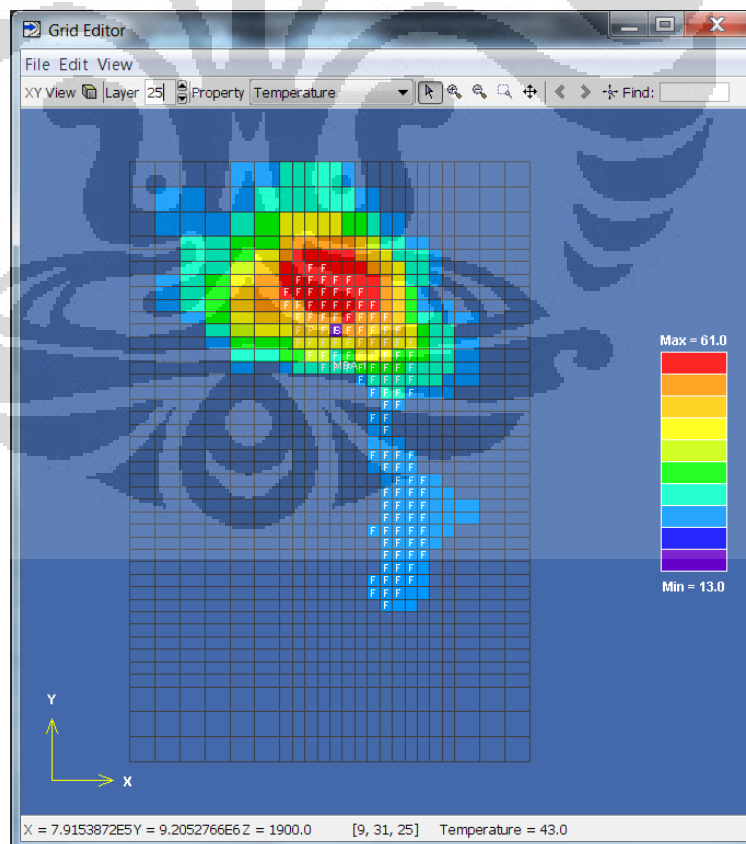
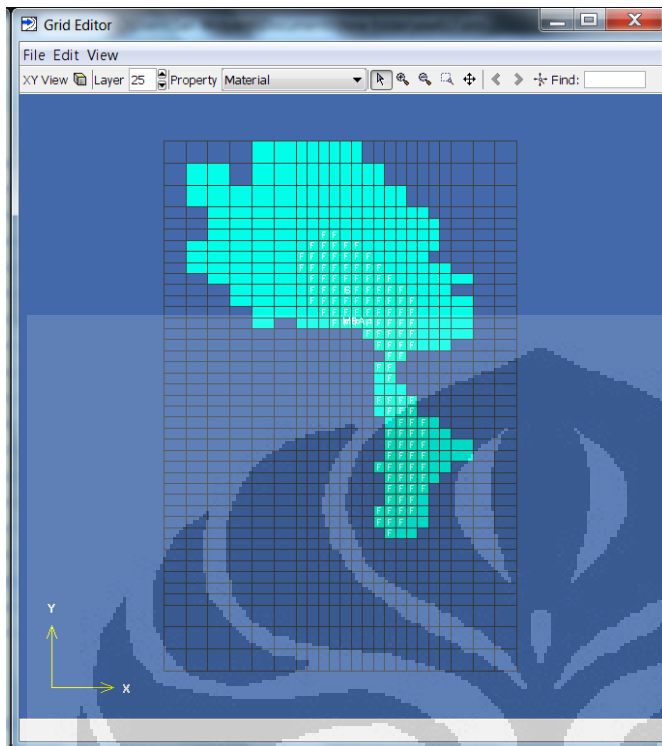
Appendix 23: Horizontal slicing of model simulation at Layer 23

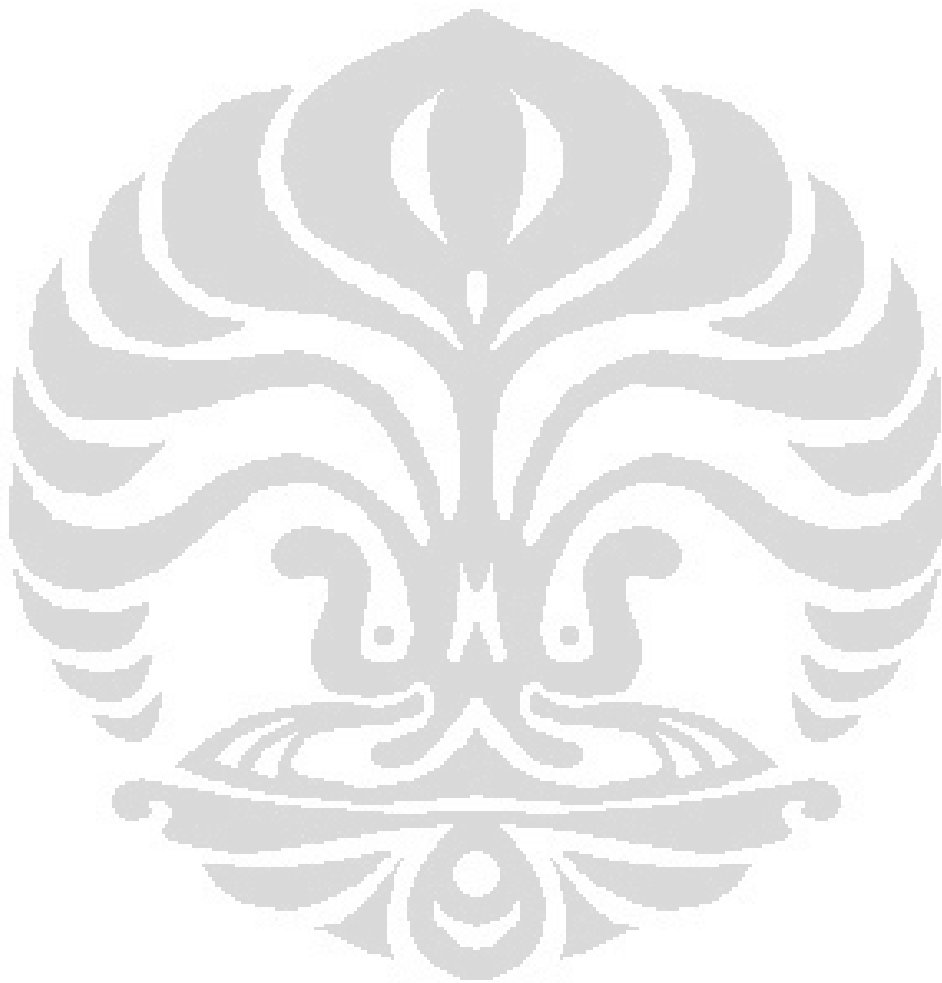


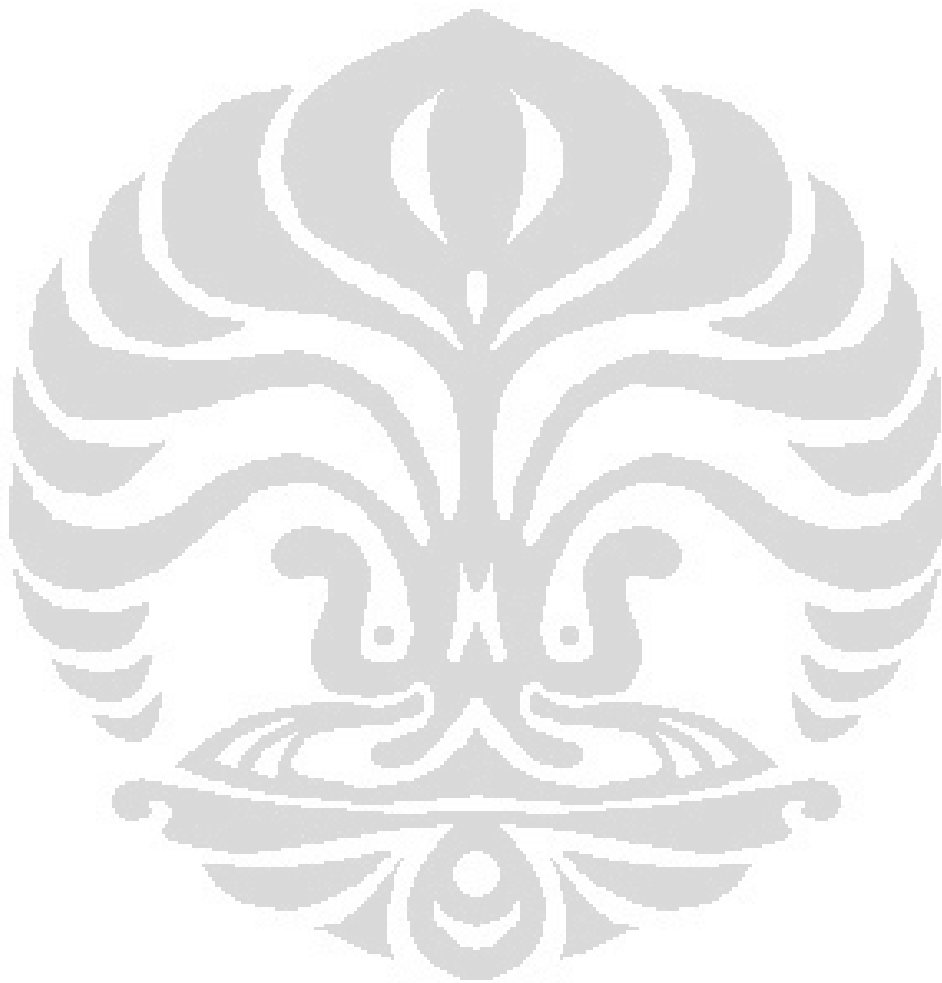
Appendix 24: Horizontal slicing of model simulation at Layer 24

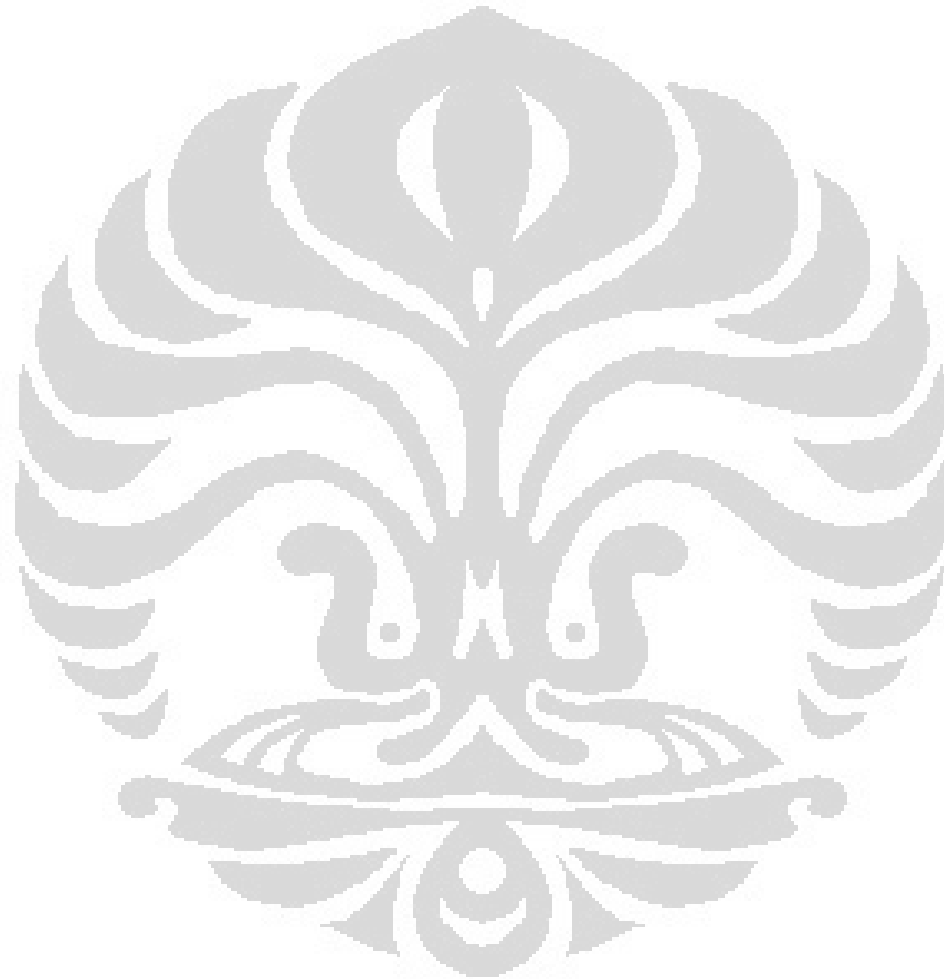


Appendix 25: Horizontal slicing of model simulation at Layer 25









University of Indonesia

